KU LEUVEN

FACULTEIT BIO-INGENIEURSWETENSCHAPPEN

# Golden opportunities in urban sewers: Nitrified urine for heterotrophic and autotrophic in-sewer denitrification, odor and corrosion control

"Gouden kansen in stedelijke riolen: Genitrificeerde urine voor heterotrofe en autotrofe denitrificatie in de riolering, geur- en corrosiebeheersing"


Promotoren:

Prof. Siegfried Vlaeminck (UAntwerpen)

Departement Bio-Ingenieurswetenschappen

Afdeling Duurzame energie-, lucht- en watertechnologie

Prof. Benjamin Horemans (KULeuven)

Departement Aard-en omgevingswetenschappen

Afdeling Bodem-en Waterbeheer


Masterproef voorgedragen tot het behalen van het diploma van Master of Science in de bio-ingenieurswetenschappen: Milieutechnologie


**Amber BROUNS**


Juni 2025


*Copyright informatie:*
*studiewerk van een student in het kader van de academische opleiding en examenbeoordeling. Na deze beoordeling vond geen correctie plaats van het studiewerk.*

# Acknowledgements

As a kid, my kindergarten teacher said I would never make it far academically, however I can gladly announce I proved her wrong. When I started this theses, I was filled with both excitement and uncertainty. Looking back now, I can say this journey has been one of growth, perseverance, and discovery. I am truly proud of how far I have come.

First and foremost, I would like to thank my tutor, Iris De Corte, for her excellent guidance throughout this thesis journey. Thank you for the many long, but fun, batch test days we endured together, and for making even the busiest moments filled with laughter and learning. I am truly grateful for everything you taught me, from scientific thinking and data processing to, perhaps most importantly, the essentials of lab clean-up and the importance of 'koffiekoeken' in daily research life. Thank you so much I am grateful for your constant support and unwavering belief in my capabilities.

I am also grateful to Professor Benjamin Horemans and Professor Siegfried Vlaeminck for establishing the connection between KU Leuven and the University of Antwerp, allowing me to work on this fascinating research topic. A special thanks to Professor Vlaeminck for his support, valuable time and for challenging me with deep and thought-provoking questions that helped me gain new insights into my work. I would also like to warmly thank Tim Van Winckel for his excellent guidance and for his insightful questions, which pushed me to approach my research from fresh and critical perspectives.

A heartfelt thank you goes to all the PhD students for welcoming me with open arms. Your openness and enthusiasm made the lab a truly inspiring and motivating environment. I am also very thankful to Maxime Bogaert for his clear explanations about the lab equipment and for his continuous support whenever technical challenges arose, whether it was mastering the IC or troubleshooting unexpected issues.

Finally, I am deeply grateful to my family for their unwavering support throughout this journey. A special mention goes to my brother, whose patience and tech-savviness helped me unravel more than one mysterious Word formatting issue. I'm also thankful to my dear friends Jana and Flore for our coffee-and-writing club days and their steady encouragement along the way. And last but not least, heartfelt appreciation goes to my dog, who provided the emotional support I needed.

Each of you made this thesis journey truly memorable, thank you.

# Abstract

Centralized wastewater treatment plants face growing challenges: capacity limitations, high carbon demands for denitrification, and energy-intensive aeration for nitrification. Simultaneously, sewer systems face operational challenges related to greenhouse gasses, odor nuisances, and corrosion. While nitrate or ferric-iron dosing is commonly used for mitigation, these rely mostly on non-renewable chemicals. Nitrified urine offers a sustainable alternative by reducing nitrogen loads on treatment plants and enabling decentralized nitrate dosing for in-sewer odor and corrosion control. This control is achieved by 1) suppressing sulphate reduction by maintaining anoxic conditions which in turn promote heterotrophic denitrification (HD), and (2) enabling the direct oxidation of hydrogen sulphide ($H_2S$) via autotrophic sulphide-driven denitrification (SAD).

This thesis explores the maximum denitrification rates ($r_{max}$) and interactions between HD and SAD under heterotrophic, autotrophic, and MIXED (*i.e.*, both acetate-COD and sulphide present as electron donors) conditions, as well as heterotrophic sulphide inhibition by performing a series of batch tests.

HD achieved the highest $r_{max}$ (303.3 ± 4.3 mg $NO_3$-N/(g VSS d)), while SAD activity was strongly influenced by enrichment, increasing from 48.29 ± 18.53 (fresh sludge) and 72.16 ± 14.05 ($S^0$) to 186.78 ± 14.45 mg $NO_3$-N/(g VSS d) ($HS^-$). No synergistic effect was found under MIXED conditions. Instead, acetate-COD availability dictated pathway dominance, favouring HD. The interplay between SAD and HD was therefore rather characterized by competition for nitrate as electron acceptor. $H_2S$ inhibition of HD occurred at low levels, but resilience varied with sludge history and dosing timing. When $H_2S$ was dosed at the start, the inhibition constant ($K_{i,H2S\text{-}NO3}$) was 1.43 mg $H_2S$-S/L, compared to 4.26-7.62 mg $H_2S$-S/L when dosed during active denitrification.

Biokinetics modelling showed that nitrate doses between 31.52 to 57.52 mg $NO_3$-N/$L_{sewage}$ are needed, depending mainly on hydraulic retention time and microbial community composition. A simulated 100-person apartment case demonstrated that nitrified urine alone can sustain anoxic conditions and enable nitrate-based odor and corrosion control, eliminating the need for non-renewable chemical inputs. These insights into microbial interactions allow for more accurate nitrate dosing estimations and contribute to more resource-efficient sewer management strategies.

# Samenvatting

Centrale afvalwaterzuiveringsinstallaties kampen steeds vaker met capaciteitsproblemen, een hoge koolstofvraag voor denitrificatie en intensieve beluchtingsbehoeften voor nitrificatie. Tegelijkertijd ondervinden rioleringssystemen operationele uitdagingen door broeikasgasemissies, geurhinder en corrosie. Hoewel nitraat- of ijzerzoutendosering vaak wordt toegepast als mitigatiestrategie, zijn deze doorgaans afhankelijk van niet-hernieuwbare chemicaliën. Genitreerde urine biedt een duurzaam alternatief doorstikstofbelasting op de installaties te verminderen en decentrale nitraatdosering mogelijk te maken voor geur-en corrosiecontrole in rioleringsstelsels. Deze controle werkt via (1) onderdrukking van sulfaatreductie door anoxische condities, wat heterotrofe denitrificatie (HD) bevordert, en (2) directe oxidatie van $H_2S$ via autotrofe, sulfide-gedreven denitrificatie (SAD).

Deze thesis onderzoekt de maximale denitrificatiesnelheden ($r_{max}$) en interacties tussen HD en SAD onder heterotrofe, autotrofe en MIXED (zowel acetaat-COD als sulfide aanwezig als elektrondonor) condities, evenals heterotrofe $H_2S$ inhibitie, via batchtesten. HD vertoonde de hoogste $r_{max}$ (303,3 ± 4,3 mg $NO_3$-N/(g VSS d)), terwijl SAD sterk beïnvloed werd door het type verrijking: van 48,29 ± 18,53 (vers slib) tot 72,16 ± 14,05 ($S^0$) en 186,78 ± 14,45 mg $NO_3$-N/(g VSS d) ($HS^-$). Er werd geen synergistisch effect waargenomen onder MIXED condities. In plaats daarvan bepaalde de beschikbare acetaat- chemische zuurstofvraag welk biologisch pad dominant werd, waarbij HD sterk werd bevoordeeld. Dus de interactie werd gekenmerkt door competitie voor nitraat als elektronenacceptor. HD bleek reeds bij lage $H_2S$-concentraties geïnhibeerd te worden, maar de inhibitie varieerde afhankelijk van de slibgeschiedenis en het doseringstijdstip. Wanneer $H_2S$ aan het begin werd gedoseerd, bedroeg de inhibitieconstante ($K_{i,H_2S\text{-}NO_3}$) 1,43 mg $H_2S$-S/L, tegenover 4,26-7,61 mg $H_2S$-S/L bij toevoeging tijdens actieve denitrificatie.

Biokinetische modellering toonde aan dat de benodigde nitraatdoseringen voor realistische riooltoepassing varieerden van 31,52 tot 57,52 mg $NO_3$-$N/L_{rioolwater}$, vooral afhankelijk van hydraulische verblijftijd en microbiële samenstelling. Een simulatie van een appartementsgebouw met 100 bewoners liet zien dat enkel genitreerde urine volstaat om anoxische condities te behouden en geur- en corrosiecontrole te realiseren, zonder externe chemicaliën. Deze inzichten maken een schatting voor nauwkeurigere nitraatdoseringen mogelijk en dragen bij aan duurzamer rioolbeheer.

# Vulgariserende samenvatting

Afvalwaterzuiveringsinstallaties staan onder toenemende druk. Ze kampen met een beperkte capaciteit, een hoog energieverbruik en de noodzaak om extra chemicaliën toe te voegen om stikstof te verwijderen. Tegelijkertijd hebben rioleringssystemen hun eigen problemen, zoals geuroverlast, aantasting van leidingen en de uitstoot van broeikasgassen. Om deze problemen aan te pakken, voegen waterbeheerders vaak nitraat of ijzerzouten toe, maar deze oplossingen zijn op lange termijn niet duurzaam.

Een veelbelovender en duurzamer alternatief is het gebruik van *genitrificeerde urine*. Dit is urine waarbij de stikstof al is omgezet naar nitraat. Deze nitraatrijke vloeistof kan rechtstreeks in de riolering worden gedoseerd. Zo helpt het om geurhinder en corrosie tegen te gaan, terwijl het ook de stikstofbelasting op de zuiveringsinstallatie verlaagt. Maar hoe reageren de micro-organismen in de riolering op deze aanpak?

Deze thesis onderzoekt hoe goed verschillende bacteriën nitraat verwijderen wanneer ze koolstof (uit acetaat), sulfide of beide als energiebron ter beschikking hebben. Uit de testen bleek dat koolstofverwerkende bacteriën (heterotrofen) nitraat het snelst verwijderen. Bacteriën die sulfide gebruiken (autotrofen) zijn trager, maar presteren beter als ze zijn aangepast aan zwavelrijke omstandigheden. Wanneer zowel koolstof als sulfide aanwezig is, krijgen de heterotrofen de overhand. In plaats van samen te werken, bleken de twee groepen bacteriën juist te concurreren om dezelfde voedingsstof: nitraat.

Daarnaast werd onderzocht hoe waterstofsulfide ($H_2S$), een stinkend en giftig gas, de heterotrofe bacteriën beïnvloedt. Zelfs kleine hoeveelheden kunnen het proces al remmen, al hangt het effect sterk af van de timing en eerdere blootstelling van de bacteriën aan $H_2S$.

Tot slot werd berekend hoeveel nitraat nodig is om geur- en corrosieproblemen in de riolering effectief te bestrijden. Een simulatie van een appartementsgebouw met 100 bewoners liet zien dat genitrificeerde urine op zichzelf al voldoende is om de juiste omstandigheden in de riolering te behouden, dit zonder dat extra chemicaliën nodig zijn.

Kortom, dit onderzoek geeft meer inzicht in hoe rioolmicroben samenwerken (of juist niet), en laat zien hoe we onze eigen afvalstromen, zoals urine, slim kunnen inzetten om afvalwatersystemen efficiënter, duurzamer en toekomstbestendiger te maken.

# List of abbreviations and symbols

Ammonia ($NH_3$)
Ammonia monooxygenase (AMO)
Ammonia oxidizing bacteria (AOB)
Autotrophic denitrifiers (AD)
Biodegradable chemical oxygen demand (bCOD)
Biological oxygen demand (BOD)
Biomass concentration (X)
Both sulphide and acetate-COD as electron donor (MIXED)
Calcium nitrate $Ca(NO_3)_2$
Carbon dioxide ($CO_2$)
Chemical oxygen demand (COD)
Chemical oxygen demand to nitrogen ratio (COD/N)
Denitrifying bacteria (DNB)
Denitrifying phosphate-accumulating organisms (DPAO)
Dissolved Inorganic Carbon (DIC)
Dissolved oxygen (DO)
Dissolved Organic Carbon (DOC)
Elemental sulphur ($S_0$)
Extracellular polymeric substance (EPS)
Free ammonia (FA)
Ferric chloride ($FeCl_3$)
Free nitrous acid (FNA)
Global warmth potential (GWP)
Greenhouse gas (GHG)
Haber-Bosch (HB)
Heterotrophic combined with autotrophic denitrification (HAD)
Heterotrophic denitrifiers (HD)
Heterotrophic sulphide-oxidizing nitrate-reducing (h-soNRB)
Hydraulic retention time (HRT)
Hydrogen sulphide ($H_2S$)
Hydroxylamine oxidoreductase (HAO)
Inhibition constant ($K_i$)
Maximum achievable denitrification/ nitrate removal rate ($r_{max}$)
Methane ($CH_4$)
Methanogenic archaea (MA)
Nitrate ($NO_3^-$)
Nitrate reductase (Nar)
Nitric oxide reductase (Nir)
Nitrite ($NO_2^-$)
Nitrite oxidizing bacteria (NOB)
Nitrogen (N)
Nitrogen gas ($N_2$)
Nitrous oxide ($N_2O$)
Nitrous oxide reductase (Nos)
Oxygen uptake rate (OUR)
Periplasmic nitrate reductase-associated cytochrome subunit G (NapG)
Periplasmic nitrate reductase catalytic subunit A (NapA)
Phosphorous (P)
Potassium (K)
Potassium acetate ($CH_3COOK$)
Potassium nitrate ($KNO_3$)
Reactive nitrogen ($N_r$)
Sequential batch reactor (SBR)
Sodium acetate ($CH_3OONa$)
Sodium acetate trihydrate ($NaAc.3H_2O$)
Sodium nitrate ($NaNO_3$)
Sodium sulphide ($Na_2S.xH_2O$)
Solid retention time (SRT)
Standard operating protocol (SOP)
Sulphate ($SO_4^{2-}$)
Sulphate reducing bacteria (SBR)
Sulphide ($S^{2-}$)
Sulphide-based autotrophic denitrification (SAD)
Sulhpide inhibition constant ($Ki,_{H2S-NO3}$)
Sulphuric acid ($H_2SO_4$)
Sulphur oxidizing bacteria (SOB)
Sulphur oxides ($SO_x$)
Thiosulphate ($S_2O_3^2$)
Total ammonia nitrogen (TAN)
Total disssolved sulphide (TDS)
Total Kieldahl Nitrogen (TKN)
Total nitrogen (TN)
Total organic carbon (TOC)
Total suspended solids (TSS)
Upward flow anaerobic sludge blanket (UASB)
Volatile suspended solids (VSS)
Volatile fatty acid (VFA)
Wastewater treatment plant (WWTP)

# List of Tables

# List of Figures

# Table of contents

# Introduction

*"Sewage is the wealth of nations if only we learn how to use it wisely." John Todd*
*Ecological Designer, Founder of Living Machines*

As the global population continues to grow at an extremely fast pace, so does the demand for food, water, energy and efficient nutrient usage. This escalating demand exerts immense pressures on the environment, contributing to issues such as eutrophication, acid rain and resource depletion. A key contributor to these environmental challenges is the inefficiency of centralized wastewater treatment plants (WWTPs), which struggle with capacity issues, loss of valuable nutrients such as nitrogen (N) and phosphorous (P), and greenhouse gas (GHG) emissions, including methane ($CH_4$) and nitrous oxide ($N_2O$).

This situation underscores the urgent need for innovative solutions to create a more sustainable approach to urban wastewater treatment (WWT) practices. In response, decentralized WWT has emerged as a promising alternative to the conventional centralized approach. Offering greater flexibility, resource conservation, and cost-effectiveness, decentralized systems can significantly reduce environmental impact while enhancing treatment efficiency (Bernal et al., 2021; Libralato et al., 2012; Otterpohl et al., 2004). However, full decentralization poses logistical and economic challenges, particularly due to infrastructure constraints and social factors. A more viable solution lies in partial decentralization and source separation, which enable optimized nutrient recovery and targeted treatment of wastewater streams (Libralato et al., 2012; Terpstra, 1999; J. Xu et al., 2023).

One major issue in existing sewer networks is the generation of harmful gases such as $CH_4$, $N_2O$ and hydrogen sulphide ($H_2S$). While $CH_4$ contributes to climate change and poses explosion hazards, $H_2S$ results in sewer corrosion, public and environmental health risks, and substantial maintenance costs (Guisasola et al., 2008; L. Zhang et al., 2008). Addressing these challenges requires an innovative approach to mitigate emissions and enhance nutrient recovery.

A potential biological solution is the use of specific in-sewer microbial communities: heterotrophic denitrifiers (HD) (using organic carbon as electron donor) and sulphide-driven autotrophic denitrifiers (SAD) (using sulphide as electron acceptor). SAD can oxidize $H_2S$ to sulphate or elemental sulphur, reducing $H_2S$ emissions, while HD, when fully carried out, can lower $N_2O$ emissions.

Both processes rely on nitrate ($NO_3^-$) as an electron acceptor, but nitrate levels in sewers are typically low (~1%) due to dilution. However, the presence of sufficient nitrate is crucial, not just for SAD and HD, but also because $NO_3^-$ acts as a redox buffer, helping to maintain anoxic conditions. This inhibits methanogenesis and sulphate reduction, thereby reducing methane ($CH_4$) emissions and $H_2S$ concentrations.

To address odor and GHG-related issues, external nitrate dosing is often applied, though this comes with additional costs. Moreover, introducing extra nitrogen into the sewer system lowers the chemical oxygen demand to nitrogen (COD/N) ratio, which may increase the need for additional external carbon dosage at central WWTPs due to potential carbon loss during the aerobic step.

To flush these problems away, a more sustainable alternative could be implemented. One promising solution is source separation and pre-treatment of urine. Although urine accounts for only 1% of the total wastewater volume, it contains about 80% of the nitrogen (N) load. It also holds significant amounts of phosphorus (P, 56%) and potassium (K, 63%), making it a valuable resource for nutrient recovery (Fittschen & Hahn, 1998; Randall & Naidoo, 2018).

By nitrifying urine before its introduction into the sewer system, $NO_3^-$ levels can be maintained to sustain its redox-buffering effect. This helps prevent $CH_4$ and $H_2S$ production, thereby reducing both GHG emissions and odor-related issues in a more cost-effective manner, while also alleviating the burden on WWTPs.

Nitrified urine will be produced in a pre-treatment nitrification step, which then will be dosed into the sewer system. This approach offers multiple benefits: (1) Usage of in-sewer denitrification reduces the carbon and N loads in wastewater. The strategy not only leads to cost, energy but also potential space savings by integrating urine collection, nitrification, and in-sewer treatment processes (F. Jiang et al., 2011; Oosterhuis & Van Loosdrecht, 2009). (2) Applicability in developing countries, where financial constraints often limit the access to clean water.

(3) Resource recovery: Key nutrients, such as P and K, can be recovered through precipitation mechanisms in the septic tank or urine storage. (4) Operating under anoxic conditions in the sewer can significantly reduce GHGs and odorous compound emissions.

This master's thesis focuses on the application of pre-treated (nitrified) urine in sewer systems, with the primary objective of optimizing nitrate retention within sewer pipes. By maintaining elevated nitrate levels, this study aims to reduce concentrations of $H_2S$, $CH_4$, mitigating odor issues and GHG emissions in the municipal wastewater infrastructure. The key goal of this thesis is to gain more insights in the kinetics of both heterotrophic and autotrophic sulphide-driven denitrification processes, gaining knowledge in the heterotrophic and autotrophic microbial interplay, and delving into the heterotrophic sensitivity to sulphur (Figure 0.1). By systematically evaluating these processes, this study will provide valuable insights into maximizing denitrification rates, minimizing inhibitory effects, and controlling $H_2S$. These findings will be critical in the next step of designing, and refining a near-realistic sewer bioreactor to evaluate the benefits of the proposed "golden opportunity". Within this reactor, parameters such as hydraulic retention time (HRT) will be adjusted to understand their impact on maintaining reduced $H_2S$ and $CH_4$ levels. However, the experimental phase involving a near-realistic sewer bioreactor falls outside the scope of this thesis. The insights gained from this work could contribute to making urban WWT systems more sustainable and resilient to future environmental challenges.

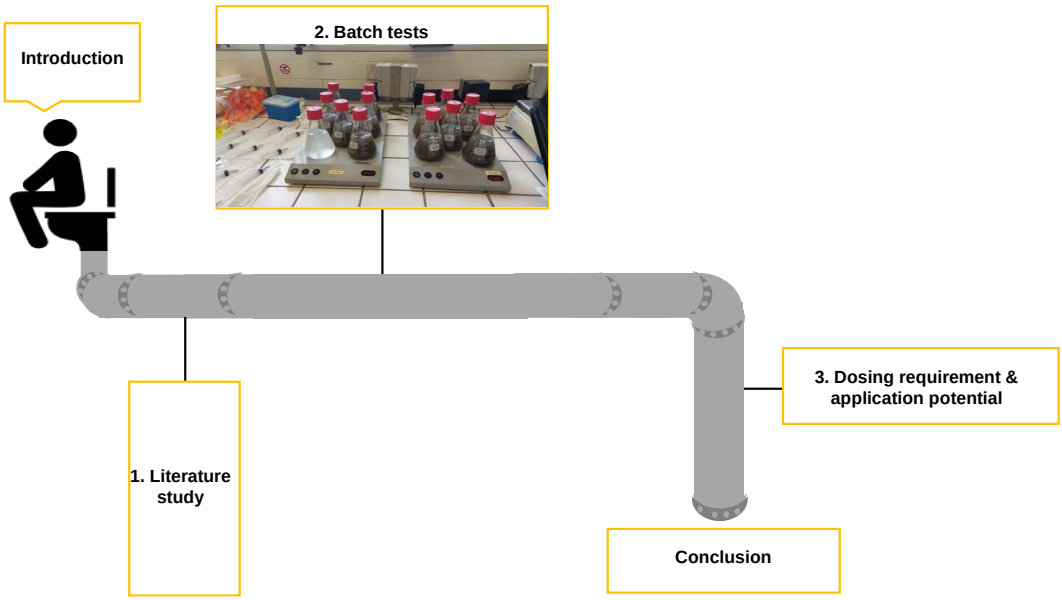


*Figure 0: Structural overview of the Thesis.*

# 1.Literature study

## 1.1 Down the drain or up the chain? The future of wastewater

Imagine a future where every drop of clean water and every nutrient it carries is as valuable as oil. In this vision, cities no longer view wastewater as a problem to be treated but as a resource to be mined. This future is approaching as growing global population drives up the demand for food, water, and energy at an unprecedented pace. Today's wastewater treatment plants (WWTPs) are the center of this challenge (H. Wang et al., 2021).

According to World Health Organisation (2024) safe water, sanitation and hygiene could have prevented 1.4 million deaths. This was equal to approximately 3.7 deaths per 100,000 population in high-income countries, and 41.7 deaths per 100,000 population in low-income countries. However, from 2015 till 2022, 902 million people gained access to safely managed sanitation. But significant gaps remain, particularly in rural and undeserved regions, where WWTPs often cannot meet local needs.

To build a more sustainable future, society must rethink its approach to wastewater management. Traditional methods are proving inadequate for the growing pressures of the 21$^{st}$ century. Among these challenges is the intensifying impact of climate change, which leads to extreme weather events such as heavy rainfall and prolonged droughts. These fluctuations dilute or concentrate the wastewater streams, complicating treatment processes and significantly increasing operational costs to adapt to these irregular and extreme events (European Environment Agency, 2019).

Other emerging problems are expanding infrastructure needs in urban and rural areas, the emergence of new pollutants requiring innovative treatments, rising energy costs, and the looming scarcity of clean water and resources. These issues lead to unwanted outcomes such as eutrophication due to limited nutrient treatment/ recovery (N, P), sewer corrosion, GHG emissions, and malodors (European Environment Agency, 2019). While conventional WWTPs were effective of their time, they are becoming outdated in an era of accelerating environmental and social demands.

### 1.1.1 From cities to countryside: centralization, decentralization, and source separation

In Flanders, where the average family (2.3 people) consumes around 89 L/p/d, most water is consumed for showering (26%), toilet- (19%) and washing machine use (16%) (VMM, 2024). Domestic wastewater consists of two main streams: blackwater (toilet waste) and greywater (from kitchens, bathrooms, laundry), with greywater comprising 73% of the total. These streams vary with habits, weather, and household behaviors (Udert & Lienert, 2013; J. Xu et al., 2023). Centralized treatment of combined streams increases the WWTP workload, energy use, and operational costs. To address this, decentralized systems present a promising solution. Decentralized systems treat wastewater closer to its source, offering greater flexibility. They enable tailored treatment approaches that improve efficiency while reducing energy and costs.

By minimizing the need for large, long pipes – especially in (dense) urban areas or (remote) rural areas - they also enhance resource recovery and lower environmental impact (Libralato et al., 2012; Otterpohl et al., 2004). However, in regions where centralized treatment infrastructures already exist, the cost per unit volume water treated remains competitive. Transitioning to full decentralization would require significant modifications to existing infrastructure, and since decentralized treatment plants process lower water volumes, the overall shift becomes more expensive due to the need for additional facilities and alignment with current networks (Libralato et al., 2012; Maurer et al., 2005). This creates an economies of scale bottleneck, sparking growing interest in solutions that can be integrated into existing infrastructure.

A related innovation is source separation, which involves separating waste streams, (*e.g.*, blackwater and greywater). By isolating blackwater, rich in N, P and K, WWTPs can focus on recovering these valuable nutrients. This approach helps to close the loop in water, energy, and resource cycles while reducing both operational and environmental burdens (Terpstra, 1999; J. Xu et al., 2023).

Urine, though only present as a mere 1% of the total wastewater, is particularly promising, as it contains 80% of the nitrogen in domestic wastewater (Fittschen & Hahn, 1998). Recycling the 30 MT of nitrogen excreted in urine globally each year could significantly reduce the 120 MT required for industrial fertilizer production.

This would reduce reliance on the Haber-Bosch (HB) process, lowering the overall energy demand for the production of synthetic fertilizers. However, market demand and consumer acceptance for such fertilizers remains negligible, limiting its environmentally beneficial potential (Larsen et al., 2021; Team Economie en Nematoden et al., 2020).

An alternative approach is the nitrification of source-separated urine and its dosing into the sewer system, offering a hybrid solution. By dosing nitrified urine into the sewer system where sufficient chemical oxygen demand (COD) is already present, a decentralized pretreatment of wastewater occurs before reaching the centralized WWTPs. This approach reduces the workload and energy demands of centralized facilities while utilizing existing infrastructure. By sidestepping the high costs and potential disruptions associated with fully decentralized systems, it offers a practical and integrative strategy for improving overall wastewater management.

## 1.2 Challenges in the sewer: biological odor and GHG formation

Sewer systems, while holding potential for pre-treatment, present significant challenges due to their complex network of pipes that create diverse microenvironments. These environments support a wide range of microorganisms, some of which contribute to the formation of problematic compounds like methane (a potent greenhouse gas) and hydrogen sulphide (a major contributor to bad odors and infrastructure corrosion). These byproducts not only affect air quality but also have a detrimental impact on the long-term sustainability of sewer infrastructure. Understanding the biological mechanisms driving their formation is crucial for developing effective control strategies.

### 1.2.1 Methane production in the sewer system

$CH_4$ in sewer systems is primarily produced through methanogenesis, an anaerobic respiration process carried out by methanogenic archaea (MA). These organisms are obligate anaerobes and strict methane producers. Organic pollutants in sewer systems are degraded into volatile fatty acids (VFAs), $CH_4$, and carbon dioxide ($CO_2$).

In rising mains, the $CH_4$ formed in the wastewater can transfer from the aqueous to the gaseous phase, particularly in places where pressure drops occur. Then $CH_4$ is vented into the atmosphere, where it may undergo aeration.

This $CH_4$ stripping also occurs when wastewater is discharged into the WWTPs. $CH_4$ has an 12 year atmospheric lifespan and global warming potential (GWP) of 21-23 (Guisasola et al., 2008). In addition to its environmental impact, $CH_4$ production by MA leads to a significant loss of soluble COD, which can negatively affect biological nutrient removal processes at WWTPs. Therefore, controlling $CH_4$ emissions is crucial, not only to mitigate its contribution to global warming and its influence on biological WWT, but also due to associated health and safety risks. Uncontrolled $CH_4$ release might lead to sewer explosion, even at low concentrations (Guisasola et al., 2008).

### 1.2.2 Sulphur in the sewer system

Sulphur is a key player in the sewer chemistry, primarily existing as sulphate in domestic wastewater. According Paing et al. (2000) and Kalogo & Verstraete (1999), sulphate concentrations typically range from 40 to 200 mg/L in the sewer. While high sulphate levels itself do not impose direct harm on health and environment, its reduced form causes bad odors, biogenic corrosion of equipment, and blockage within pipelines (Guisasola et al., 2008; G. Jiang et al., 2015; Jimenez et al., 2015; Libralato et al., 2012; Park et al., 2014). To mitigate odors it is necessary to reduce the $H_2S$ concentration below 0.5 ppm $H_2S$ (Weissenberger, 2002). Also, Despot et al. (2022) stated that to mitigate corrosion to a rate of 10 mm/a, it must be kept below 3 ppm. Figure 1.1 illustrates key speciation and transformations, highlighting pathways of reduction, oxidation, and the interplay between chemical and biological processes.

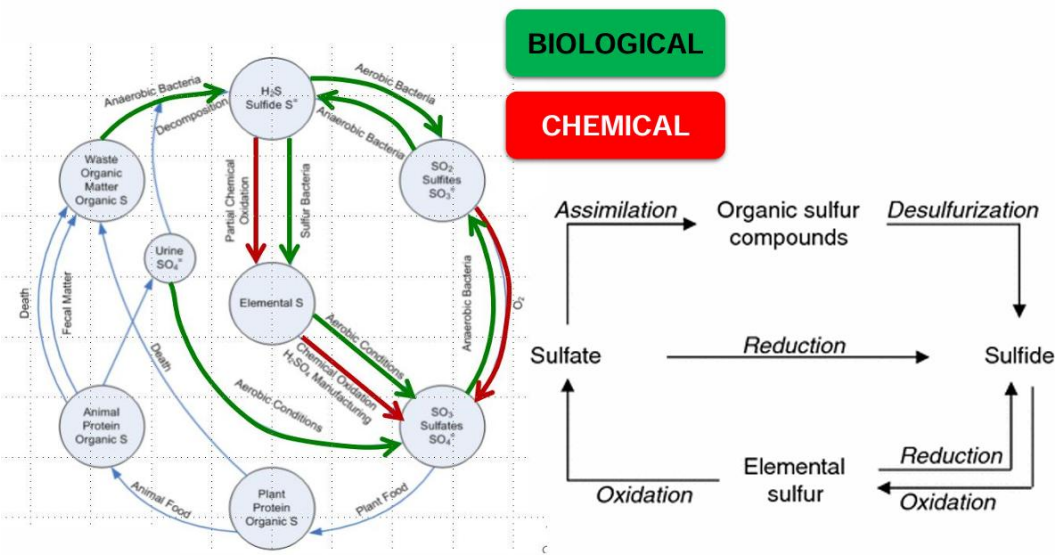


*Figure 1.1: Sulphur speciation and reactions, both biological (green) and chemical (red) (Figure taken from Horemans (2023)).*

#### 1.2.2.1 Sewer corrosion

The presence of $H_2S$, in the sewer contributes to several undesirable effects. One of these effects is sewer corrosion, resulting in a substantial annual costs worldwide. For instance, annual maintenance of affected sewer infrastructure in Germany costs approximately € 100 billion, and in Flanders (Belgium) € 5 million, representing around 10% of the region's wastewater collection and treatment expenses. In Los Angeles, ± 10% of sewer pipes suffer from notable corrosion, requiring an estimated € 5 million annually for rehabilitation. The corrosion severity depends on the numerous parameters like $H_2S$ concentration in the wastewater, and piping material. Minor corrosion occurs at sulphide levels of 0.1-0.5 mg S/L, whereas severe corrosion is observed at ≥ 2 mg S/L. In sewers in Bruges (Belgium), severe corrosion rates were found (1.1-1.8 mm/y) (G. Jiang et al., 2015; L. Zhang et al., 2008).

#### 1.2.2.2 Biogenic formation of $H_2S$ in the sewer system by sulphate-reducing bacteria

Biological sulphate reduction to $H_2S$ occurs trough the activity of sulphate-reducing bacteria (SRB), particularly in biofilms and sediments under anaerobic conditions in submerged parts of sewer systems. However, SRB and MA compete for the same electron donors, creating a stratified biofilm structure (G. Jiang et al., 2015; Jin et al., 2018; J. Sun et al., 2014). SRB inhabits the outer layers (0-300 µm), and MA the inner layer (> 200 µm), highlighting the importance of taking their interaction into account when evaluating biogenic sulphide production (Figure 1.3) (J. Sun et al., 2014, 2015)**.** $H_2S$ production occurs in pressure pipes and sediments of gravity pipes, in (almost) complete absence of oxygen. In pressure pipes, this can be described by the Hvitved-Jacobsen model (Equation 1) (Coördinatiecomissie Intergraal Waterbeleid, 2014).

$$\Delta H_2S = k \cdot \sqrt{COD_f - 50} \cdot \frac{A}{V} \cdot HRT \cdot 1.07^{(T-20)}$$

*Equation 1: Rising sulphide in pressure pipes. With k = sulphide formation speed [g S/ $m^2h^1$], A = inner wall surface of the pressure pipes [$m^2$], V = volume of the pressure pipes [$m^3$], HRT = hydraulic retention time [h], T = temperature of the wastewater [°C] and $COD_f$ = chemical oxygen demand of the filtered sample [mg/L] (Equation taken from Coördinatiecomissie Integraal Waterbeleid (2014)).*

SRB oxidize low-molecular-weight substrates, like ethanol, to acetic acid salts (incomplete oxidation) or $CO_2$ (complete oxidation) while reducing sulphate (L. Zhang et al., 2008; Z. Zhang et al., 2022). This process primarily reduces sulphate to $H_2S$, although elemental sulphur ($S^0$) can also form under certain conditions.

### 1.2.2.3 Sulphuric acid formation by sulphur oxidizing bacteria (SOB)

Sewer corrosion primarily occurs in gravity pipes due to transfer of $H_2S$ into the gas phase (Figure 1.3). Among these compounds, only $H_2S$ can move across the air-water interface. However, $H_2S$ emissions are influenced by several parameters: temperature, water flow conditions, ventilation in the air phase and pH. The speciation of $H_2S$ is highly pH-dependent (Figure 1.2). In sewage (pH 7.5-9.5), both $HS^-$ and $H_2S$ are the predominant and bioavailable forms of sulphide (Horemans, 2023; Phscale Core Team, 2024; L. Zhang et al., 2008).

$$H_2S \leftrightarrow H^+ + HS^-, pK_{a1} \sim 7.04 \ (1)$$

$$HS^- \leftrightarrow H^+ + S^{2-}, pK_{a2} \sim 11.96 \ (2)$$

$$H_2S_{(aq)} \leftrightarrow H_2S_{(g)}, \ k_c \sim 468^1 atm \ (x)^{-1} \ (3)$$

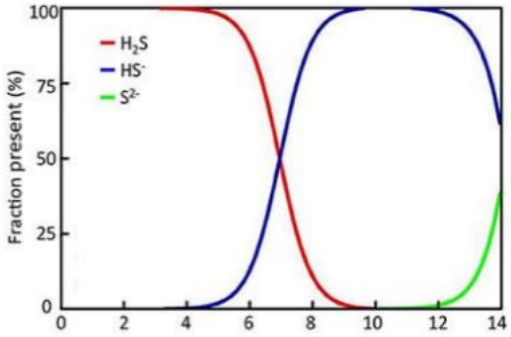


*Figure 1.2: Speciation of $H_2S$: reactions (left) (1) dissociation of $HS^-$, (2) dissociation of $S^{2-}$, (3) transfer across the air-water interface, with x the mole fraction; (right) pH dependence of sulphur speciation (Figure taken from Zhang et al., 2008; Horemans, 2023).*

When $H_2S$ enters the sewer gas phase, it diffuses into the thin, liquid aerobic biofilm on the sewer surface. Here, sulphur-oxidizing bacteria (SOB), chemoautotrophic organisms, oxidize sulphide to sulphuric acid in the presence of oxygen, as illustrated in Figure 1.3. This biogenic sulfuric acid reacts with the concrete of the sewer pipes, converting it into gypsum and ettringite (an expansive compound). As this corrosive layer thickens and penetrates further into the concrete, structural damage exposes more surface area, accelerating acid penetration and further weakening the sewer pipes' structural integrity, which can ultimately lead to their collapse (Horemans, 2023; G. Jiang et al., 2015).

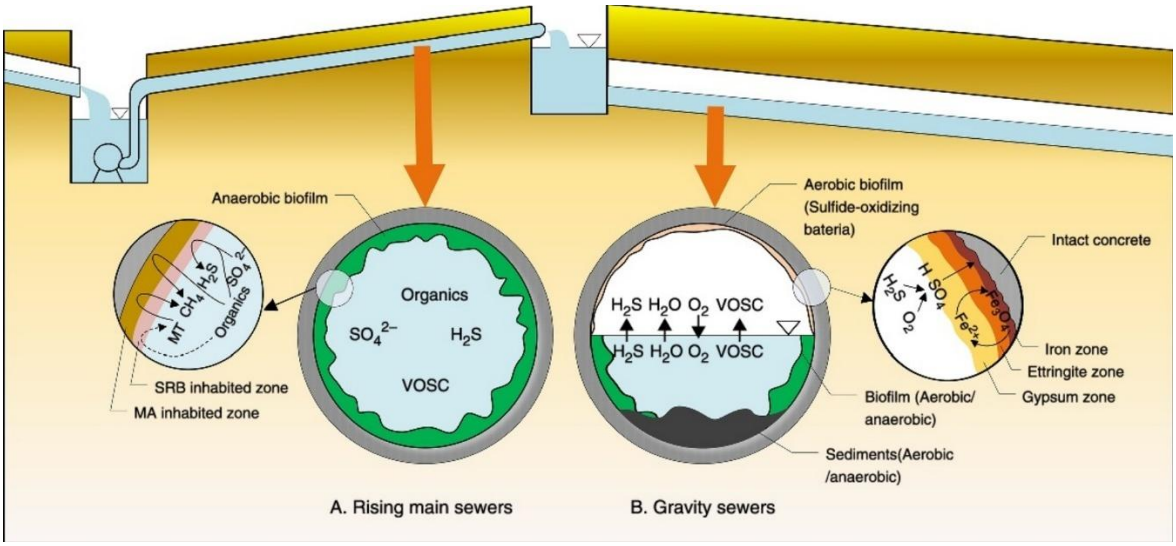


*Figure 1.3: Biogenic sulphate reduction by sulphate-reducing bacteria (SRB) in rising main (A) and sewer corrosion through sulphur-oxidizing bacteria (SOB) in the biofilm wall of the aerated zone in gravity main (B) (Figure taken from Jiang et al. 2015).*

## 1.3 Factors influencing biological pathways for $CH_4$ and odorous compounds, inconvenient products within the sewer

Several factors influence biological pathways for methane and sulphur-related compounds within the sewer systems, including the type of sewer system (gravity pipes or pressure pipes). Each system type has distinct operational characteristics that affect microbial interactions and the dynamics of sewer biofilms (W. Li et al., 2019).

### 1.3.1 Influence of system type

#### 1.3.1.1 Gravity Pipes (Gravity Mains)

Gravity sewer systems rely on the downward slope of pipes to move wastewater from households to the WWTP without mechanical pumping (Figure 1.4). This flow requires a sufficient speed to prevent scaling of debris and solid buildup. These systems could be preferred in areas with suitable terrain (not hilly or flat), as they are more energy-efficient and easier to maintain compared to pressure systems (Coördinatiecomissie Intergraal Waterbeleid, 2014; Muller, 2024).

#### 1.3.1.2 Pressure pipes (Rising Mains)

Pressure mains, on the other hand, use mechanical pumps to move wastewater through pipes, making them less energy efficient (Figure 1.4). A small pump is typically installed for each household or cluster of households.

Pressure mains are often used in specific situations, such as when pipes need to be installed at great depths, in areas with flat or hilly landscapes, or when there is a large distance between buildings, making gravity flow impractical. Due to the constant pressure in the system, pressure mains are less prone to sedimentation compared to gravity mains, as faster flow rates help keep solids suspended within the wastewater (Coördinatiecomissie Intergraal Waterbeleid, 2014; Muller, 2024).

#### 1.3.1.3 Distribution in Flanders by Aquafin

According to G.Wellens, personal communication (18 September 2024), based on the 'Afvalwater Informatie Systeem' (AWIS) sewer inventory, Flanders has approximately 53,000 km of gravity mains and only 1,850 km of pressure mains. This distribution suggests a preference for gravity mains, though the choice depends on topography and infrastructure needs. Where gravity mains are unsuitable, pumping stations are used to move wastewater. Given their widespread use and unique microbial interactions influenced by the headspace environment, this research primarily focusses on gravity pipes.

### 1.3.2 Influence of sewer biofilms

#### 1.3.2.1 Sewer biofilms and microbial interactions

Sewer systems don't solely contain piping, but function as diverse ecosystems, hosting both eukaryotic organisms (*e.g.*, protozoa, fungi and mammals) and prokaryotes, primarily bacteria and archaea. These microorganisms are categorized into planktonic organisms and those forming biofilms at the sewer system interfaces. Their metabolic activity is influenced by the availability and quantity of carbon sources and the electron acceptors present (oxygen, nitrate, and sulphate) (Augustyniak et al., 2021).

Biofilms consist of diverse microbial communities embedded in an extracellular polymeric substance (EPS) matrix. The EPS contains of 25% proteins, 16% humus, and 7% polysaccharides, along with nucleic acids, and fatty acid supporting specific microorganisms (Augustyniak et al., 2021; Jahn & Nielsen, 1998; W. Li et al., 2019). In sewers, biofilms are either submerged or unsubmerged. Submerged biofilms form as floating microorganisms that settle on pipe surfaces, grow, and mature over months. As they age, they may detach, releasing planktonic and dispersed cells back into the flow (Chua et al., 2014).

In contrast, unsubmerged biofilms develop in areas with higher dissolved oxygen (DO) and are not subjected to the flushing action of sewage (W. Li et al., 2019).

Biofilms play a crucial role in pre-treating organic and nitrogen pollutants, reducing the pollutant load before wastewater enters the WWTPs. The biofilm matrix offers protection from antimicrobials, regulates macromolecule penetration, and reduces shear stress. Throughout the sewer, the microbial community undergoes changes in response to changing environments (Augustyniak et al., 2021; Verma et al., 2023).

#### 1.3.2.2 Impact on biofilm formation and greenhouse gas emissions

In the sewer, wastewater contains a significant portion of biodegradable organic compounds, typically measured as biological oxygen demand (BOD). These serve as a food source for microorganisms, promoting their degradation. As these microorganisms consume organic matter, the oxygen levels in the sewer decrease, creating more anoxic and anaerobic processes. In turn, these conditions lead to the production of GHGs such as $CH_4$ and $N_2O$, as well as odorous compounds like $H_2S$ (Augustyniak et al., 2021; Guisasola et al., 2008; Park et al., 2014). However, the extent of oxygen depletion, biofilm formation, and GHG production differs between gravity and pressure sewer systems in their hydraulic characteristics.

#### 1.3.2.3 Oxygen availability and reaeration

One of the key factors influencing microbial activity and GHG emissions in sewer systems is the oxygen availability. DO levels decrease with biofilm depth, creating gradients that lead to distinct microbial habitats. According to Hvitved-Jacobsen et al. (2013), gravity sewers generally offer better reaeration than pressure sewers. This is because gravity sewers typically have gaseous headspace above the wastewater, allowing easier oxygen exchange between the sewer atmosphere and the flowing wastewater. In contrast, pressure sewers lack this headspace, resulting in more anaerobic conditions and consequently, more pronounced anaerobic sewer biofilm formation (Hvitved-Jacobsen et al., 2013; W. Li et al., 2019).

Ventilation also plays an crucial role, as poorly ventilated gravity sewers (DO < 5 mg $O_2$/L) tend to develop a more anaerobic sewer biofilm (Jin et al., 2018; W. Li et al., 2019). The variation in microbial biofilm composition and their DO levels are illustrated in Figure 1.4.

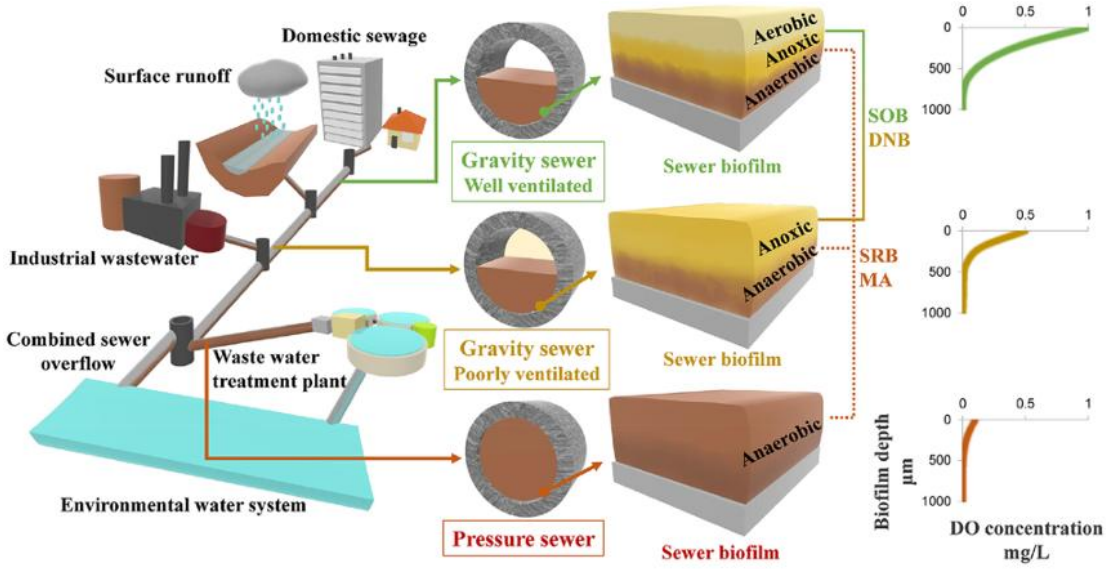


*Figure 1.4: Graphical overview of the microbial biofilm composition in gravity and pressure sewers. MA = methanogenic archaea, SOB = sulphur oxidizing bacteria, DNB = denitrifying bacteria, and SRB = sulphate reducing bacteria, as well as their corresponding DO gradient with varying biofilm depth (Figure taken from Li.W. et al., 2019).*

#### 1.3.2.4 Shear stress and biofilm formation

Another important factor influencing biofilm development is the shear stress, being the force exerted by the flowing wastewater on the walls of sewer pipes. This is related to the slope and hydraulic radius of gravity sewers ((Duque et al., 2022; W. Li et al., 2019).

Biofilm formation in the sewer is promoted under low shear stress conditions, such as those found in flat or slow-flowing sections of the sewer, which accelerate clogging of the sewer and reduced sewer capacity over time (Möhle et al., 2007; S. Wang et al., 2022; T. Wang et al., 2020). On the other hand, when shear stress increases, typically in steeper or more hydraulically efficient systems, it can lead to reduced biofilm porosity, lower oxygen uptake rates, and decreased COD removal (Li W. *et al.,* 2019).

##### 1.3.2.4.1 Impact of low shear stress in gravity versus pressure sewers

In gravity sewers, low shear stress is often observed in areas with insufficient slope or irregular flow patterns. These conditions promote the accumulation of sediments and growth of anaerobic biofilms, which can exacerbate the production of odorous compounds and GHGs (Guisasola et al., 2008; Hvitved-Jacobsen et al., 2013; L. Zhang et al., 2008). In pressure sewers, where the flow is generally more uniform, low shear stress can still occur whereas flow velocities are insufficient, leading to similar issues with biofilm formation and sediment buildup (Hvitved-Jacobsen et al., 2013).

## 1.4 Mitigation options for $H_2S$ and $CH_4$ production in the sewer

Among the various techniques to mitigate $CH_4$ and $H_2S$ emissions in sewers, biological nitrate dosing stands out as one of the most comprehensive approaches. As shown in Table 1.1, nitrate promotes anoxic conditions that suppress anaerobic microbial activity, thereby inhibiting both sulphate-reducing bacteria (SRB) and methanogens (MA). This dual action enables the simultaneous reduction of odor ($H_2S$) and greenhouse gas emissions ($CH_4$), while also promoting denitrification and sulphur oxidation. Unlike chemical precipitating agents such as ferric chloride, which remove sulphide after its formation, nitrate acts preventively at the microbial level. This helps avoid the formation of sulphide-rich biofilms and adds the co-benefit of nitrogen removal. However, challenges such as sulphide rebound after nitrate depletion and potential nitrite or $N_2O$ formation during incomplete denitrification remain.

Despite these drawbacks, nitrate dosing provides a strong balance of efficacy and added value. Other techniques often fall short: oxygen injection is expensive; electrochemical oxidation is still emerging; sediment flushing requires maintenance and is less effective in sewers with deep sediments; and air ventilation mainly targets gaseous components, which promotes $H_2S$ transfer to the headspace, increasing odors. Compared to these, nitrate dosing offers a more integrated solution with multiple environmental benefits (Table 1.1).

While nitrate dosing offers clear technical advantages over other mitigation strategies, its practical implementation remains limited in certain regions. In Flanders, for instance, its high cost has hindered widespread adoption, leading to the continued use of ferric chloride despite its drawbacks: high dosage requirements, clogging risks, and the absence of nitrogen removal (Haaningnielsen et al., 2005; G. Jiang et al., 2010; Mohanakrishnan et al., 2009). More broadly, chemical dosing strategies depend on a continuous supply of non-renewable resources, limiting their long-term sustainability.

A promising alternative is nitrified urine, a renewable nitrogen source that can replace synthetic nitrate. This enables the benefits of chemical nitrate dosing, while lowering costs and supporting a circular wastewater strategy. When coupled with controlled dosing and monitoring, biological nitrate dosing emerges as a highly effective and future-proof option for managing sewer emissions.

*Table 1.1: Overview of techniques reducing $CH_4$ and $H_2S$ in sewers, alongside their (dis)advantages.*

| Technique | Compound/ pathway | Principle | Advantages | Disadvantages | Sources |
|---|---|---|---|---|---|
| **Chemical dosing ($NO_3^-$)** | $H_2S$, SRB, $CH_4$ | Nitrate promotes anoxic conditions resulting in the suppression of anaerobic pathways (*e.g.*, MA and SRB) | Promotes denitrification; reduces odor; readily available | High cost; Risks including $NO_3^-$ overloading, $NO_2^-$ and $N_2O$ accumulation from incomplete denitrification, and sulphide rebound after depletion | (Auguet et al., 2015; G. Jiang et al., 2010; Mohanakrishnan et al., 2009) |
| **Intermittent sediment flushing** | $H_2S$, $CH_4$ | Removes organic-rich sediments that serve as substrate for anaerobic microbial activity. Thereby reducing gas production. | Effective $H_2S$ and $CH_4$ reduction; low cost; carbon source retention; | Limited for deep sediments; frequent maintenance | (Ren et al., 2022) |
| **Iron salts (*e.g.*, $FeCl_3$)** | $H_2S$, $CH_4$ | Ferric iron forms insoluble FeS precipitates, removing $H_2S$ from the system. | precipitates sulphides; effective $H_2S$ control | High costs, high dosages; potential downstream effects (sulphide rebound after nitrate depletion) | (Haaningnielsen et al., 2005; L. Zhang et al., 2009) |
| **Oxygen injection** | $H_2S$, SRB, $CH_4$ | Injecting oxygen creates aerobic conditions. Oxidizes $H_2S$ (aq), and inhibits SRB and MA. | Inhibits anaerobic conditions (SRB, $CH_4$) | Expensive; may increase biofilm growth | (Gutierrez et al., 2008; G. Jiang et al., 2015) |
| **Air ventilation** | $H_2S$, $CH_4$ | Facilitates gas exchange between sewer atmosphere and outside air, reducing gas accumulation and anaerobic zones. | Reduces anaerobic sewer gases; cheaper than $O_2$ injection | Ineffective for dissolved components; nearby air release causes issues (odors, etc.) | (R. Gao et al., 2020; Talaiekhozani et al., 2016) |
| **Electrochemical oxidation** | $H_2S$ | Applies electric current to oxidize dissolved sulphide to $S^0$/ $SO_4^{2-}$ (without chemicals). | Energy efficient; avoids chemical transport | High initial cost; still in early stages | (Lin et al., 2015; Pikaar et al., 2012, 2019) |

## 1.5 $H_2$Oh! Nitrified urine for resource-efficient water treatment

### 1.5.1 Biological pathways for nitrogen removal from urea

Daily, humans produce approximately 1270 g urine, containing around 15 grams of nutrients (N, P, K) per person per day. Urine also contributes to nearly two-third of the pharmaceuticals and hormones found in wastewater (Gundlach et al., 2021; Randall & Naidoo, 2018). Figure 1.5 illustrates the biological conversion of urea to $N_2$. In fresh urine, ~85% of nitrogen is in urea form, which is hydrolysed to ammonium via urease during storage. This ammonium is then converted to $N_2$ through nitrification and denitrification (Mazzei et al., 2020; Randall & Naidoo, 2018).

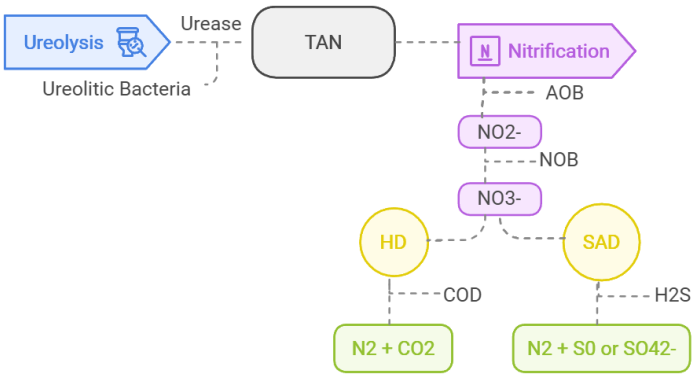


*Figure 1.5: Graphical overview of the pathways involved in urea conversion to $N_2$. With HD being heterotrophic denitrification and SAD sulphide-driven autotrophic denitrification.*

#### 1.5.1.1 Nitrification

Nitrification is a two-step biological oxidation of ammonia to nitrate, performed by ammonia-oxidizing (AOB) and nitrite-oxidizing bacteria (NOB). Both use $CO_2$ as a carbon source and derive energy from inorganic compounds in the presence of oxygen (Soliman & Eldyasti, 2018; Udert & Jenni, 2013). AOB convert ammonia to $NO_2^-$ via nitritation, then NOB rapidly oxidize $NO_2^-$ to $NO_3^-$.

#### 1.5.1.2 Denitrification

Nitrate, the end product of complete nitrification, is a widespread contaminant that poses risks to both human health and the environment. To mitigate these risks, regulatory standards limit nitrate concentrations to ≤ 5 mg Total nitrogen (TN)/L (European Parliament, 2023). Denitrification offers an approach to meet this standard (Di Capua et al., 2019). Denitrification is the process by which $NO_3^-$ is reduced to $N_2$ in the absence of oxygen.

Not only is this biological nitrogen removal method frequently used in daily WWT for both industrial and domestic wastewater, but it is also the main topic of this thesis. Denitrifying microorganisms, primarily facultative aerobes like *Nitrospira* and *Thiobacillus denitrificans* (Smets, 2024). The reduction of $NO_3^-$ is catalyzed by four nitrogen reductase enzymes: (1) Nitrate reductase (Nar), (2) nitrite reductase (Nir), (3) nitric oxide reductase (Nor) and lastly nitrous oxide reductase (Nos). This cascade results in intermediate gaseous forms such as nitric oxide and $N_2O$ (Reaction 1).

If denitrification is incomplete due to substate limitations, inhibition or imbalances within microbial community, these intermediates may accumulate. This could result in $N_2O$, a potent GHG, being released into the atmosphere (Di Capua et al., 2019; Udert & Jenni, 2013; Zumft, 1997).

$$NO_3^- \xrightarrow[2e^-]{Nar} NO_2^- \xrightarrow[1e^-]{Nir} NO \xrightarrow[1e^-]{Nor} \frac{1}{2}N_2O \xrightarrow[1e^-]{Nos} \frac{1}{2}N_2$$

*Reaction 1.1: Complete denitrification cascade with reductase enzymes and electron flow per step. Nar = nitrate reductase, Nir: nitrite reductase, Nor: nitric oxide reductase and Nos: nitrous oxide reductase.*

Recent studies suggest denitrification is not exclusively performed by complete denitrifiers. Instead, it can happen through a consortium of partial denitrifiers as well, each specializing in one or a few steps of the process. This division of metabolic labor appears to be the dominant strategy in complex environments, such as soil and WWTPs, where microbial diversity is high and resource availability fluctuates. In contrast, complete denitrifiers are more prevalent in controlled laboratory conditions with stable substrate availability (Roothans et al., 2025).

Denitrification requires an electron donor (organic or inorganic). The type depends on the type of denitrifier. Currently, two main groups of denitrifying microorganisms are recognized: heterotrophic (HD) and autotrophic (AD) denitrifiers (Kleerebezem & Mendezà, 2002; Knowles, 1982; Metcalf & Eddy, 2014). The denitrification rate depends on donor concentration, pH, microbial affinity, hydrophilicity, particle size, and temperature (Di Capua et al., 2019). It can occur over a wide temperature range (5-60°C). The optimal pH for denitrification is 7-8 (Metcalf & Eddy, 2014; Smets, 2024).

A variant of denitrification, denitritation, uses nitrite ($NO_2^-$) as electron acceptor. This pathway requires fewer resources, such as COD. However, high nitrite levels can be inhibitory, potentially leading to nitrous oxide and $N_2O$ emissions (Udert & Jenni, 2013).

## 1.5.2 Nitrate/ nitrified urine removal pathways in the sewer system

### 1.5.2.2 Heterotrophic denitrification

Heterotrophs, also known as chemoorganoheterotrophs, constitute the majority of denitrifiers. As their classification suggests, these organisms obtain energy from chemical compounds and utilize organic compounds (mainly short-chain fatty acids) as both electron donors and carbon sources (Smets, 2024; H. Wang et al., 2021). Heterotrophic denitrification reactions are shown in Reaction 1.2 (Fu et al., 2022; Metcalf & Eddy, 2014). Denitritation requires only 1.71 g acetate-COD/ g N compared to 2.86 g acetate-COD/ g N for denitrification (Udert & Jenni, 2013).

$$3\ CH_3COOH + 8\ NO_2^- + 8\ H^+ \rightarrow 4\ N_2 + 6\ CO_2 + 10\ H_2O \quad (1)$$

$$5\ CH_3COOH + 8\ NO_3^- + 8\ H^+ \rightarrow 4\ N_2 + 10\ CO_2 + 14\ H_2O \quad (2)$$

*Reaction 1.2: Complete denitritation (1) and complete denitrification (2) of acetic acid.*

Heterotrophic denitrifiers exhibit higher biomass yields (0.8-1.2 g volatile suspended solids (VSS)/ (g $NO_3$-N)) than autotrophs (0.74 or 0.61 g VSS/ (g $NO_3$-N) using $S^0$ or sulphide as electron donor, respectively (Campos et al., 2008; Di Capua et al., 2019).

### 1.5.2.3 Autotrophic denitrification (sulphide-driven)

Autotrophs (chemolithoautotrophs), derive energy from inorganic compounds, such as hydrogen gas, sulphur compounds, pyrite, thiocyanate, arsenic and ferrous iron. The kinetics of autotrophic processes strongly depend on the electron donor choice (Di Capua et al., 2019; Metcalf & Eddy, 2014). They must allocate more energy to biosynthesis (Di Capua et al., 2019; Metcalf & Eddy, 2014). Despite their slower growth rates and lower biomass yields, their application remains attractive. In conventional WWTPs that rely on HD, the addition of external organic carbon is necessary to satisfy microbial demands, leading to increased sludge production and possible toxic organic compound formation during chlorination, like trihalomethanes (Di Capua et al., 2019).

This thesis focuses on sulphide-driven autotrophic denitrification (SAD). Sulphide, referred to as total dissolved sulphide (TDS = $HS^-$ + $H_2S$ + $S^{2-}$), serves as an inexpensive electron donor capable of achieving complete nitrate removal under anoxic conditions. But, as mentioned before, under typical sewage conditions (pH 7.5-9.5) both $HS^-$ and $H_2S$ are the predominant and bioavailable forms of sulphide (Phscale Core Team, 2024).

A key objective of this work is to mitigate the formation of bad odors and harmful products, such as $H_2S$, which can be achieved through the SAD process. The SAD process involves two key mechanisms (Reaction 1.3): partial SAD (4) and short SAD (3), both of which reduce nitrate to $N_2$ (Wang et al.,2023). However, (5) and (6) demonstrate partial oxidation of sulphide with nitrite accumulation. Other sulphur sources can be used as electron donors, including $S^0$ (7) and thiosulphate ($S_2O_3^{2-}$) (8) (Ren et al., 2022). If complete denitrification to sulphate occurs depends on the physiological conditions (Cardoso et al., 2006).

$$S^{2-} + 1.6\,NO_3^- + 1.6\,H^+ \rightarrow SO_4^{2-} + 0.8\,N_2 + 0.8\,H_2O \quad (3)$$

$$S^{2-} + 0.4\,NO_3^- + 2.4\,H^+ \rightarrow S^0 + 0.2\,N_2 + 1.2\,H_2O \quad (4)$$

$$S^{2-} + 4\,NO_3^- \rightarrow SO_4^{2-} + 4\,NO_2^- \quad (5)$$

$$S^{2-} + 0.4NO_3^- + 2\,H^+ \rightarrow S^0 + NO_2^- + H_2O \quad (6)$$

$$S^0 + 1.2\,NO_3^- + 0.4\,H_2O \rightarrow SO_4^{2-} + 0.6\,N_2 + 0.8\,H^+ \quad (7)$$

$$S_2O_3^{2-} + 1.6\,NO_3^- + 0.2\,H_2O \rightarrow 2\,SO_4^{2-} + 0.8\,N_2 + 0.4\,H^+ \quad (8)$$

*Reaction 1.3: Complete sulphide-driven autotrophic denitrification (SAD) (3 and 5) and incomplete SAD (4 and 6), denitrification using $S^0$ (7) and thiosulphate (8) as electron donor.*

Yuan et al (2019) demonstrated that under anoxic conditions, the rate of $S^{2-}$ oxidation to $S^0$ is approximately 3.31 times higher than the subsequent oxidation of $S^0$ to $SO_4^{2-}$. This is also supported by Dolejs et al.(2015).

#### 1.5.2.4 Mixotrophic denitrification

In addition to HD and AD, mixotrophic denitrifiers exist as well. These organisms can use both inorganic and organic sources to wield their energy for metabolic processes (*e.g.*, *Paracoccus* and *Pseudomonas*). The metabolic pathway for mixotrophic denitrification is shown in Figure 1.6, but are not studied within the scope of this thesis.

#### 1.5.2.5 MIXED denitrification

Instead, the focus is on the interaction between SAD and HD in MIXED conditions (both COD and sulphur as available electron donor). Research on the impact on their performance is limited, as well as the assumed synergistic and/ or competitive relation between SAD and HD (Y. Li et al., 2022; Pang et al., 2022; Q. Sun et al., 2023). Table 1.2 shows literature findings on the maximal observed nitrate removal rates in the different setups. All rates are corrected to 21°C using Arrhenius.

$$k_2 = k_1 \cdot \theta^{(T_2 - T_1)}$$

With:

$k_1$ and $k_2$ [mg $NO_3$-N/ (g VSS d)]: Denitrification rates found at the temperatures from literature, and for 21°C.

$\theta$ [-]: Temperature constant, equal to 1.04 (Shen et al., 2020).

T [°C]: Temperature.

*Table 1.2: Overview of the maximal observed nitrate removal rates. All values are corrected for temperature (21°C) using Arrhenius. The type of enrichment is the same as the row's type.*

| **Type** | **$r_{max}$ [mg $NO_3$-N/ (g VSS d)]** | **Differences** Enriched (E)/ notes | **pH** | **T [°C]** | **Sources** |
|---|---|---|---|---|---|
| **HD** | 11-740.48 | **E**; 230 mg MLSS/L | 7.7 ± 0.5 | 28.1 ± 0.5 | (F. Jiang et al., 2013a) |
| | | Acid phase digestion | 6.28 ± 0.29 | 21.0 ± 2.0 | (Elefsiniotis & Wareham, 2007) |
| | 2304 | Only 5.97% *Thauera* Low C/N | 7.0-8.5 | | (Liang et al., 2020a) |
| **SAD** | 35.37-168.56 | **E** ; 230 mg MLSS/L | 7.7 ± 0.5 | 28.1 ± 0.5 | (F. Jiang et al., 2013a) |
| | | **E**; SRB reactor; 4.54 g VSS/L | 8.0 | 30.0 ± 1.0 | (Fajardo et al., 2012) |
| | | SRB reactor ; 2.49 g MLSS/L | 8.0 | 30.0 | (S. Huang et al., 2021) |
| | | **E**; 3.0 g VSS/L | 7.0 ± 0.1 | 25.0 ± 2.0 | (Lu et al., 2018a) |
| | 577 | | 9.5 ± 0.1 | 24.0 | (Dolejs et al., 2015) |
| | 2051.04 | **E** | 7.5 | 30.0 | (Manconi et al., 2007) |
| | 72-96 | **E**; high salinity; donor: $S^0$ | 7.0-8.0 | 30.0 | (Koenig & Liu, 2004) |
| **MIXED** | 38.88-534 | Activated sludge | 7.3-7.5 | 25.0 | (Z. Xu et al., 2020) |
| | | Activated sludge, 230 mg MLSS/L | 7.7 ± 0.5 | 28.1 ± 0.5 | (Manconi et al., 2007) |
| | 225.81 | Activated sludge, 230 mg MLSS/L | 7.7 ± 0.5 | 28.1 ± 0.5 | (F. Jiang et al., 2013a) |
| | 1495.6 | Low C/N | 7.0-8.5 | | (Liang et al., 2020a) |

### 1.5.2.6 Inhibition of the in- sewer- denitrification by $H_2S$ toxicity

As mentioned before, sulphur speciation is strongly pH depended. When the pH < 6, $H_2S$, the most toxic form, becomes the most pronounced species. $H_2S$ is toxic due to its neutral charge, allowing it to pass easily through the negatively charged microbial cell membranes. Excessive levels can cause structural damage to microorganisms and lead to the deactivation of essential enzymes, ultimately disrupting metabolic activity and inactivation of the electron transport chain (D. Wang et al., 2023).

Overall, HD is more sensitive to $H_2S$ toxicity than SAD. For example, Pan et al. (2013) reported that Nos is already inhibited at 0.04-0.1 mg $H_2S$-S/L, while Nar remains unaffected even at 2.0 mg $H_2S$-S/L. While, Liang et al. (2020) observed a 50% inhibition at approximately 3.88 mg $H_2S$-S/L, with a maximum achieved inhibition of 71% at 17.43 mg $H_2S$-S/L (pH 7.5). However, Reyes-Avila et al. (2004) achieved a 42% decrease in HD at 3.76 mg $H_2S$-S/L (pH 8.3). Finding consistent data on SAD sulphur inhibition is challenging. While Lu et al (2018) reported toxicity above 200 mg S/L (pH 7) (98.4 mg $H_2S$-S/L), Cardoso et al. (2006) observed inhibition at 320 mg S/L (pH 7) (= 157.44 mg $H_2S$-S/L) . In contrast, An et al. (2010) recorded maximum SAD rates at 480 mg S/L (pH 6.8-7.2) (= 184.64- 286.61 mg $H_2S$-S/L) in oil-rich conditions.

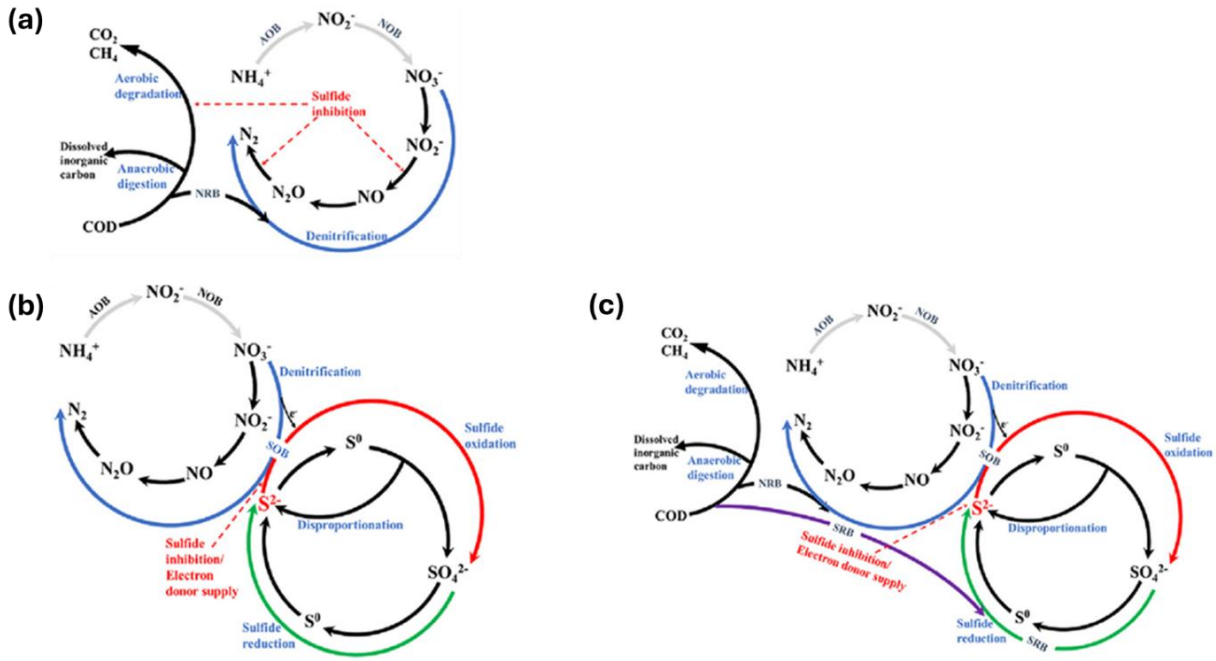


*Figure 1.6: Metabolic pathways of (a) heterotrophic denitrification, (b) autotrophic denitrification, and (c) mixotrophic denitrification. The red dashed lines show the effect of sulphide on each pathway (Figure taken from Wang et al., 2023).*

## 1.6 Dosing nitrified urine for in-sewer HD and SAD

Urine source separation enables an approach to sustainable urban wastewater management by supporting nitrogen recovery or reuse nitrate source in sewers .While using recovered nitrogen in fertilizers could reduce reliance on the Haber-Bosh (HB) process, market demand remains low. Localized systems managed by municipalities could instead reuse nitrified urine within the urban water cycle, reducing nitrogen loads and chemical dosing needs to WTTPs (Fittschen & Hahn, 1998; F. Jiang et al., 2011; Libralato et al., 2012; Oosterhuis & Van Loosdrecht, 2009; Randall & Naidoo, 2018).

Conventional nitrification-denitrification processes require high aeration energy and external carbon sources to sustain nitrate removal. Urine, which contains biodegradable organic compounds (biodegradable COD (bCOD)), offers a promising alternative. But, urine alone lacks sufficient carbon to achieve full heterotrophic denitrification (2.82 g acetate-COD/ g N), with a COD/N of 1 to 1.1 g COD/ g N in fresh urine (Faust et al., 2024; F. Jiang et al., 2013a; Udert & Jenni, 2013). Nevertheless, the high COD levels already present in the sewer could reduce external carbon dosing needs, optimizing chemical and energy use in centralized systems.

Introducing nitrified urine into sewer networks creates a favourable environment for HD and SAD, which enhances redox control and mitigates odors and GHG's. Nitrate acts as a redox buffer, inhibiting sulphate and/or $S^0$ reduction by maintaining residual nitrate within the sewer network and thereby minimizing the production of $H_2S$, a malodorous and corrosive compound. Simultaneously, SAD oxidizes sulphide to $S^0$ (incomplete) or $SO_4^{2-}$ (complete), further reducing sewer corrosion and emissions. By achieving anoxic sewer conditions, MA activity decreases as well, lowering the in-sewer methane production (Auguet et al., 2015; G. Jiang et al., 2010; Mohanakrishnan et al., 2009). Also, in $H_2S$ hotspots like rising mains and pumping stations, where HD struggles due to its sensitivity to $H_2S$, SAD is more likely to thrive. The slow-moving wastewater, anaerobic conditions, and biofilm formation within these hotspots make it an ideal environment for SRBs, but increased SAD activity can help reduce $H_2S$ production.

Furthermore, in rural areas where households are not yet connected to the sewer system, or in developing countries with an underdeveloped sewer system, nitrified urine dosage is beneficial. Here, septic tanks are used to pretreat the sewage stream (Kang et al., 2020; Withers et al., 2014).

However, these settlement chambers are hotspots for man-made GHG production due to their lack of effective electron acceptors (*e.g.*, $O_2$, $NO_3^-$). On top of that, the mainly anaerobic conditions are inefficient in reducing nitrogen loading (Gill et al., 2009). Even within this setup, nitrified urine dosage could pose a possible solution as Z. Gao et al. (2024) reported that its addition decreased emissions.

### 1.6.1 Working principle

In this part, the working principle will be clarified. (Figure 1.7).

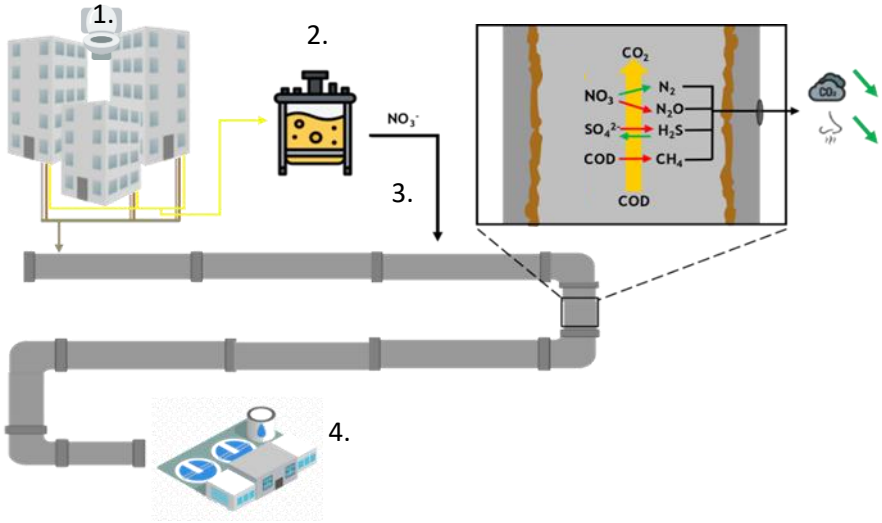


*Figure 1.7: Implication of the suggested approach in chronological order. (1) Collection and source separation of the urine stream via NoMix toilets. (2) Nitrification of the collected urine within a nitrification reactor. (3) Dosage of the nitrified urine to the urban to the urban sewer system, inducing anoxic conditions, lowering $H_2S$, $N_2O$, and $CH_4$ production (GHGs and odors). (4) Further treatment of the waste stream in the centralized WWTP.*

In the first part of the process, urine will be source separated using a NoMix toilet. Both urine (N, P) and faeces contain valuable nutrients. When combined, these nutrients are bound in sludge, requiring intensive processing for nutrient recovery. However, by separating them at the source, nutrient recovery becomes easier and more efficient.

Urine can be stored in a dedicated storage tank. But, because source-separated urine is highly unstable, stabilization is necessary. Storage tanks will be placed both before and after the nitrification reactor, then the collected urine will be nitrified. Afterwards, it will be dosed back into the sewer system. Here, interactions of HD and SAD will take place lowering GHGs and odors, causing a pretreatment. In the end, the wastewater will be collected by the centralized WWTP for further treatment.

### 1.6.2 Challenges

While economic feasibility of decentralized systems poses challenges, especially in terms of economies of scale, this strategy holds long-term potential, particularly for urban developments (Libralato et al., 2012). Retrofitting existing buildings with dual-pipe systems for source-separated urine collection is costly, and transportation of separated urine can be inefficient, especially in less densely populated regions. However, in high urbanized and densely populated areas, like Hong Kong, urine collection system may prove more efficient and therefore more viable for source separation efforts (F. Jiang et al., 2011; Randall & Naidoo, 2018).

Maintenance issues further compound these challenges. Issues such as pipe blockages from salt precipitation (*e.g.*, struvite) and odor problems, especially in waterless urinals, add operational complexity and costs. Social acceptance also poses a barrier, with public resistance to handling urine-separated systems requiring education and outreach to gain support (Randall & Naidoo, 2018). In addition, fluctuating urine flow rates can create inconsistent dosing, although buffer systems, like septic tanks, can help may mitigate this issue (Udert & Lienert, 2013). Another concern is the large amount of nitrate required to control $H_2S$ levels . As a result, this application is suitable for limited applications (in addition to other mitigating techniques) in areas with high $H_2S$ formation potential (Oosterhuis & Van Loosdrecht, 2009). Additionally, dosing nitrate/ nitrified urine can result in potential downstream effects, due to elevated sulphate levels reaching anaerobic downstream conditions when nitrate is depleted (Table 1.1).

## 1.6 Research questions, hypothesis, objectives and challenges

This thesis aims to explore HD and SAD biokinetics to estimate nitrified urine dosing requirements within the urban sewer, while understanding potential inhibitory effects on HD and the dynamics between SAD and HD in MIXED conditions. In addition to nitrate/ nitrite removal rates, sulphide oxidation rates were observed. These provide indications of SAD activity and highlight the potential to remove $H_2S$ from the sewer. A critical aspect of this research is addressing key denitrification parameters, including maximum denitrification rates ($r_{max}$), half-saturation constants ($K_s$), and inhibition constants ($K_i$), by varying sulphur-to-nitrogen ratios. These kinetic parameters provide critical insights into $NO_3^-$ removal dynamics and requirements, and inhibition.

However, limited uniform data on $K_s$ and $K_i$ (Table 1.3 a-b) hinders accurate prediction and optimization of denitrification performance.

*Table 1.3a: Literature study of half-saturation constant for nitrate, sulphide and COD in SAD and HD.*

| Compound | Heterotrophs | Autotrophs | Sources |
|---|---|---|---|
| $NO_3^-$ [mg $NO_3$-N/L] | 0.10-0.76 | 3-10 | (Abdul-Talib et al., 2002; Barker & Dold, 1997; Calise et al., 2020; DHI, 2023; S.-E. Oh et al., 2000) |
| Sulphide [mg $H_2S$-S/L] | - | 20.16; 31.20 | (Gadekar et al., 2006; Lu et al., 2018a) |
| Acetate [mg sCOD/L] | 38.1 +/- 16.2<br>0.5 | - | (Cherchi et al., 2009a; DHI, 2023) |

*Table 1.3b: Literature study of inhibitory values of important components for both autotrophic and heterotrophic denitrification.*

| Compound | Heterotrophs | Autotrophs | Sources |
|---|---|---|---|
| **$H_2S$-S** [mg $H_2S$-S/L] | IC50: 3.88 (pH 7.5)<br>IC71: 17.43 (pH 7.5)<br>IC42: 3.76 (pH 8.3)<br>$K_{H2S-NO3}$: 2.03<br>$K_{H2S-NO2}$: 11.30 | > 98.40<br>> 157.55<br>$K_{H2S-NO3}$: 118.95 | (Cardoso et al., 2006; Liang et al., 2020b; Lu et al., 2018b; Reyes-Avila et al., 2004) |
| **$SO_4^{2-}$** [mg $SO_4^{2-}$-S/L] | - | Partial: 500<br>Complete:<br>≥ 6400<br>>2000 | (S.-E. Oh et al., 2000; Peirano et al., 2020) |
| **COD** [mg $O_2$/L] | > 2000* (glucose) | >200 | (Campos et al., 2008; S.-E. Oh et al., 2000) |
| **Salts** [g NaCl/L] | IC50: 4.3 +/- 0.3 | IC50: 1.0-2.5 | (D'Aquino et al., 2023) |
| **$NO_2^-$** [mg $NO_2^-$/L] | ≥ 250 | $K_i$: 34.7<br>$K_i$: 36-60 | (Fajardo et al., 2014; S.-E. Oh et al., 2000) |
| **$NO_3^-$** [mg $NO_3^-$-N/L] | - | ≥ 660 | (S.-E. Oh et al., 2000) |
| **FA** [mg $NH_3$-N/L] | IC50: 76.31<br>$K_i$= 64.74+/- 0.02 (high strength water)<br>IC20: 16 | ≥ 53 | (X. Wang et al., 2019; Yang et al., 2018) |
| **FNA** [mg $HNO_2$-N/L] | IC40: 0.010-0.025<br>IC40: 0.020 | $K_i$: 0.7-1.0 $.10^{-3}$<br>$K_i$: 4.0 $.10^{-3}$ | (Lan et al., 2019; Zhou et al., 2007) |
| **DO** [mg $O_2$/L] | > 2.0 | Signifiant inhibition: 5.5-6.5 | (Fu et al., 2022; Kou et al., 2024) |

**not specified for heterotrophs, however, this value shows inhibition in MIXED conditions.*

### 1.7.1 Novelties and research gaps

The concepts of using nitrified urine as a nitrate source to elevate N removal efficiency, dosing nitrate to lower GHG emissions, and reduce odorous compounds, alongside leveraging biological pathways for $H_2S$ oxidation, are not entirely new (Table 1.1). However, there are significant research gaps that make this topic extremely valuable to explore. Current literature often provides varying data under different conditions, making it difficult to draw reliable conclusions. True, standardized, and comparable data on the subject remains scarce. Key knowledge gaps include: 1) The interaction between HD and SAD remains poorly understood. While Pang et al. (2022) and Q. Sun et al. (2023) suggest a synergistic relation, Zhan et al. (2024) report competition. 2) The inhibitory effect of $H_2S$ by HD, particularly the determination of condition-specific $K_i$ values, and the influence of sludge enrichment on process efficiency, also requires further investigation. Additionally, it suggests potential acetate-induced suppression of autotrophic denitrification by competing HD, offering a new perspective on pathway competition 3) Lack of a standard operating protocol (SOP) to assess SAD activity.

Contributions to existing concepts: 1) Development of an SOP for SAD activity to gain fundamental insights to support practical applications, including within the sewer context using sulphide as electron donor, enabling standardized and reproducible batch testing under sewer-relevant conditions. 2) Application of nitrified urine for in-sewer denitrification. The practical application for dosing in sewers remains partly unexplored. This thesis offers a framework to determine dosing quantities to enhance $H_2S$ oxidation, reducing corrosion and odors. 3) Exploratory testing of MIXED (COD and sulphide) setup, offering insights into potential synergy between SAD and HD. This thesis could ignite ideas for future studies on microbial interplay in such environments. Understanding sulphide removal routes (volatilization, precipitation, and biological and chemical oxidation) under nitrified urine dosing, contributing to a more integrated view on sulphur fate.

### 1.7.2 Key research questions

0. What are the **maximum achievable heterotrophic and autotrophic** sulphide-driven **denitrification rates $r_{max}$** [mg $NO_3$-N/ (g VSS d)] ?
1. How do heterotrophic and autotrophic sulphide-driven denitrificatiers interact (synergistically, competitive, etc.) in a MIXED setup?
2. What is the **$K_{i,H2S-NO3}$** of fresh sludge from a wastewater treatment plant?

3. **How much nitrate from urine** must be dosed to the sewer **[mg $NO_3$-N/ $L_{sewage}$]** to maintain **anoxic conditions**?

### 1.7.3 Hypothesis

1. The maximum achievable **HD rates** will be **higher** than SAD due to the slower growth of autotrophs.
2. A **synergistic interaction between HD and SAD** will enhance nitrate removal in the batch tests. SAD will efficiently reduce $NO_3^-$ to $NO_2^-$, while HD are more efficient in converting $NO_2^-$ to $N_2$. Without HD, $NO_2^-$ accumulation is more likely to inhibit SAD activity ($K_i$ = 34.7 mg $NO_2^-$-N/L, Fajardo et al. (2014)). However, HD reduce $NO_2^-$ buildup, benefiting SAD activity. Conversely, HD (sensitive to $H_2S$), but SAD oxidize $H_2S$, lowering its in-sewer levels, benefiting HD activity.
3. **Heterotrophs are more sensitive to sulphide toxicity**, and will be inhibited at lower concentrations than autotrophic denitrifiers.
4. Nitrified urine dosing requirements **depend on inhibition and microbial interactions**. HD will be dominate at high COD levels, while being inhibited by the sulphide present. Depending on those levels, more (or less) dosing is required. The possible synergistic effect could elevate nitrified urine consumption.

### 1.7.4 Research objectives

This study aims to examinate the biokinetics of HD and SAD, including their inhibition and interactions, through batch tests. These insights will support the next step, which is outside the scope of this thesis: the operation of a near-realistic sewer reactor under more dynamic conditions and aid in developing a protocol to assess microbial activity within this dynamic system, with a focus on their impact on nitrate removal efficiency. However, in this thesis a proposal will be made for the reactor design.

### 1.7.5 Overall research challenges

1. **Balancing inhibitory factors:** Prevent the accumulation of unwanted intermediates (*e.g.,* $NO_2^-$) and toxic compounds (*e.g.*, excessive sulphide or $NH_3$). Adress the pH dependency of complex sulphur pathways.
2. **Maintaining autotrophic activity:** Ensure sufficient active autotrophic biomass in the sludge to sustain sulphur oxidation and prevent toxic $H_2S$ accumulation.

3. **Understanding MIXED interactions:** Explore the relation between HD and SAD, under fluctuating dosing conditions (different S/N, acetate-COD, etc.).
4. **Handling sulphur:** Maintain the sulphur cycle as closed as possible, handling sulphur is challenging due to its volatility and complex pathways.

In conclusion, this thesis provides key insights into the kinetics of HD and SAD, focusing on their dynamics with nitrified urine dosing. By addressing existing research gaps, this work will contribute to optimizing nitrified urine dosing strategies in order to reduce odorous emissions and GHG in the urban sewer system.

# 2. Materials and methods

Before constructing the batch tests, a deep literature study was done on the type of tests which were already conducted in the field. These literature findings are presented in Table A.7. These gave valuable insights into the trial and error performed by fellow scientists. Furthermore, these tests gave an idea about the nitrate removal rates which were found through HD and SAD, providing insights in substrate dosing, test duration and time between sampling.

## 2.1 Experimental setup batch tests

The setups of the proposed batch tests were designed based on existing literature. To obtain maximum denitrification rates for heterotrophs and autotrophs, knowledge must be gathered on their inhibition constants ($K_i$) and half-velocity constant constants ($K_s$) (Table 1.3a-b). As visible, not all parameters were (consistently) available in literature.

Next, a literature study was performed on the maximum observed denitrification rates to make an estimation on the amount of sludge (g VSS/ L) and duration of the test (Table 1.2). As heterotrophs grow much faster, their test are conducted over a much shorter timeframe compared to the autotrophs.

### 2.1.1 Sludge and autotrophic enrichment:

For each heterotrophic batch test, fresh active sludge from Aquafin Zuid or Aartselaar was obtained to inoculate the flasks.

For the autotrophic batch tests, active sludge from Aquafin Aartselaar was collected on the 4$^{th}$ of December 2024 and incubated for 156 days to stimulate SAD. Throughout this work, the incubated sludge is referred to as “enriched sludge”.

The enrichment setup is shown in Figure 2.1. A big glass vessel, filled with 5 L active sludge, was wrapped in aluminium foil to prevent sulphur-photo oxidation (An et al., 2010). The lid was sealed using a septum and connected to a smaller flask filled with water to prevent explosion risks due to gas buildup. Prior to enrichment, total suspended solids (TSS)/ VSS was performed to determine the biomass concentration (g VSS/ L) which was used to calculate the required nitrate and sulphur dosages.

To buffer at neutral pH, 7.008 g dipotassium hydrogen phosphate ($K_2HPO_4$) and 4.732 g potassium dihydrogen phosphate ($KH_2PO_4$) where added at the start of the enrichment (equivalent to 15 mM P). Nitrate was supplied using $Ca(NO_3)_2.4H_2O$ (MW 236.15). The dosage was calculated based on an indicative denitrification rate from Jiang et al. (2013), who reported a rate of 2.236 mg $NO_3$-N/ (g VSS h).

The total nitrate concentration to be dosed ($C_{NO3,\ dosed}$) was estimated using the following equation:

$$C_{NO3,\ dosed}\left[\frac{mg\ NO3-N}{L}\right] = r\left[\frac{mg\ NO3-N}{\left(\frac{g\ VSS}{d}\right)}\right] \cdot t\ [days] \cdot V\ [L] \cdot X\ \left[g\frac{VSS}{L}\right]$$

With:

r: Nitrate removal rate [mg $NO_3$-N/ (g VSS d)].

t: Duration without additional feeding [days].

V: Volume present in the vessel [L].

X: Biomass concentration [g VSS/ L].

Initially, 447.15 mL of a 1 g/L $Ca(NO_3)_2.4H_2O$ stock solution was dosed. As electron donor, elemental sulphur (99.5% MW 32.05 g/mole) was fed. Elemental sulphur was chosen since this is less toxic to the microorganisms (at lower pH, $H_2S$ becomes more dominant), and less volatile. Initially 0.8535 g $S^0$ was dosed. On the 13th of March 2025, the incubation switched to $Na_2S.xH_2O$ (65% purity; MW 78.04 g/mole). This switch is expected to further increase SAD activity since the oxidation of $S^{2-} \rightarrow S^0$ is more rapid compared to $S^0 \rightarrow SO_4^{2-}$. Based on anion chromatography results ($NO_3$-N, $NO_2$-N and $SO_4$-S), sulphur and nitrate were periodically dosed to maintain SAD activity.

Assuming that denitrification activity was primarily driven by SAD, sulphur was dosed following stoichiometric requirements: 1.91 g $S^\circ$-S/ g $NO_3$-N during $S^0$ enrichment, and 1.43 g S/ g $NO_3$-N during $Na_2S.xH_2O$ enrichment.


A: vessel with enriched sludge, wrapped in aluminium foil.
B: plastic tube to connect the outflowing gas of the enriched sludge with C.
C: 250 mL flask, filled with water to unleash gasses produced from A
D: stirring plate
E: needle + syringe for sampling

*Figure 2.1: Setup for sludge enrichment.*

To monitor the enrichment process, 8 mL sludge samples were periodically collected to measure pH, using a portable pH probe (HI2020-02, Hanna Instruments), and EC, using a conductivity meter (HI2030-212 02a, Hanna Instruments, Woonsocket, USA). Also, anion chromatography (Metrohm 930 with Metrosep 208 A supp 5-150/4.0 column, Herisau, Switzerland) was performed to quantify $NO_3$-N and $SO_4$-S concentrations. For rapid estimations of nitrate and nitrite, commercial test strips (QUANTOFIX, Machinerey-Nagel, Alemania) were used. All values were logged in an Excel tracking sheet.

### 2.1.2 Synthetic medium composition

Synthetic medium was used to ensure reproducibility across tests and to provide trace elements essential for microbial growth. The medium recipe was adapted from the recipe provided by (Peirano et al., 2020).

The synthetic medium included the following: 100 mg/L $NaHCO_3$ was added to provide adequate inorganic carbon, for autotrophic microbial activity during denitrification.

Also, 0.1 g /L $NH_4Cl$ was added to make sure sufficient nitrogen source is present for assimilation. Furthermore, tap water was used as solvent to provide essential trace elements: 2.5 mg $NO_3^-$-N/L, 16 mg $SO_4^{2-}$-S/L, 39 mg $Cl^-$/L, 30.05 mg $Na^+$/L, 4.3 mg $K^+$/L, 63.7 mg $Ca^{2+}$/L, and 7.562 mg $Mg^{2+}$/L. Lastly, to maintain a stable pH of 7.5 for optimal denitrification, a phosphate buffer was prepared by adding 0.008046 M $K_2HPO_4$ and 0.006954 M $KH_2PO_4$ (15 mM P) to the medium.

### 2.1.3 Nitrified urine

To introduce nitrified urine, a purified solution in which 99% of the nitrogen has been removed is added to each flask. The nitrified human urine has a concentration of approximately 4.45 g $NO_3$-N/L. It is essential that the concentration of nitrified urine in the test setup does not exceed the target nitrate concentrations intended for each of the experiments.

### 2.1.4 TSS/VSS

Before every experiment, a triplicate TSS/ VSS test was performed on the (enriched) sludge to gain insights on the suspended active biomass concentration (VSS) which is needed to reach the desired biomass concentration (g VSS/ L) within each flask. The determination of the TSS provides valuable insides about cell lysis, and precipitation. The APHA 2540D Standard Method was followed (APHA, 1992). Filtration was performed using 50 mL samples with 0.7 µm glass microfiber filters (WAT No. 1825-047, Whatman) connected to a vacuum pump (ME 4R NT, Vacuubrand, Germany). The biomass concentrations from Aquafin Aartselaar or Zuid depended on the batch collected, since this depends on parameters such as rainfall events. The biomass concentration of the enriched sludge differed as well from time to time due to feeding regimes and biomass growth and decay. For each batch test, a sludge concentration of 0.5 to 1 g VSS/ L/ flask was opted for.

The TSS and VSS calculations where performed using following equation:

$$\mathrm{TSS}\left(\frac{\mathrm{mg}}{\mathrm{L}}\right) = \frac{(\mathrm{B}-\mathrm{A})\cdot 10^6}{\mathrm{V_{sample}}} \qquad \mathrm{VSS}\left(\frac{\mathrm{mg}}{\mathrm{L}}\right) = \frac{(\mathrm{B}-\mathrm{C})\cdot 10^6}{\mathrm{V_{sample}}}$$

With:

A [g]: The weight of the clean filter.

B [g]: The filter weight after drying the filtered sample in the oven.

C [g]: The filter weight after ignition in the muffle oven.

$V_{sample}$ [mL]: The volume of the sample.

## 2.2 Experimental setup batch tests and sampling preparation

Prior to the sludge dosing, the sludge was thoroughly shaken to ensure homogeneous sampling. To minimize residual carbon and nutrients in the sludge medium, the sludge was washed three times with an isotonic buffer (tap water) before being added to each flask (except for the abiotic control). The experimental setup is displayed in Figure 2.2. Before starting the test, samples were taken for TSS/ VSS and Dissolved Inorganic Carbon (DIC) and Dissolved Organic Carbon (DOC) analysis.

### 2.2.1 Electron acceptors and donors

As electron acceptor, a 1 g $NO_3$-N/L $Ca(NO_3)_2.4H_2O$ stock solution was used. Electron donors were selected based on the experimental conditions. For the heterotrophic or MIXED flasks, a 20 g $O_2$/L $CH_3COONa$) stock solution was used. Acetate-COD was chosen as a simple (fast) COD source, one of the advantages of acetate compared to other simple COD-sources like methanol and glucose is its lower nitrite accumulation potential (Rocher et al., 2015). All reagents where dosed into the designated 250 mL flasks. A 1 g S/L $Na_2S.xH_2O$ stock solution was prepared by adding 5 mL 5% NaOH ultra-pure to 499.5 mL deionized water in a Schott bottle. This was sparged for 5 minutes using $N_2$-gas to prevent sulphide oxidation. After purging the headspace with $N_2$, 1.93 g $Na_2S.xH_2O$ (MW = 78.04 g/ mole and 63% purity) was added and dissolved using magnetic stirring.

### 2.2.2 Pre-treatment and buffering

To create an anoxic environment, the liquid phase in each flask was purged with $N_2$ gas using an aeration stone until the DO level reached ≤ 0.5 mg $O_2$/L. The DO was measured using a polarographic DO probe (LDO probe, HQ30d, Hach, USA).

To ensure sufficient inorganic carbon availability for autotrophic denitrification, a $NaHCO_3$ (10 g/L) buffer stock solution was added to obtain a concentration of 30 mg/L. The pH was then adjusted to 7.5 using 1 M HCl or NaOH as needed.

At this stage, 50 mL was sampled using a 10 mL syringe, filtered through a 0.2 µm filter (PET syringe filter, CHROMAFIL), and stored in a 50 mL falcon tube without headspace, to prevent compounds from leaking to the gas phase, for DIC and DOC measurements. Next, the headspace of the flasks were sparged using $N_2$ for ± 10s.

### 2.2.3 Sulphur addition and final preparations

For flasks requiring a sulphur source (electron donor/inhibitor), a **fresh** 1 g S/L $Na_2S.xH_2O$ (MW 78.04 g/mole) stock solution was carefully dosed by perforating the septum with a needle. Sulphur was added **after** sparging to minimize volatilization losses. To counteract the $OH^-$ generated from TDS addition, 1M HCl was dosed into each flask. The containers were then sealed with a septum (PTFE-protected, DWK Life Sciences, Germany). Each sulphur containing flask was wrapped in aluminium foil or covered with a dark container to prevent sulphur photo-oxidation (An et al., 2010). To measure total dissolved sulphide, an TDS dilution liquid was prepared by adding 5 mL 5% NaOH and 0.5 mL formaldehyde to 499 ML of deionized water in a Schott bottle. The solution was then bubbled with $N_2$-gas for 5 minutes to remove oxygen.

### 2.2.4 Sampling and sample analysis

Batch tests were conducted on stirring plates at 200 rpm (Figure 2.2). All samples were collected by puncturing the septum with a needle connected to a syringe and filtering the sample through a 0.2 µm filter (PET syringe filter, CHROMAFIL). Samples containing TDS were immediately diluted in the TDS dilution liquid and measured photometrically using a Spectroquant® test kit (range: 0.020-1.50 mg/L ($S^{2-}$); Merck KGaA, Darmstadt, Germany). After sampling, samples were stored at 4°C until further analyses was conducted.

At each sampling period, pressure was monitored using a barometer connected to a needle to maintain overpressure (0.3-0.4 bar) (to prevent leakages and contamination from outside, but also explosion risks) in the system. If a pressure drop was detected, $N_2$ gas was added to restore to initial conditions. To minimize potential gas leakages, a water lock method was applied at the lid of each flask. Furthermore, at each time point, the pH was maintained between 7.5 and 8, as this range is optimal for denitrification. If deviations occurred, adjustments were made using 1M NaOH or 1M HCl. The experiments where conducted until a significant level of nitrate depletion (close to zero) was reached or TDS was close almost zero.

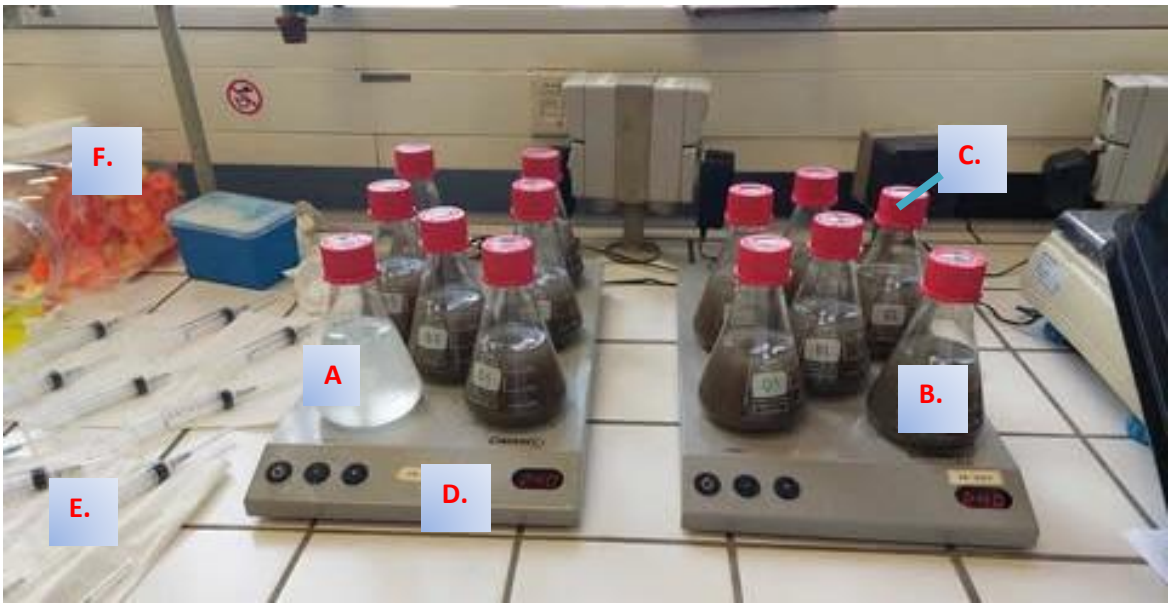


A: 250 mL flask Abiotic control

B: 250 mL flask containing sludge, prepared for SAD, HD or MIXED favoured conditions

C: Cap, sealed with a septum (PTFE-protected, DWK Life Sciences, Germany) and water lock

D: Stirring plate (unheated)

E: 10 mL syringe for sample taking

F: 0.2 µm filters (PET syringe filter, CHROMAFIL) to filter each sample

*Figure 2.2: General setup of the proposed batch tests.*

At the beginning and end of each batch test the pH, EC, DO, and COD were measured using manual probes. The EC was determined with a conductivity meter (HI2030-212 02a, Hanna Instruments, Woonsocket, USA), while pH was measured with a portable pH probe (HI2020-02, Hanna Instruments). The DO was measured inside each flask using a polarographic DO probe (LDO probe, HQ30d, Hach, USA).

#### 2.2.4.1 Acetate-COD

COD measurements were performed using the COD40 or COD600 testkits (Nanocolor photometric tests, Macherey-Nagel, Pennsylvania). These measurements were done to provide insights into heterotrophic denitrification and potential cell lysis.

However, in tests where sulphur was added and the sample was kept without gaseous headspace, a correction was applied to account for its contribution to the COD measurements. This ensured more accurate determination of the acetate-COD. This correction was based on a sulphur-to-COD ratio of 2:1, calculated from the chemical oxidation reaction of sulphide (Reaction 2.1).

$$S^{2-} + 2O_2 \rightarrow SO_4^{2-} + H^+$$

*Reaction 2.1 : Chemical oxidation of sulphide.*

Since one mole of sulphur ($S^{2-}$, $HS^-$ or $H_2S$) requires 2 moles of $O_2$, the oxygen demand equals ~2 g $O_2$/g S. This stoichiometric value was validated through a mini batch test "Mini batch test 1: TDS correction for COD". The TDS-COD was calculated by multiplying the measured TDS concentration with an empirically determined ratio of 1.81 mg $O_2$/mg S (Figure A.1) as follows:

$$COD_{corrected}\left[mg\frac{O_2}{L}\right] = COD_{measured}\left[mg\frac{O_2}{L}\right] - \frac{S\left[\frac{mg\ S}{L}\right]}{1.81\left[\frac{mg O_2}{mg\ S}\right]}$$

With:

S [mg S/L]: The measured concentration TDS.

$COD_{measured}$ [mg $O_2$/L]: The measured COD concentration.

COD correction was only applied to samples containing TDS.

#### 2.2.4.2 Ion Chromatography

Furthermore, to asses denitrification performance and potential nutrient limitations, anion (Metrohm 930 with Metrosep 208 A supp 5-150/4.0 column, Herisau, Switzerland)and cation chromatography (Metrohm 930 with Metrosep C6 150/4.0 with Metrosep C6 Guard/4.0, Herisau, Switzerland) were performed. Prior to measurement, all samples where filtered over 0.2 µm filters and diluted with a 1:12.5 dilution factor. Following anion concentrations were measured: chloride ($Cl^-$), nitrite-N ($NO_2$-N), nitrate-N ($NO_3$-N), phosphate-P ($PO_4$-P) and sulphate-S ($SO_4$-S).

Next to anions, several cation concentrations were measured to gain insights in nutrient limitations, inhibition, and (unexpected) nitrification indications: ammonium ($NH_4^+$), calcium ($Ca^{2+}$), magnesium ($Mg^{2+}$), potassium ($K^+$) and sodium ($Na^+$). Measurements where conducted using cation-exchange chromatography. All ion chromatography values were corrected for dilution.

#### 2.2.4.3 DIC DOC

To validate autotrophic denitrification (characterized by a decrease in Dissolved inorganic carbon, DIC) or heterotrophic denitrification (indicated by a decrease in dissolved organic carbon, DOC), DIC and DOC measurements were performed on samples at the beginning and end of each batch test.

DIC and DOC concentration where measured using the Skalar Formacs HT machine. Prior to analysis, samples were sequentially filtered through a 0.2 µm filter.

10 mL of the filtered samples was then transferred into glass tubes without dilution, as no interference was expected.

## 2.3 Batch test maximum observable denitrification rates

### 2.3.1 Denitrification performance- Fresh sludge (Aquafin Zuid)

The parameters used for the batch test are explained in detail in Table A.2. Each proposed setup is done in triplicate except for the abiotic control. The role of the abiotic control is to correct for sulphide losses via precipitation, volatilization, and chemical oxidation with residual oxygen or nitrate. The test was performed using fresh sludge from Aquafin Zuid obtained at 13$^{th}$ of November 2024.

### 2.3.2 SAD performance- $S^0$ enriched sludge (Aquafin Aartselaar)

The experiment was conducted using enriched sludge (Figure 2.1), taken 15 days after onset of $S^0$ enrichment. An abiotic control was included for the same reasoning as 2.3.1. The philosophy and concentrations of the parameters added to each flask are visible in Table A.3. To mitigate risks of substrate inhibition, the experiment was conducted fed-batch mode. TDS was added after each sampling in steps of 9 mg S/L to obtain a total volume of 45 mg S/L. Each flask was performed in duplicate, except the controls.

### 2.3.3 SAD performance- $HS^-$ enriched sludge (Aquafin Aartselaar)

The enriched sludge (Figure 2.1) is used 6 days after enrichment with $HS^-$. In this test mixed control was included to account for HD contributions. All experimental conditions were performed in triplicate, except for the abiotic control. The fed-batch approach was not applied, as a more in-depth literature study revealed that the concentrations used in our tests do not cause (significant) SAD inhibition, particularly within the pH range selected for this study (Table A.4).

### 2.3.4 Sulphide inhibition on heterotrophic denitrification performance- Sludge Aquafin Aartselaar

All setups were operated in batch mode rather than fed-batch, as a more in-depth literature study revealed that the concentrations used in the tests do not cause (significant) SAD inhibition.

Each heterotrophic inhibition setup was accompanied by a dedicated autotrophic control to account for potential SAD at the given S/N ratio (Table A.5). All experimental conditions, with the exception of the controls, were performed in triplicate. Also, this test was performed two times (Test A and Test B). All conditions were the same in each test, except the sulphide concentrations shown in Table A.5. Here, blue indicates the concentration of Test B and green the concentrations of Test A.

### 2.3.5 Mini batch tests

#### 2.3.5.1 Mini batch test 1: TDS correction for COD

A calibration curve was prepared using a dilution series of three different TDS concentrations. A 1 g S/L $Na_2S.xH_2O$ standard solution was added to deionized water to create dilutions of 1:50, 1:100, and 1:200, resulting in final concentrations of 20 mg S/L, 10 mg S/L and 5 mg S/L, respectively. The concentrations where measured using the sulphide test kit with following dilutions in the blank: 1:20, 1:10 and 1:5.

Based on Reaction 2.1 indicating a COD/N ratio of 2:1, additional dilution was applied to the 20,10 and 5 mg S/L samples. The 20 and 10 mg S/L were further diluted twofold using deionized water, while the 5 mg S/L remained undiluted.

This was done to measure the COD using the COD40 test kit (Nanocolor photometric tests, Macherey-Nagel, Pennsylvania). The exact components used as well as their philosophy are presented in Table A.6.

#### 2.3.5.2 Mini batch test 2: Sulphide Removal via Adsorption and/or precipitation at varying VSS

An abiotic control was added to assess if sulphide losses resulted from chemical oxidation or leakage. Additionally, three different VSS concentrations were tested to investigate a potential correlation between fresh sludge concentration and sulphide losses (Table A.7). No nitrate source ($Ca(NO_3)_2.4H_2O$ or Nitrified urine) was added, since the aim was to evaluate sulphide losses due to adsorption or precipitation rather than SAD.

## 2.4 Determination of biological denitrification activity

A key approach to evaluate if nitrate and nitrite removal in the batch tests were due to biological HD or SAD, was to measure and calculate the COD/N and S/N ratios (g/g) for each setup. These values were compared with the stoichiometric values (Table 2.1).

*Table 2.1: Overview of denitrification and denitritation, S/N and COD/N ratios in [mole/mole] and g/g according to stoichiometry, shown with their appropriate reactions for HD and SAD.*

| **Reactions for SAD** | **S/N [mole/mole]** | **S/N [g S/g $NO_3$-N] Or [g S/ g $NO_2$-N]** |
|---|---|---|
| $S^{2-} + 0.4\ NO_3^- + 2.4\ H^+ \rightarrow S^0 + 0.2\ N_2 + 1.2\ H_2O$ | 1:0.4 | 5.72:1 |
| $S^{2-} + 1.6\ NO_3^- + 1.6\ H^+ \rightarrow SO_4^{2-} + 0.8\ N_2 + 0.8\ H_2O$ | 1:1.6 | 1.43:1 |
| $S^0 + 1.2\ NO_3^- + 0.4\ H_2O \rightarrow SO_4^{2-} + 0.6\ N_2 + 0.8\ H^+$ | 1:1.2 | 1.91:1 |
| $S^0 + 2\ NO_2^- \rightarrow SO_4^{2-} + 0.6\ N_2 + 0.8\ H^+$ | 1:2 | 1.14 |
| $2\ NO_2^- + 3\ HS^- + 5\ H^+ \rightarrow N_2 + 3\ S^0 + 4\ H_2O$ | 3:2 | 3.43:1 |
| $8\ NO_2^- + 3\ HS^- + 5\ H^+ \rightarrow 4\ N_2 + 3\ SO_4^{2-} + 4\ H_2O$ | 3:8 | 0.86:1 |
| **Reactions for HD** | **COD/N [mole/mole]** | **COD/N [g $O_2$/g NO3-N] Or [g $O_2$/ g $NO_2$-N]** |
| $3\ CH_3COOH + 8\ NO_2^- + 8\ H^+ \rightarrow 4\ N_2 + 6\ CO_2 + 10\ H_2O$ | 3:8 | 2.86:1 |
| $5\ CH_3COOH + 8\ NO_3^- + 8\ H^+ \rightarrow 4\ N_2 + 10\ CO_2 + 14\ H_2O$ | 5:8 | 1.71:1 |

## 2.5 Biomass growth modelling using Monod kinetics

To assess the nitrate removal potential of nitrified urine in sewer systems, specific biomass growth rates (μ(S)) were derived from batch experiments and modelled using Monod kinetics. These models allow estimation of nitrate removal under varying substrate and inhibition conditions.

### 2.5.1 General Approach

The classic Monod equation was used as a starting point to describe the substrate-dependent growth of the biomass:

$$\mu(S) = \mu_{max} \cdot \frac{S}{K_s + S}$$

With:

μ(S) [1/h]: The specific growth rate.

$\mu_{max}$ [1/h]: The maximum specific growth rate.

Ks [(g $NO_3$-N)/L]: The half-saturation constant.

S [(g $NO_3$-N)/L]: The substrate concentration.

### 2.5.2 Assumptions

1. Constant pH around 7.5.
2. Temperature remains constant at ± 21°C during the tests.
3. Biomass decay is neglected, as it is assumed that biomass growth is in its exponential phase.
4. DO is stable at approximately 0.5 mg $O_2$/L.
5. The $K_{NO3}$ values for nitrate used: 0.5 mg $NO_3$-N/L (HET) and 3 mg $NO_3$-N/L (AUT).
6. The $K_{S2-}$ values for sulphide: 0.5 mg S/L (AUT).
7. The $K_{COD}$ values for COD: 0.5 mg $O_2$/L (HET).
8. No inhibition of SAD by $H_2S$ was considered (2.5.1).
9. $K_{i,\ H2S\text{-}NO3}$ for heterotrophs: 7.62 mg $H_2S$-S/L (results experiment). COD inhibition of HD was neglected.
10. $Y_{X/S}$ [g VSS/ g $NO_3$-N]: 0.82 and 0.61 for acetate-based HD and SAD using sulphide (Di Capua et al., 2019).

These assumptions allowed simplification of the growth models.

### 2.5.3 Determination of $r_{max}$, $\mu_{max}$ and $K_i$

These maximal nitrate removal rates were calculated based on the following formulas:

$$r_{max,observed} = \frac{slope}{C_{biomass}}$$

$$r_{max,actual} = r_{max,observed} - r_{max,abiotic\ control}$$

With:

$r_{max,\ observed}$ [mg $NO_3$-N/ (g VSS h)]: The calculated $r_{max}$.

$r_{max,\ abiotic\ control}$ [mg $NO_3$-N/ (L h)]: The measured $r_{max}$ in the abiotic control (due to chemical reactions).

$C_{biomass}$ [g VSS/L]: The active biomass concentration.

$t_i$ [h]: The time the sample was taken after the start of the test.

Slope: The slope over the nitrate concentration versus time.

The maximum specific growth rate was calculated from the yield ($Y_{X/S}$) [g VSS/ ( g $NO_3$-N)] was and the observed maximum substrate removal rate ($r_{max}$) [g $NO_3$-N/ (g VSS h)]:

$$\mu_{max} = Y_{X/S} \cdot r_{max}$$

Using a Lineweaver-Burk graph (*e.g.*, Figure A.6), the $K_i$ can be calculated via:

$$K_{i,H2S-NO3} = \frac{1}{\mu_{max}.\,slope}$$

With

$\mu_{max}$ = maximum specific growth rate [$h^{-1}$].

$K_{i,H2S-NO3}$ = the inhibition constant with $H_2S$ the inhibitor and $NO_3$ the substrate.

## 2.5.4 Inhibition terms

To reflect real sewer conditions, substrate inhibition effects were incorporated.

### 2.5.4.1 Autotrophic growth (sulphide-driven denitrification)

In the sewer system, autotrophic activity primarily decreases at high COD concentrations. This is due to the outcompeting of faster growing HD (Guerriero et al., 2022). This is not included in the Monod model of the pure autotrophic community since here no substrate ($NO_3$) competition is expected by HD:

$$\mu(S)_{AUT} = \mu_{max,AUT} \cdot \frac{[NO_3^-]}{K_{NO3} + [NO_3^-]} \cdot \frac{[S^{2-}]}{K_{S2-} + [S^{2-}]}$$

With:

$\mu(S)_{AUT}$ [$h^{-1}$]: The specific growth rate of pure autotrophic denitrifiers at a given substrate concentration ($NO_3$ and $S^{2-}$).

$\mu_{max,\ AUT}$ [$h^{-1}$]: The maximum specific growth rate of pure autotrophic denitrifiers in substrate excess conditions.

$K_{NO3}$ [mg $NO_3$-N /L] : The half-saturation constant of nitrate.

$K_{S2-}$ [mg S/L]: The half-saturation constant of sulphide.

Since inhibitory concentrations for $H_2S$ (typically > 200 mg S/L) are not realistic in sewer environments, $H_2S$ inhibition was excluded for SAD organisms.

### 2.5.4.2 Heterotrophic growth

Heterotrophs were modelled with inhibition by $H_2S$ due to their high sulphide sensitivity, this is highly relevant to determine more realistic growth of sewer systems:

$$\mu(S)_{HET} = \mu_{max,HET} \cdot \frac{[NO_3^-]}{K_{NO3} + [NO_3^-]} \cdot \frac{[COD]}{K_{COD} + [COD]} \cdot \frac{1}{1 + \frac{I}{K_{I,H2S-NO3}}}$$

With:

$\mu(S)_{HET}$ [$h^{-1}$]: The specific growth rate of pure heterotrophic denitrifiers at a given substrate concentration ($NO_3$ and COD).

$\mu_{max,\ HET}$ [$h^{-1}$]: The maximum specific growth rate of pure heterotrophic denitrifiers in substrate excess conditions.

$K_{NO3}$ [mg $NO_3$-N /L] : The half-saturation constant of nitrate.

$K_{COD}$ [mg $O_2$/L]: The half-saturation constant for COD.

I [mg $H_2S$-S/L] : The concentration of the inhibitor ($H_2S$-S/L).

$K_{i,H2S-NO3}$ [mg $H_2S$-S/L]: The inhibition constant where 50% inhibition $H_2S$-S occurs.

### 2.5.4.3 Mixed Community growth

For batch tests containing both autotrophic and heterotrophic denitrifiers, the specific growth rate was modelled as the weighted sum of both populations:

$$\mu(S)_{mixed} = \mu(S)_{HET} \cdot \%HET + \mu_{AUT}(S) \cdot \%AUT + \alpha$$

With:

%HET : The heterotrophic contribution to nitrate or nitrite.

%AUT: The autotrophic contribution to nitrate or nitrite.

α: The synergistic effect between autotrophic and heterotrophic denitrification.

### 2.5.4.4 Determination of Community Composition

The relative abundance of autotrophs (AUT%) and heterotrophs (HET%) in the MIXED batch was estimated based on their maximum specific growth rates ($\mu_{max}$). To model the mixed growth rate ($\mu_{max,mixed}$), the formula from section 2.5.4.3 was used, replacing the substrate-dependent growth rates ($\mu(S)_{AUT}$ and $\mu(S)_{HET}$) with their respective $\mu_{max}$ values.

Since nitrate reduction was assumed to occur exclusively via autotrophic or heterotrophic denitrifiers, the relative abundance of heterotrophs was expressed as HET% = 1 – AUT%.

The AUT% was determined iteratively: for each tested AUT% value, the resulting $\mu_{max,mixed}$ was calculated and compared to the experimentally derived $\mu_{max,mixed}$. The AUT% that yielded the smallest absolute difference between the modelled and experimental $\mu_{max,mixed}$ was selected as the estimated autotrophic contribution for the MIXED test.

### 2.6 Statistical analysis

Mean values of the $r_{max}$ were compared in JMP Pro 17 (Sas Institute, Tervuren, Belgium) with the all pairs Tukey Kramer test at a significance level of 5%.

## 3. Results and discussion

## 3.1 Batch tests

The batch tests aimed to determine the maximum achievable denitrification rates ($r_{max}$) for autotrophic sulphide-driven (SAD), and heterotrophic (HD) denitrification under both pure and mixed conditions while also exploring the inhibition constant of $H_2S$ on HD, and gaining a better understanding of the interplay between SAD and HD when both sulphide and acetate-COD are available as electron donors (MIXED setup).

The measured $r_{max}$ values served as input to estimate nitrate removal and biomass growth by applying Monod-based kinetic modelling as detailed in *Materials and Methods – Biomass growth modelling using Monod kinetics*. Inhibitory compounds can significantly lower biomass growth. In the proposed batch tests, sulphide is the most prominent one for heterotrophic denitrification. However, significant sulphide inhibition for SAD is unlikely to happen under realistic sewer conditions, as its $K_{i,H2S-NO3}$ value is higher than the expected in-sewer sulphide levels (Table 1.2b).

The estimated biomass growth is crucial to determine the appropriate dosing of nitrified urine required to maintain anoxic conditions in the sewer (reactor) and to reduce emissions of hydrogen sulphide and methane. The experimental setups used to investigate these dynamics are described in detail in *Materials and Methods*.

It was hypothesized that autotrophic organisms would display lower denitrification rates due to their inherently slower growth compared to heterotrophs (Di Capua et al., 2019). Under optimal conditions, the MIXED condition was expected to outperform both individual systems due to potential synergistic interactions as suggested by the studies of Pang et al. (2022) and Y. Sun & Nemati (2012). The microbial growth was assumed to follow Monod kinetics. However, the $r_{max}$ and thus maximal specific growth rate will depend on the COD/N/S ratio, particularly due to the potential inhibitory effect of $H_2S$ at elevated concentrations.

This section presents the results for autotrophic and heterotrophic nitrate removal along with sulphate production, total dissolved sulphide (TDS) removal, and the microbial growth kinetics, the sulphur-to-nitrogen and acetate-COD-to-nitrogen ratio and DIC DOC measurements per test. In addition, a series of mini-batch tests were performed to better understand the TDS removal pathways aside from denitrification to correct for these losses, and to adapt the SOP to mitigate these abiotic losses as much as possible. Lastly, it is important to note that the denitrification rates presented here are indicative and serve to estimate nitrate dosing needs in sewers. Actual rates may differ, as sewer COD sources are mixed and not pure acetate. As noted by Lu et al. (2014), different carbon sources can influence the microbial community and denitrification efficiency.

## 3.1.1 Denitrification performance- Fresh sludge (Aquafin Zuid)

### 3.1.1.1 Nitrate removal rates, sulphate production and nitrite accumulation

Performance of nitrate, COD, and TDS removal, as well as sulphate production from fresh activated sludge in HD-, SAD- and MIXED-favoured conditions was assessed to confirm denitrification activity (HD or SAD, or both). Figure 3.1 presents the average of nitrate removal and sulphate concentration over time for each triplicate condition. The observed nitrate removal rate followed the following order: HET > MIXED > AUT.

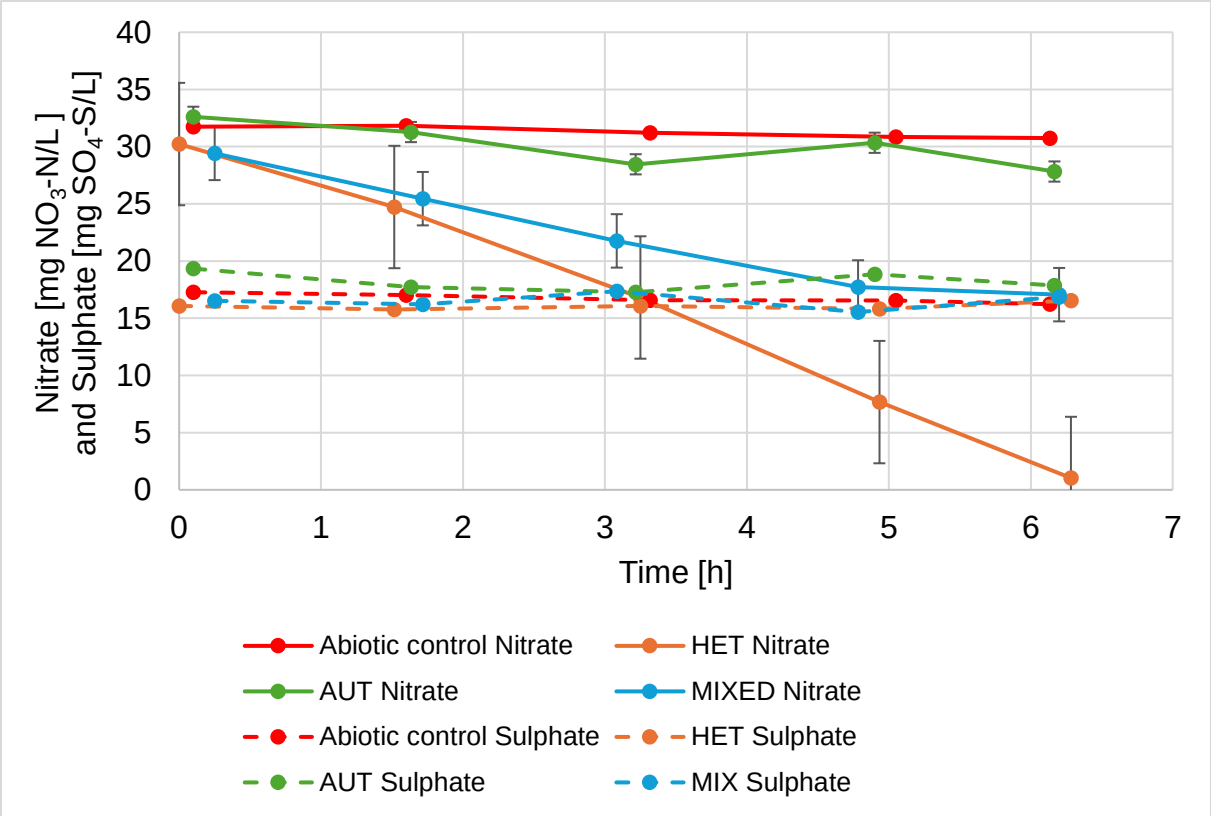


*Figure 3.1: Nitrate [mg $NO_3$-N/L] and sulphate [mg $SO_4$-S/L] over time [h] under heterotrophic (HET), autotrophic (AUT), and MIXED conditions. Each line represents the triplicate average with error bars.*

The observed maximal nitrate removal rates ($r_{max}$) of this test were 167.61 ± 5.64 mg $NO_3$-N/ (g VSS d) (HD), 48.29 ± 18.53 mg $NO_3$-N/ (g VSS d) (SAD) and 119.07 ± 13.71 mg $NO_3$-N/ (g VSS d) (MIXED). The observed $r_{max}$ values were averaged over the triplicates. Nonetheless, this $r_{max}$ is relatively low compared to peak values reported in literature (740.48 for HD, 168.56 for SAD and 534 mg $NO_3$-N/ (g VSS d) for MIXED, Table 1.2).

Statistical analysis shows that the observed $r_{max}$ values for all conditions differ significantly ($p < 0.05$). As anticipated based on faster growth rates, and faster nitrate removal capacity of heterotrophs, their $r_{max}$ is higher compared to the autotrophs (Y. Sun & Nemati, 2012; Metcalf & Eddy, 2014). Contrary to the expected trend pattern MIXED > HD > AUT, as previously suggested by Pang et al. (2022) and Q. Sun et al. (2023), the MIXED conditions resulted in a lower $r_{max}$ value compared to the HET setup.

Furthermore, in Figure 3.1 no significant sulphate production was observed. However, this does not completely exclude SAD activity, as $S^0$ can form as an intermediate.

Moreover, C. Huang et al. (2021) indicated that the oxidation process to sulphate or $S^0$ is influenced by the ratio of autotrophs to heterotrophs present. While comparing removal rates, heterotrophic denitrifiers appear to be more dominant; however, a more detailed explanation will be provided in section 3.1.1.3.

During the test, nitrite started to accumulate. The highest accumulation was observed in the heterotrophic condition (Figure 3.2).

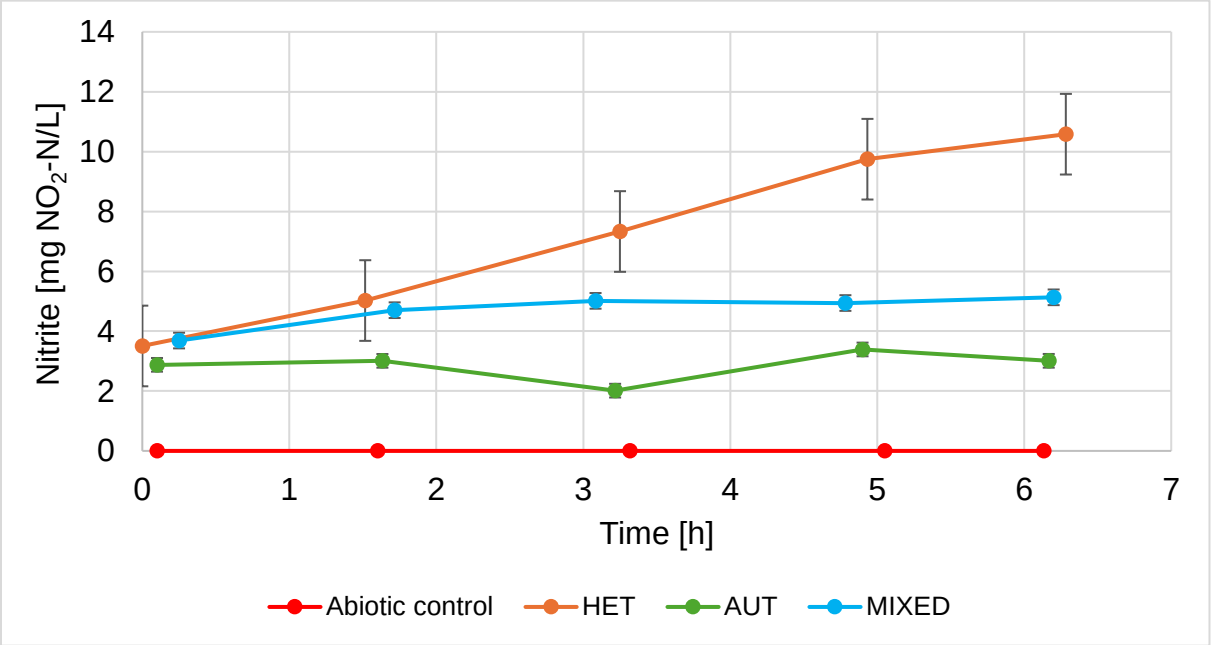


*Figure 3.2 : Nitrite [mg $NO_2$-N /L] over time under heterotrophic (HET) and autotrophic (AUT) and MIXED conditions. In each conditions, the average is taken over the triplicates and vertical error bars are shown.*

### 3.1.1.2 TDS removal

Figure 3.3 presents the total dissolved sulphide (TDS) concentration for each condition tested. The HET condition was excluded due to the absence of added sulphide. The aim of this figure is to boost insights into the biological activity as the S/N values are calculated in Table 3.1 and compared to stoichiometry. The abiotic controls shows the TDS losses, possibly due to chemical oxidation, leakages or losses due to sampling. Interestingly, the most pronounced TDS decrease was observed under MIXED conditions.

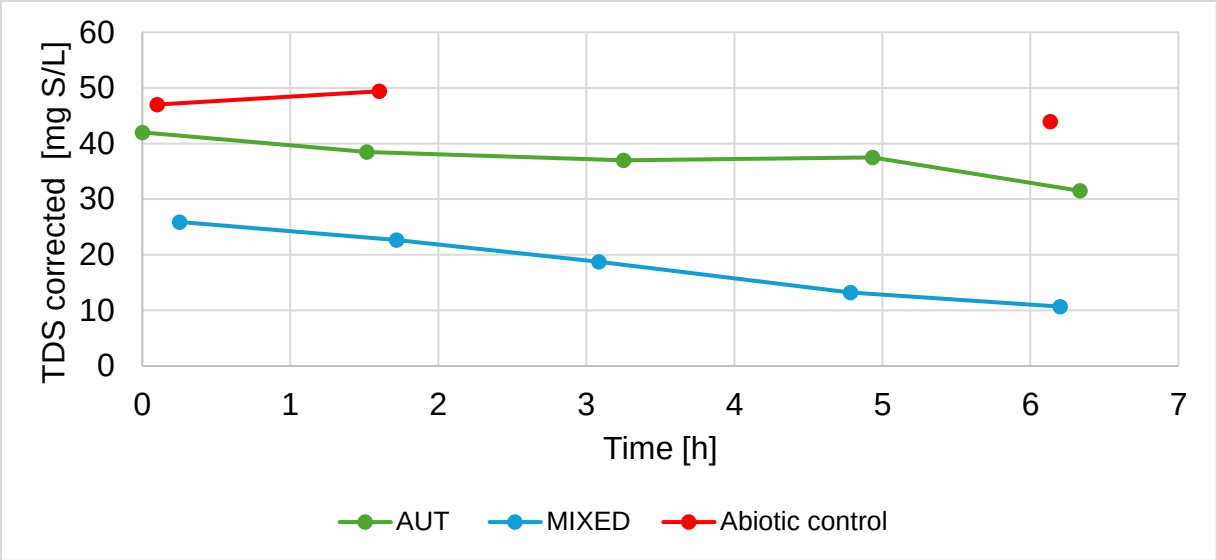


*Figure 3.3:TDS [mg S/L] over time [h] for autotrophic (AUT) and MIXED conditions.*

#### 3.1.1.3 DIC DOC analysis

Figure 3.4 displays the trend in dissolved organic carbon (DOC) and dissolved inorganic carbon (DIC). These measurements were performed as an extra control to confirm whether the nitrate removal was due to HD, SAD or both. The abiotic control showed a small decrease in both DIC and DOC. The decrease in DIC could be due to $CO_2$ losses when stored in the fridge.

The heterotrophic condition showed a clear decrease in DOC. Interestingly, towards the end a complete depletion was observed which contradicts expectations, since the organic carbon source was supplied in excess, meaning that residual DOC should have remained even after full nitrate depletion. Despite this, the linear trend in nitrate removal (Figure 3.1) suggests that the measured $r_{max}$ reflects the maximum nitrate removal rate achievable under the tested conditions. There was no DOC measured in the autotrophic condition. But interestingly, a DIC increase was visible instead of the expected decrease. Lastly, the MIXED control showed minimal changes in both DOC and DIC, suggesting limited HD or SAD activity.

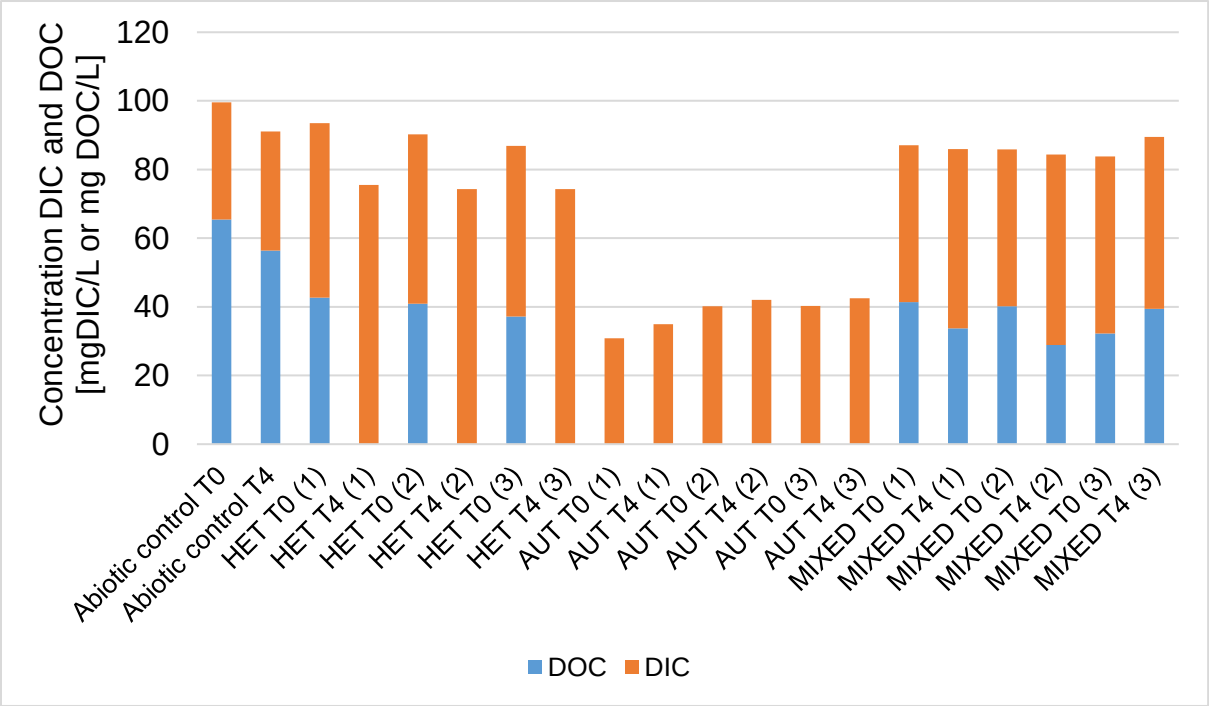


*Figure 3.4: Average dissolved organic carbon (DOC) and dissolved inorganic carbon (DIC) concentrations [mg DIC/L or mg DOC/L] for each sample at the start (T0) and end (T4) of the test.*

#### 3.1.1.4 Biological activity insights and apparent growth kinetics

Table 3.1 summarizes the nitrate, acetate-COD, and TDS concentration changes over the course of the experiment, providing insight into the biological removal pathways under different conditions. Negative values indicate an a gain in a compound. No S/N ratios are reported for the heterotrophic conditions, as no sulphide was added. Similarly, COD/N ratios are not applicable under autotrophic conditions, where no external organic carbon was dosed. For the mixed conditions, S/N removal could only be assessed for MIXED 1, which was monitored in fed-batch mode over time.

*Table 3.1:Overview of COD/N and S/N removal [g/g] across HET, AUT and MIXED conditions. 'NA' indicate values that were not measured in the flasks with TDS dosing.*

| Sample | Acetate-COD/$NO_3$-N removed over test (g $O_2$/g $NO_3$-N) | S/N removed over test (g S/g $NO_3$-N) |
|---|---|---|
| **HET 1** | 2.37 | - |
| **HET 2** | 3.26 | - |
| **HET 3** | 2.40 | - |
| **AUT 1** | - | 1.09 |
| **AUT 2** | - | 2.85 |
| **AUT 3** | - | 11.45 |
| **MIXED 1** | -1.49 | 1.27 |
| **MIXED 2** | -1.38 | NA |
| **MIXED 3** | 0.73 | NA |

Furthermore, to compare the nitrate-dependent growth kinetics of heterotrophic- , autotrophic, and mixed- favoured conditions, Monod kinetics (using nitrate as a substrate) (Figure 3.4) were used to estimate the maximum specific growth rate ($\mu_{max}$) for each condition. The maximum calculated growth rates for this test were: 0.00573 $h^{-1}$ (HET); 0.00123 $h^{-1}$ (AUT) and 0.00339 $h^{-1}$ (MIXED).

Figure 3.5 shows the increase in specific growth rate for HET, AUT and MIXED activity for different substrate levels. The assumptions made are presented in *Materials and methods*. Based on the $r_{max}$ found, an almost complete absence of SAD can be assumed.

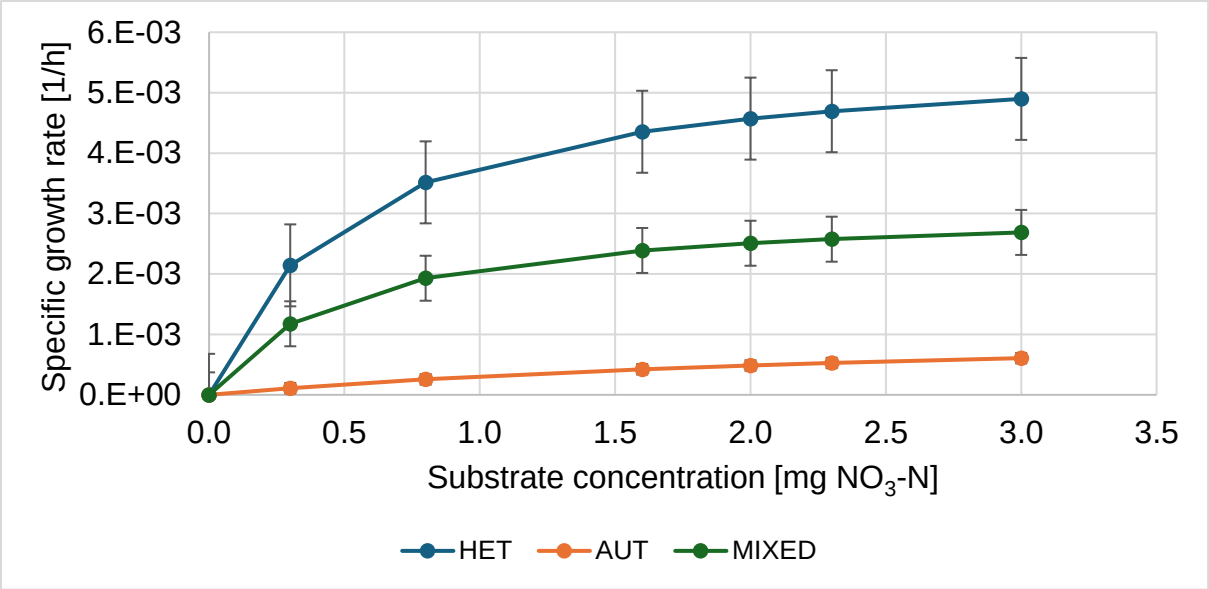


*Figure 3.5: Comparison of the average specific growth rate μ [1/h] per substrate concentration [g $NO_3$-N/L], for the maximal observed heterotrophic, autotrophic and mixed activity of fresh sludge from Aquafin Aartselaar. Each performed in triplicate.*

### 3.1.1.5 Unravelling denitrification pathways: Insights activity trends

Under **heterotrophic conditions**, the observed acetate-COD/ N removal ratios closely approached the theoretical value of 2.86 g $O_2$/g $NO_3$-N for full heterotrophic denitrification. Nonetheless, values in HET 1 and 2 fell slightly below this stoichiometry, suggesting partial nitrite accumulation, as visible in Figures 3.1-3.2. This is consistent with the preference of heterotrophs for nitrate over nitrite as an electron acceptor, and aligns with observations by Rocher et al. (2015), who reported typical nitrite accumulation patterns during acetate-driven denitrification.

Despite these relatively good stoichiometric ratios, the overall nitrate removal rates were unexpectedly low compared to literature. This may be due to the observed elevated nitrite concentrations of 10 mg $NO_2$-N/L (~0.0079 mg $HNO_2$-N/L), which approach reported inhibitory levels ($IC_{40}$ of 0.01–0.025 mg $HNO_2$-N/L) (Lan et al., 2019; Zhou et al., 2007). Furthermore, COD/N ratio of around 5 in these batch tests may have been suboptimal, as later experiments with a ratio of 7 showed more favourable outcomes. However, a COD/N around 5 should be sufficient for denitrification. Thus, it could be that the sludge was not active enough anymore as it was kept in the fridge without aeration. Another possible reason to explain the lower $r_{max}$ of the fresh sludge compared to literature, was because many studies used enriched sludge. These combined factors probably explain the suboptimal rates observed.

In the **autotrophic conditions**, S/N removal in AUT 1 approached the theoretical value for full SAD to sulphate (1.43 g S/g $NO_3$-N), whereas AUT 2 fell between partial oxidation to $S^0$ (5.72 g S/ g $NO_3$-N) or full SAD. AUT 3 presented an interesting anomaly. The S/N ratio of 11.45 is nearly twice the stoichiometric value required for partial SAD to $S^0$. Despite the high S/N removals in each conditions, and signs for full SAD to sulphate, no significant sulphate productions was visible (Figure 3.2). The AUT 3 flask showed a much lower $r_{max}$ (17.71 mg $NO_3$-N/ (g VSS d), compared to AUT 1 and AUT 2 (45.44 and 81.70 mg $NO_3$-N/ (g VSS d). Also, the observed $r_{max}$ for SAD (48.29 ± 18.53 mg $NO_3$-N/ (g VSS d)) was markedly lower compared to literature findings in Table 1.2 (66.4-192.4 mg $NO_3$-N/ (g VSS d)).

The simultaneous increase in DIC and high TDS losses in AUT flasks could suggest misinterpretation of sulphur oxidation dynamics, possibly influenced by non-biological interactions such as precipitation with metals like iron or adsorption to sludge flocs, which is later explained in mini-batch test 2. The lower $r_{max}$'s could indicate $H_2S$ inhibition inside the autotrophic flasks due to potential dominance of heterotrophs present inside the inoculated sludge and thus insufficient amounts of active autotrophic denitrifiers. If no inhibition was present, the autotrophic flasks would show nearly the same $r_{max}$ as the heterotrophic flaks, assuming almost no autotrophs are present.

**MIXED conditions** presented a more complex picture. Initially, the stronger reduction in TDS hinted at potential synergistic interactions between HD and SAD. However, when the observed $r_{max}$ was compared to the sum of the pure conditions, a substantial reduction was seen rather than enhancement. This negative 'synergy' suggested that inhibitory and or competition rather than cooperative interactions occurred. Given the low activity observed in the autotrophic setup, the mixed rates likely reflect predominantly heterotrophic denitrification. Furthermore, MIXED conditions did deviate from the full HD stoichiometry. However, this was not excluded since previous findings did suggest cell lysis. Therefore, no exact measurements were performed to out rule these increases in COD, meaning the true acetate-COD/ N removed could be closer to stoichiometry. On the other hand, S/N ratios close to stoichiometry for full SAD were observed. But, here as well, no significant sulphate production was observed.

This discrepancy led to the hypothesis that partial oxidation to $S^0$ occurred, possibly facilitated by heterotrophic sulphide-oxidizing nitrate-reducing bacteria (h-soNRB) such as *Pseudomonas* spp., which are known to oxidize sulphide incompletely under high acetate and sulphide concentrations. Since SAD like *Thiobacillus denitrificans* generally prefer low-sulphide environments and oxidize sulphide fully to sulphate, the conditions present in the batch tests (excess sulphur relative to nitrate) likely favoured the heterotrophic pathway (Di Capua et al., 2019). This interpretation aligns with Zhan et al. (2024), who observed that under excess organic carbon, HD outcompetes SAD due to faster substrate uptake and higher growth rates. Their gene expression analyses confirmed this by showing increased expression of *napA* (HD-related) and decreased expression of *napG* (SAD-related). However, high $H_2S$ levels might inhibit HD, explaining the reduced $r_{max}$ observed under MIXED conditions.

Interestingly, in MIXED 1 and 2, a net increase in $H_2S$-corrected acetate-COD was observed over time (from 147.61 to 165.56 mg $O_2$/L in MIXED 1 and from 116.01 to 133.24 mg $O_2$/L in MIXED 2). This could suggest DOC accumulation, but a more detailed interpretation is needed. To investigate this, measured DOC values were converted to acetate-COD equivalents using a conversion factor of 0.375 mg $O_2$/mg C. These DOC-derived COD values were much lower than the COD values measured. A possible explanation could be the contribution of $S^0$ to the COD measured, however this was insufficient to explain the COD increase. To proof this, all TDS removed is assumed to be transformed to $S^0$ (as no significant sulphate production was visible, and thiosulphate is expected to be neglectable) This way, the nitrate reduction attributed to SAD was estimated. The remaining nitrate removal was ascribed to HD.

The hypothesis regarding the presence of partial oxidation to $S^0$ might be supported by Zhan et al. (2024). Under excess organic carbon, they observed that the HD pathway becomes dominant over SAD. This is attributed to faster uptake of (fast) organic carbon sources, higher growth rates and substrate affinity of the heterotrophs. In contrast, SAD rely on slower metabolic pathways and are outcompeted under excess COD conditions. These conditions limit the oxidation of $S^0$ as nitrate and nitrite are competitively reduced by HD.

The hypothesized microbial community shift towards HD was supported in Zhan et al. (2024) by their gene expression data, showing increased expression of periplasmic nitrate reductase catalytic subunit A (NapA) (for HD) and decreased expression of periplasmic nitrate reductase-associated cytochrome subunit G (NapG) (SAD). However, elevated $H_2S$ levels can suppress heterotrophic activity, which might explain the lower $r_{max}$ compared to full HD.

But, MIXED 1 and 2, DOC remained higher than expected. Notably, MIXED 1 showed a sharp VSS decline and MIXED 2 a moderate one (Figure A.2), pointing towards cel lysis. The release of intracellular carbon likely caused the apparent DOC to increase again reaching nearly equal values as at T0. This biomass decay might also indicate the proposed inhibition in the MIXED setup, and may explain the lower $r_{max}$ values found in MIXED conditions compared to HET conditions. In contrast, MIXED 3 did not show such a discrepancy, and the DOC-based COD matched the expected HD contribution more closely.

In the literature, the nature of interactions between HD and SAD in MIXED systems remains debated. While some studies (*e.g.*, Pang et al. (2022) and Q. Sun et al. (2023)) report synergistic effects, others like Y. Sun & Nemati (2012) have shown that in the presence of both acetate and sulphide, only acetate is utilized as the electron donor. Li et al. (2022) demonstrated that the contribution of HD is strongly dependent on the COD/N ratio, with higher organic loading favouring heterotrophic dominance and enhancing nitrate removal rates. The findings of the current study support the notion of competitive or inhibitory interactions under MIXED conditions, rather than synergy. Thus, the observed outcomes align more closely with the results of Li et al. (2022) and Y. Sun & Nemati (2012)

In conclusion, comparing the $r_{max}$ values and stoichiometric balances between the pure and MIXED conditions suggests that HD likely dominated under MIXED conditions, but faced inhibition, possibly from elevated $H_2S$ concentrations or competitive substrate dynamics. The absence of sulphate formation across all setups further supports the hypothesis that $S^0$ was the dominant end product, especially under carbon-rich conditions where HD outcompeted SAD. The lack of clear DIC reduction and inconsistent TDS trends in the autotrophic flasks suggest low autotrophic activity overall.

While it remains possible that longer adaptation periods could eventually stimulate SAD activity, as proposed by Huang et al. (2021) the current batch test timeframe was likely too short to capture such transitions.

## 3.1.2 SAD performance- $S^0$ enriched sludge (Aquafin Aartselaar)

### 3.1.2.1 Nitrate and sulphate trends (SAD indicator) under varying S/N ratios

This test assessed the impact of $S^0$ enrichment on maximal autotrophic nitrate removal ($r_{max}$) under different S/N ratios to gain insights in the effect or $r_{max}$ when nitrate is overdosed, dosed in equal ratio with S, or when nitrate becomes limited. As literature generally advises operating below stoichiometry regarding S/N ratios to avoid sulphide toxicity (*e.g.*, Dolejs et al., 2015; Huang et al., 2021), the following S/N ratios were tested: 0.75, 1.0 g S/ g $NO_3$-N (sulphur limited) and 1.5 g S/ g $NO_3$-N (excess sulphur compared to nitrogen, slightly above the stoichiometric ratio of 1.43 g S/ g $NO_3$-N).

The $S^0$ enriched sludge was expected to yield higher $r_{max}$ values compared to the previous test, especially under higher sulphur concentrations since more autotrophic activity was expected due to the acclimatization to sulphur, without a COD-source present causing a microbial community shift.

Figure 3.6 shows that S/N ratio 1.5 indeed resulted in the highest $r_{max}$ (72.16 ± 14.05 mg $NO_3$-N/ (g VSS d)), which is 49.5 ± 21.3% higher compared to the $r_{max}$ reached in previous test (48.29 ± 18.53 mg $NO_3$-N/ (g VSS d)). Compared to literature, this value is in range (72-96 mg $NO_3$-N/ (g VSS d), Table 1.2). However, the there was no significant difference between intermediate S/N ratio (1.0) (48.46 ± 3.16 mg $NO_3$-N/ (g VSS d)) and the most sulphur-limited condition (0.75 g S/g $NO_3$-N; 53.20 ± 12.61 mg $NO_3$-N/ (g VSS d)) ($p > 0.05$), which contradicted expectations based on stoichiometry.

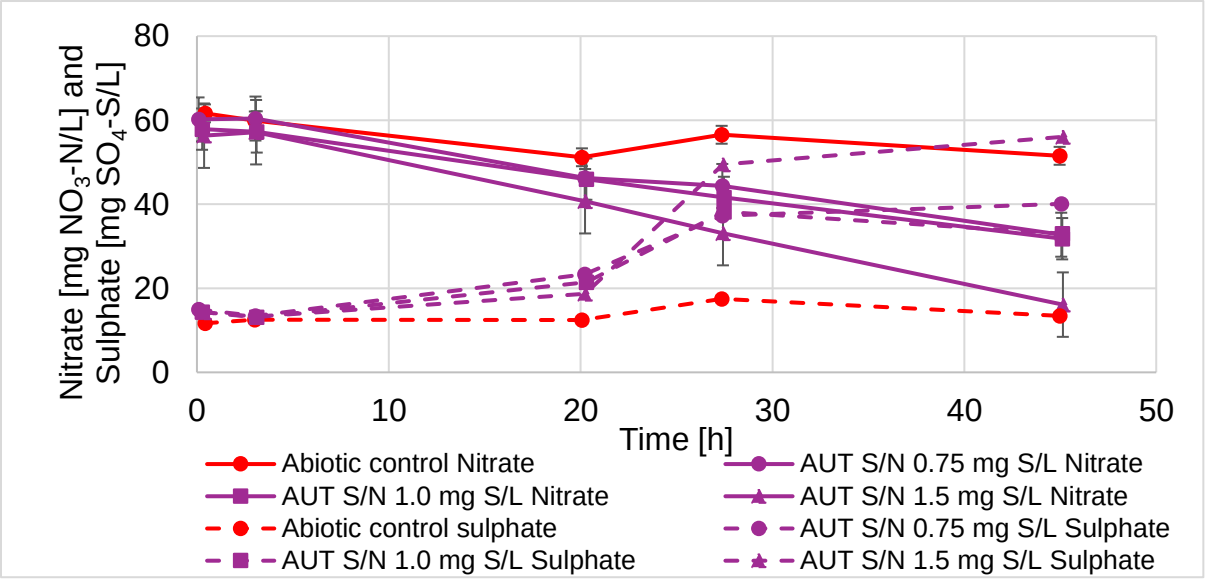


*Figure 3.6: Nitrate [mg $NO_3$-N/ L] and sulphate [mg $SO_4$-S/L] over time for autotrophic (AUT) conditions under S/N ratios of 0.75, 1.0 and 1.5 [g S/ g $NO_3$-N]. For each conditions, the average is taken over the duplicates and vertical error bars are shown.*

Sulphate production mirrored nitrate removal trends, as shown in Figure 3.6. The S/N 1.5 condition yielded the highest sulphate formation (119.49 ± 6.27 mg $SO_4$-S/ (g VSS d)), nearly doubling the values observed at S/N 0.75 (67.16 ± 11.73 mg $SO_4$-S/ (g VSS d)) and S/N 1.0 (64.31 ± 15.87 mg $SO_4$-S/ (g VSS d)).

### 3.1.2.2 Overview table

During this period, there was a shortage on the Spectroquant® test kit for TDS measurement, so an estimation was made to calculate the S/N removal ratios (Table 3.2). Two key assumptions were made: 1) All TDS was assumed to be depleted at the end of the test, based on similar trends observed in other tests, and 2) all formed sulphate results from complete denitrification (1.43 g S/ g $NO_3$-N) (Table 3.2). The S/N values shown in Table 3.2 are residuals, calculated after accounting for sulphur converted to sulphate and the nitrate used in the process. These values are intended to give an indicative reflection on the observed $r_{max}$ trend. True values probably deviate from the estimates, since the S/N 1.5 flasks are expected to show partial S oxidation patterns due to the excess sulphur conditions (Dolejs et al., 2015).

Both S/N 0.75 and 1.5 show insufficient TDS removal to obtain $S^0$ production (5.72 g S/ g $NO_3$-N). The S/N for AUT S/N 1.5 are relatively close to $S^0$ production when keeping in mind that these values are calculated based on estimations. However, AUT S/N 1.0 does show the potential for $S^0$ production.

*Table 3.2: Estimation of the S/N removed over the whole test, calculated after accounting for sulphur conversion to sulphate (1.43 g S/ g $NO_3$-N) for autotrophic conditions with three different S/N ratios (0.75, 1.0 and 1.5 mg S/L).*

| **Conditions with S/N [g S/g $NO_3$-N]** | **Residual S/N removed [g S/g $NO_3$-N] over test** |
|---|---|
| **AUT S/N 0.75 (1)** | 2.95 |
| **AUT S/N 0.75 (2)** | 1.67 |
| **AUT S/N 1.0 (1)** | 5.82 |
| **AUT S/N 1.0 (2)** | 8.63 |
| **AUT S/N 1.5 (1)** | 4.43 |
| **AUT S/N 1.5 (2)** | 5.00 |

### 3.1.2.2 Estimation on the sulphur oxidizing pathway

The differences in sulphate production between S/N 0.75 and S/N 1.0 was almost negligible, which is in line with the $r_{max}$ findings. Moreover, the elevated sulphate production and $r_{max}$ at S/N = 1.5 confirmed that SAD were most active when sulphur was in excess (relative to nitrogen), in line with findings from Dolejs et al. (2015).

While pH dynamics are not the primary basis to deduce the biological sulphur transformation, they offer additional insights into the underlying process. The pH trends support this interpretation: In both S/N 0.75 and S/N 1.0, an initial pH increase was observed. However, this increase persisted longer in S/N 0.75. This is intriguing, as S/N 0.75 exhibited insufficient S/N removal to support substantial $S^0$ production, potentially suggesting direct oxidation of sulphide to sulphate instead. This aligns with sulphate production and nitrate removal (Figure 3.6). In contrast, the shorter pH lies in S/N 1.0 supports the hypothesis of transient $S^0$ formation, which aligns with findings from Table 3.2 that suggest potential $S^0$ oxidation in the AUT S/N 1.0 condition. Since incomplete oxidation (to $S^0$) occurs more rapidly than full oxidation, the observed pH profiles may amplify the hypothesis' made in 1.2.2. Meanwhile, S/N 1.5 did not exhibit a notable initial pH increase in the early stage, the S/N 1.5 conditions did also show the lowest sulphate production in early phases. The low sulphate production and S/N values found in Table 3.2 might hint towards $S^0$ formation as the dominant pathway in the first 20 hours of the experiment. However, a marked pH drop occurred later.

This drop coincided with a strong increase in sulphate levels (Figure 3.6), suggesting potential oxidation of previously formed $S^0$ to sulphate.

In conclusion, the results demonstrate that $S^0$-enrichment significantly enhances the autotrophic $r_{max}$, this was most prominent under conditions of excess sulphur (S/N = 1.5). When sulphur was dosed in stoichiometric or limiting ratios (S/N = 1.0 and 0.75), $r_{max}$ values did not significantly differ, suggesting that the full potential of SAD is only realised under sulphur-rich conditions. Interestingly, the S/N = 1.0 condition showed signs of partial sulphur oxidation and potential $S^0$ formation, suggesting that even sulphur-limited conditions may support $S^0$ accumulation. This is particularly relevant for in-sewer applications, as partial oxidation to $S^0$ alone could already be sufficient to mitigate odour and corrosion issues.

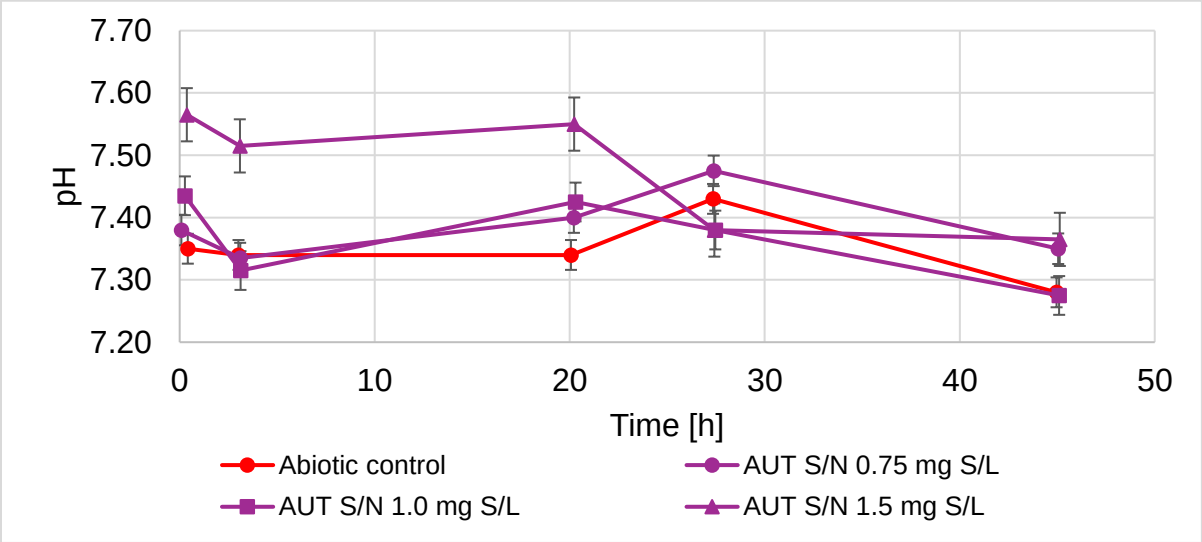


*Figure 3.7: Average pH values over time for autotrophic (AUT) conditions under S/N ratios of 0.75, 1.0 and 1.5 [g S/ g $NO_3$-N]. and the controls. Each condition (except the control) was performed in duplicate.*

## 3.1.3 SAD performance- $HS^-$ enriched sludge (Aquafin Aartselaar)

### 3.1.3.1 Nitrate removal comparison

This test evaluated whether $HS^-$ enrichment enhanced the $r_{max}$ compared to the $S^0$-enriched and fresh sludge. These batch tests were conducted at an S/N ratio of 1.5 g S/ g $NO_3$-N. Mixed conditions were included to understand how acetate-COD influences nitrate removal by sulphide-acclimated sludge and to account for the presence of HD. As shown in Figure 3.8, nitrate declined most steeply under autotrophic conditions, reaching a significantly higher $r_{max}$ of 186.78 ± 14.45 mg $NO_3$-N/ (g VSS d), compared to 108.55 ± 20.55 mg $NO_3$-N/ (g VSS d) for the MIXED control ($p < 0.05$).

The addition of acetate-COD led to a 41.9 ± 13.5% decrease in $r_{max}$. Furthermore, the autotrophic $r_{max}$ under $HS^-$ enrichment was significantly higher compared to both fresh sludge and $S^0$ enrichment ($p < 0.05$). This was expected, as sulphide oxidation generally proceeds faster than $S^0$ oxidation (Dolejs et al., 2015; Yuan et al., 2019). Chemically produced $S^0$, used in the previous enrichment (3.1.2), is poorly soluble in water and presents mass transfer limitations. In contrast, biogenic produced $S^0$ is more hydrophilic and bioavailable (Di Capua et al., 2019). Hence, it was hypothesized that $HS^-$ enriched sludge would obtain higher $r_{max}$ values. Interestingly, a small lag phase in nitrate removal was visible in both enrichment experiments. This was not visible in the heterotrophic setups and is likely due to the slower mechanism of autotrophs (Campos et al., 2008; Di Capua et al., 2019).

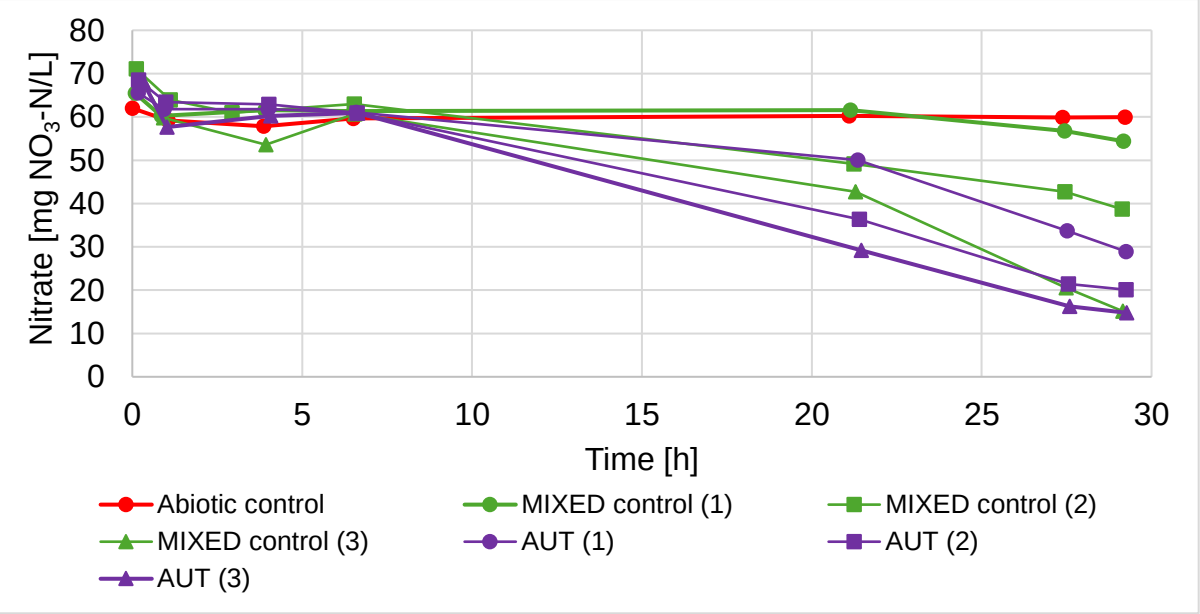


*Figure 3.8: The nitrate [mg $NO_3$- N/L] over time for autotrophic (AUT) and MIXED (MIXED control) conditions. The abiotic control was performed as a single replicate.*

Sulphate production closely mirrored nitrate removal trends (Figure 3.9), indicating coupling of denitrification to sulphide oxidation. The average maximal observed sulphate production rate was 452.97 ± 49.88 mg $SO_4$-S/ (g VSS d) (AUT), which is significantly higher than the 352.99 ± 94.41 mg $SO_4$-S/ (g VSS d) observed in the MIXED control. Notably, $HS^-$ enriched sludge produced 73.63 ± 6.1% more sulphate than $S^0$ enriched sludge and 93.66 ± 7.5% more than fresh sludge, confirming the success of enrichment. The observed complete oxidation of sulphide to sulphate rather than partial oxidation to $S^0$ is particularly noteworthy.

This trend likely results from the depletion of available $H_2S$, leaving the bacteria no alternative but to fully oxidize the remaining sulphur species. As sulphate is more stable and reduces much slower to toxic $H_2S$ compared to $S^0$, this may offer process-level advantages in mitigating odor and corrosion risks.

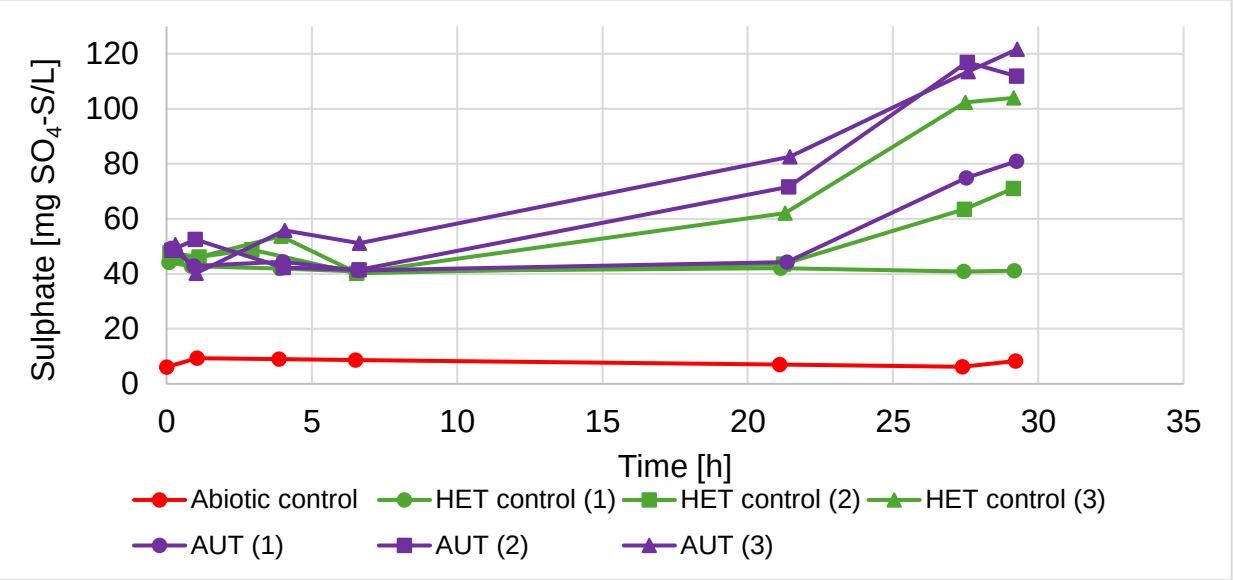


*Figure 3.9: The sulphate concentrations (b) [mg $SO_4$-S/L] over time for autotrophic (AUT) and MIXED (MIXED control) conditions. The abiotic control was performed as a single replicate.*

### 3.1.3.2 TDS removal

TDS levels declined rapidly between T3-T4, coinciding with accelerated nitrate removal and sulphate production. Interestingly, this acceleration occurred when sulphide was (almost) depleted. A similar dynamic is expected in the sewer systems, where nitrate is dosed to suppress $H_2S$ and maintain anoxic conditions. Increased sulphate production elevates nitrate consumption, requiring more dosing. The AUT flasks exhibited the steepest drop, while MIXED control 1 decreased more slowly (Figure 3.8-9), which is interesting as synergistic interactions were hypothesized, which would result in higher denitrification rates in the MIXED condition.

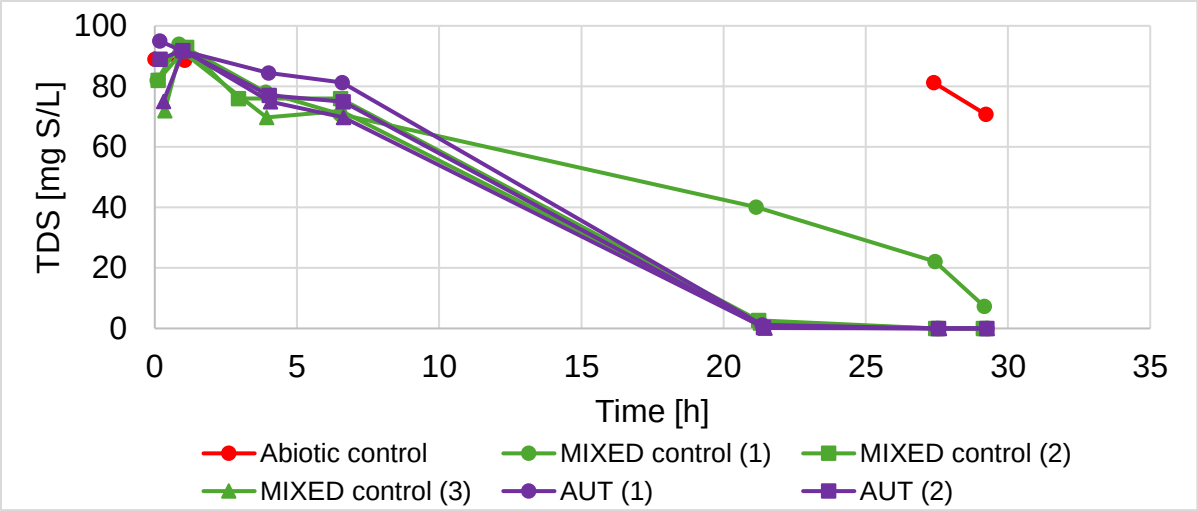


*Figure 3.10: The TDS concentration [mg S/L] over time for each condition. MIXED conditions contain both acetate-COD and TDS, while no acetate-COD is added to the AUT conditions.*

#### 3.1.3.3 DIC DOC

These measurements aimed to confirm HD and SAD activity. A decrease in DIC in the abiotic control (Figure 3.11) may have resulted from $CO_2$ losses during storage. DOC increased in both abiotic control and AUT setup, possibly due to measurement inaccuracies or contamination. Abiotic acetate-oxidation is unlikely as these reactions occur at high temperatures (Fanning, 2000). A slight DIC decrease in autotrophic flasks may indicate SAD activity. MIXED controls showed a clear decrease in DOC and increase in DIC, indicating organic carbon oxidation to $CO_2$ by heterotrophs. However, this test ran under 90 mg S/L, equivalent to 23 mg $H_2S$-S/L at pH 7.5. These conditions are highly inhibitory for HD, what might explain the lower rates compared to Test 1.1.

When $r_{max}$ is split in pure HD and SAD, it becomes clear that a small majority of the nitrate removal was performed by HD activity. In MIXED control 1, almost all nitrate removal was attributed to HD, while HD accounted for 60.87% and 44.13% of nitrate removal in MIXED control 2 and MIXED control 3, respectively. This highlights the important contribution of HD activity (especially in MIXED control 1). Since only a small part of the activity in the MIXED controls is attributed to SAD, it could be noted that when COD is present, the HD becomes dominant which was also one of the conclusions made by Y. Sun & Nemati, (2012). The lower $r_{max}$ found in the MIXED condition compared to SAD is probably due to a combination of the HD outcompeting SAD, and $H_2S$ inhibition on HD**.** However, another interesting theory to explain the lower $r_{max}$ in the MIXED compared to the pure SAD conditions could be acetate inhibition.

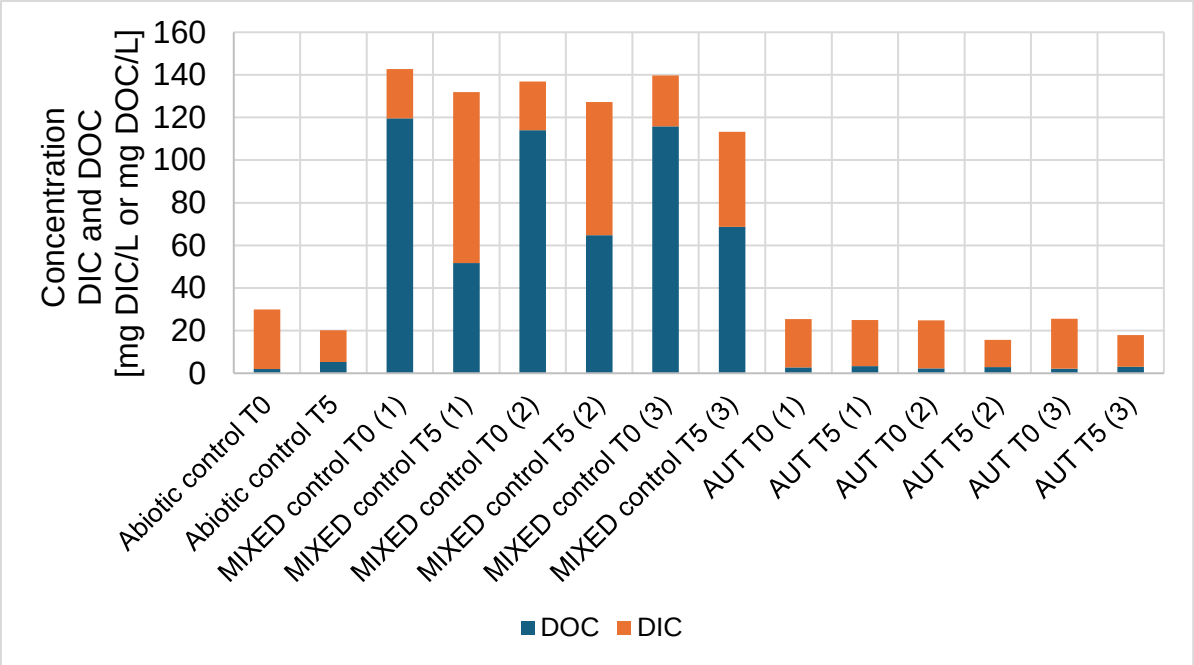


*Figure 3.11: The average dissolved organic carbon (DOC) and dissolved inorganic carbon (DIC) concentrations [mg DIC/L or mg DOC/L] for each flask at the start (T0) and end (T5) of the test.*

### 3.1.3.4 Overview table and metabolic insights

Table 3.3 presents the acetate-COD/N and S/N ratios removed during the batch tests.

*Table 3.3: Overview of COD/N and S/N removal [g/g] across, AUT and MIXED conditions.*

| **Sample** | **Acetate-COD/$NO_3$-N removed over test (g $O_2$/g $NO_3$-N)** | **S/N removed over test (g S/g $NO_3$-N) corrected for abiotic $H_2S$ removal*** |
|---|---|---|
| **MIXED CONTROL 1** | 3.62 | - |
| **MIXED CONTROL 2** | 1.61 | 2.28 |
| **MIXED CONTROL 3** | 1.00 | 1.57 |
| **AUT 1** | - | 4.61 |
| **AUT 2** | - | 2.10 |
| **AUT 3** | - | 1.35 |

**The S/N for the MIXED controls are corrected for the HD contribution to the $NO_3$-N removal.*

AUT 1 had the highest $r_{max}$ over all flasks. AUT 2 showed a lower nitrate removal compared to AUT 1. This could be because the S/N ratio of AUT 2 is close to complete $S^0$ oxidation (1.91). In contrast, the S/N ratio of AUT 1 lies between $S^0$ oxidation and partial oxidation to $S^0$ (5.72). However, the data suggest that AUT 1 leans more towards partial oxidation to $S^0$. If $S^0$ oxidation would be the dominant pathway, the $r_{max}$ was expected to be lower compared to the other AUT flasks. In addition, the sulphate production rate of AUT 1 (371.06 mg $SO_4$-S/ (g VSS d)) would be closer to that of AUT 2 (593.41 mg $SO_4$-S/ (g VSS d)) if full $S^0$ oxidation were occurring. AUT 3 showed an S/N ratio close to that of full SAD (1.43), which could explain its higher sulphate production rate. The highest sulphate production was observed in AUT 2.

MIXED control 3 had the highest $r_{max}$ among the MIXED controls and the lowest HD contribution, as also indicated by lower DOC removal (Figure 3.11). This is notable, as it suggests that HD was strongly inhibited: MIXED controls with a higher HD contribution exhibited a slower $r_{max}$.

This interpretation is further supported by MIXED control 1, where almost no sulphate production was observed. The rate found in MIXED 3 was slightly lower compared to the designated autotrophic flask, indicating elevated acetate concentrations in these flasks could have hindered autotrophic denitrification (G. Xu et al., 2015). Estimated nitrate requirement (13.98 mg $NO_3$-N/L) to match COD removal in this flask supports this COD concentrations were the highest in MIXED control 1 (518 mg $O_2$/L), followed by MIXED control 2 (488 mg $O_2$/L), and MIXED control 3 (474 mg $O_2$/L, MIXED), resulting in a higher COD/N ratio in MIXED control 1. This likely intensified competition between HD and SAD.

As Zhan et al. (2024) noted, under COD-rich conditions, sulphur oxidation may stop at $S^0$, which could explain the lower sulphate production in MIXED compared to AUT conditions (Figure 3.9). HD dominance may also explain lower TDS removal in MIXED conditions. Despite enrichment in the absence of organic carbon, HD activity was observed in MIXED conditions. Two hypotheses may explain this: (1) Residual HD population: A small heterotrophic community may have persisted by utilizing organic matter released from lysed cells during enrichment (Biradar et al., 2010). Upon COD addition, this population could have rapidly expanded due to its high growth rates and substrate affinity.

Or (2) the presence of h-soNRB: These organisms might have relied on sulphur compounds in COD absence, but shifted toward organic carbon oxidation when it became available (Di Capua et al., 2019).

However, the first hypothesis appears more plausible in this experiment, as h-soNRB are specialised in sulphide oxidation. While Di Capua et al. (2019) reported their metabolic flexibility, this was observed under MIXED conditions from the outset. Since no organic carbon was present during autotrophic enrichment, such conditions were not established. Another interesting finding is that the $r_{max}$ found in this test for MIXED conditions does not differ significantly with the $r_{max}$ found for MIXED conditions in 1.1 (predominantly HD, 119.71 ± 13.71) ($p < 0.05$). Nonetheless, pure autotrophic and heterotrophic process rates differed: autotrophic nitrate removal in enriched sludge was 3.8 times higher, while heterotrophic activity was 7.4 times lower, indicating a microbial shift. Lastly, MIXED control 3's S/N ratio and high sulphate production aligns with full SAD (1.43). In contrast, MIXED control 2 showed an S/N ratio close to $S^0$ oxidation (1.91), which might explain its lower $r_{max}$ compared to MIXED 3.

#### 3.1.3.5 Apparent growth kinetics in autotrophic-, and mixed-favoured conditions

Figure 3.12 compares the average specific growth rates between autotrophic and mixed conditions for $HS^-$ enriched sludge. Notably, the AUT flask does show a higher growth rate already at relatively low substrate concentrations. This was expected, as $HS^-$ enrichment favoured SAD growth. However as mentioned before the resulting MIXED conditions are a combination of HD (mostly dominating) and SAD activity. Since HD activity becomes dominant in higher acetate-COD conditions, but is very sensitive to $H_2S$, a lower growth rate was observed compared to the $HS^-$ enriched conditions, which is also visible in the Figure 3.12. In these MIXED conditions, SAD growth was limited due to HD dominance, competing for nitrate.

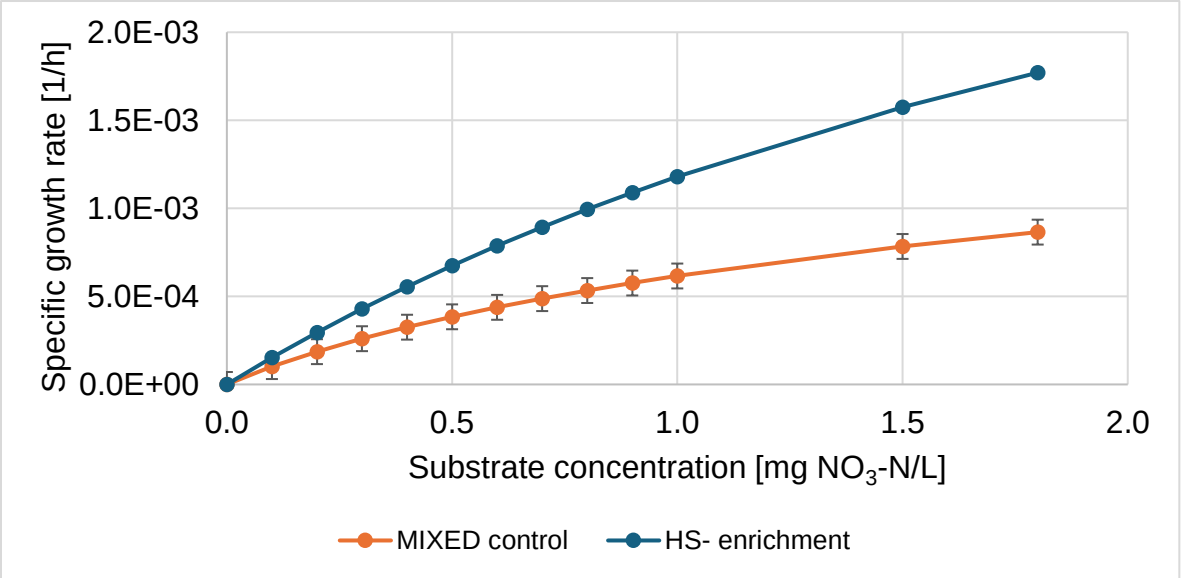


*Figure 3.12: Comparison of the specific growth rates [1/h] for enriched sludge $HS^-$ over different substrate concentrations [mg $NO_3$-N/L]. In autotrophic, and mixed favoured conditions.*

## 3.1.4 Sulphide inhibition on heterotrophic denitrification performance sludge Aquafin Aartselaar

The aim of these tests was to investigate the inhibitory effect of increasing sulphide concentrations (mg $H_2S$-S/L) on HD using fresh sludge from Aquafin Aartselaar. The goal was to derive the sulphide inhibition constant ($K_{i,H2S-NO3}$), a crucial parameter for modelling microbial kinetics in sewer (reactor) systems. The test was performed two times. The first time (Test A), the $H_2S$ concentrations dosed were 0 mg $H_2S$-S/L, 0.66 mg $H_2S$-S/L and 4.29 mg $H_2S$-S/L. In this test, sulphur was dosed before rapid denitrification could take place. The second time, fresh sludge was used (Test B) and the $H_2S$ concentrations dosed were 0, 1.54 and 5.89 mg $H_2S$-S/L. This time, the sulphur was dosed 2 hours after nitrate addition.

### 3.1.4.1 Test A: Nitrate removal, nitrite trend comparison and sulphate production

The heterotrophic setups revealed a clear decline in nitrate removal rates with increasing $H_2S$ concentrations (Figure 3.13a). The control flask (0 mg $H_2S$-S/L) exhibited the highest $r_{max}$ at 303.29 ± 4.23 mg $NO_3$ -N/ (g VSS d), which dropped to 172.54 ± 6.96 at 0.66 mg $H_2S$-S/L, and further declined to 73.89 ± 4.03 mg $NO_3$-N/ (g VSS d) at 4.26 mg $H_2S$-S/L, causing a total reduction of 75.64%. These decreases were statistically significant ($p < 0.05$), indicating progressive inhibition of HD by $H_2S$. This justifies the need to determine the inhibition constant ($K_i$) for $H_2S$.

In contrast, the autotrophic controls showed negligible nitrate removal and unsignificant sulphate production in all flasks. Since significant sulphate generation is expected under SAD activity, especially at high N/S, the lack of sulphate suggest no substantial SAD occurred (Di Capua et al., 2019).This was also the case in 3.1.1.

Figure 3.13b presents nitrite accumulation patterns. Significant nitrite buildup was only observed in HET 0 mg $H_2S$-S/L. The HET 0.66 mg $H_2S$-S/L conditions showed a minor increase in nitrite, followed by a decrease. This decrease collides with the TDS values falling below 0.55 mg $H_2S$-S/L, suggesting that Nir became less inhibited (Figure A.4). Similar findings were observed by Pan et al. (2013).

However, the conditions with the highest $H_2S$ dosed showed almost no nitrite accumulation. This, together with the lower nitrate removal rates could potentially imply inhibition of Nar.

In Table A.8, the acetate-COD/N ratio is above the stoichiometric value for HD (2.86). Negative values were obtained due to a COD increase. A possible reason could be cel lysis, which is interesting as this was not observed in Test B. However Test A did show a more pronounced inhibition at lower sulphur values compared to Test B.

Only the autotrophic control (4.26 mg $H_2S$-S/L) showed an S/N ratio above stoichiometric ratio for either $S^0$ oxidation (1.91) or complete sulphide oxidation (1.43). Despite this, the absence of both sulphate production and increase in $r_{max}$ compared to the other autotrophic conditions indicates the absence of complete SAD activity (Figure 3.13 a). Therefore, the observed sulphide losses likely have another origin, the most plausible ones for these test will be explained in 3.1.5.

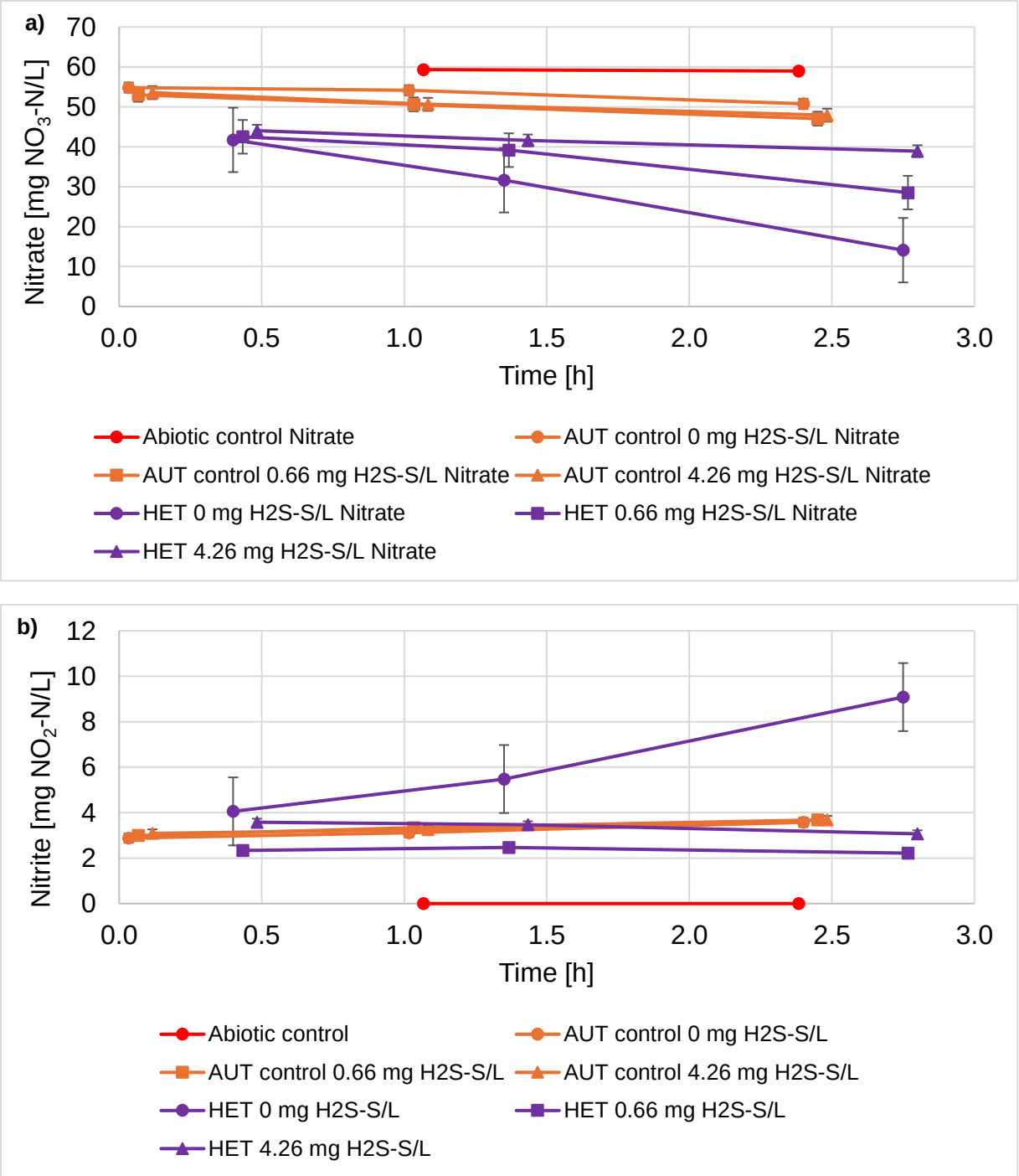


*Figure 3.13: The average nitrate [mg $NO_3$-N/ L] (a) and nitrite [mg $NO_2$-N/L] (b) concentrations over time for autotrophic (AUT control) and heterotrophic (HET) conditions with three different sulphide concentrations (0, 0.66, and 4.26 mg $H_2S$-S/L). For each condition, the average was taken over the triplicates and vertical error bars are shown. Each abiotic control was performed as a single replicate.*

### 3.1.4.2 Test B: Nitrate removal, nitrite trend comparison and sulphate production

The heterotrophic setups clearly showed nitrate removal, although removal rates decline with increasing sulphide levels (Figure 3.14 (a)). All setups started with 60 mg $NO_3$-N/L, but the first sampling already revealed lower nitrate values.

This is likely due to delayed sulphide dosing (2 hours **after** nitrate dosing), allowing uninhibited denitrification to occur. Sulphate production remained negligible, similar to Test A.

Nitrite accumulation was observed in all heterotrophic setups, with the highest peak in the 0 mg $H_2S$-S/L setup (Figure 3.14 b). As nitrate was preferentially reduced, nitrite levels rose and subsequently declined once nitrate was depleted (J. Oh & Silverstein, 1999). The sharpest nitrite decline occurred in HET 1.54 mg $H_2S$-S/L, while HET 5.86 mg $H_2S$-S/L showed a more gradual decrease. Notably, this pattern aligns with the moment when TDS dropped below 2 mg S/L. This is below the reported threshold for Nir inhibition, supporting sulphide's inhibitory role on Nir (Pan et al., 2013) (Figure A.5).

The $r_{max}$ significantly decreased at higher sulphide concentrations ($p < 0.05$). In the heterotrophic flasks, $r_{max}$ dropped from 510.33 ± 16.69 mg $NO_3$-N/ (g VSS d) in the control (0 mg $H_2S$-S/L) to 290.66 ± 11.13 mg $NO_3$-N/(g VSS d) (5.89 mg $H_2S$-S/L). Even at 1.54 mg $H_2S$-S/L, inhibition was evident with $r_{max}$ reduced to 487.79 ± 3.29 mg $NO_3$-N/ (g VSS d).

Interestingly, $r_{max}$ values in Test B were generally higher than those in Test A, even in the heterotrophic control. This may be attributed to differences in experimental design: Test A had fewer sampling points, potentially missing the true $r_{max}$. In contrast, Test B allowed HD to proceed before inhibition due to delayed sulphide addition, which might have led to higher apparent $r_{max}$ values. Furthermore, the sludge in Test B was pre-activated with aeration and acetate-COD. While Test A used freshly collected sludge, possibly explaining the higher activity. These methodological differences should be taken into account when interpreting $H_2S$ inhibition and estimating $K_i$ values.

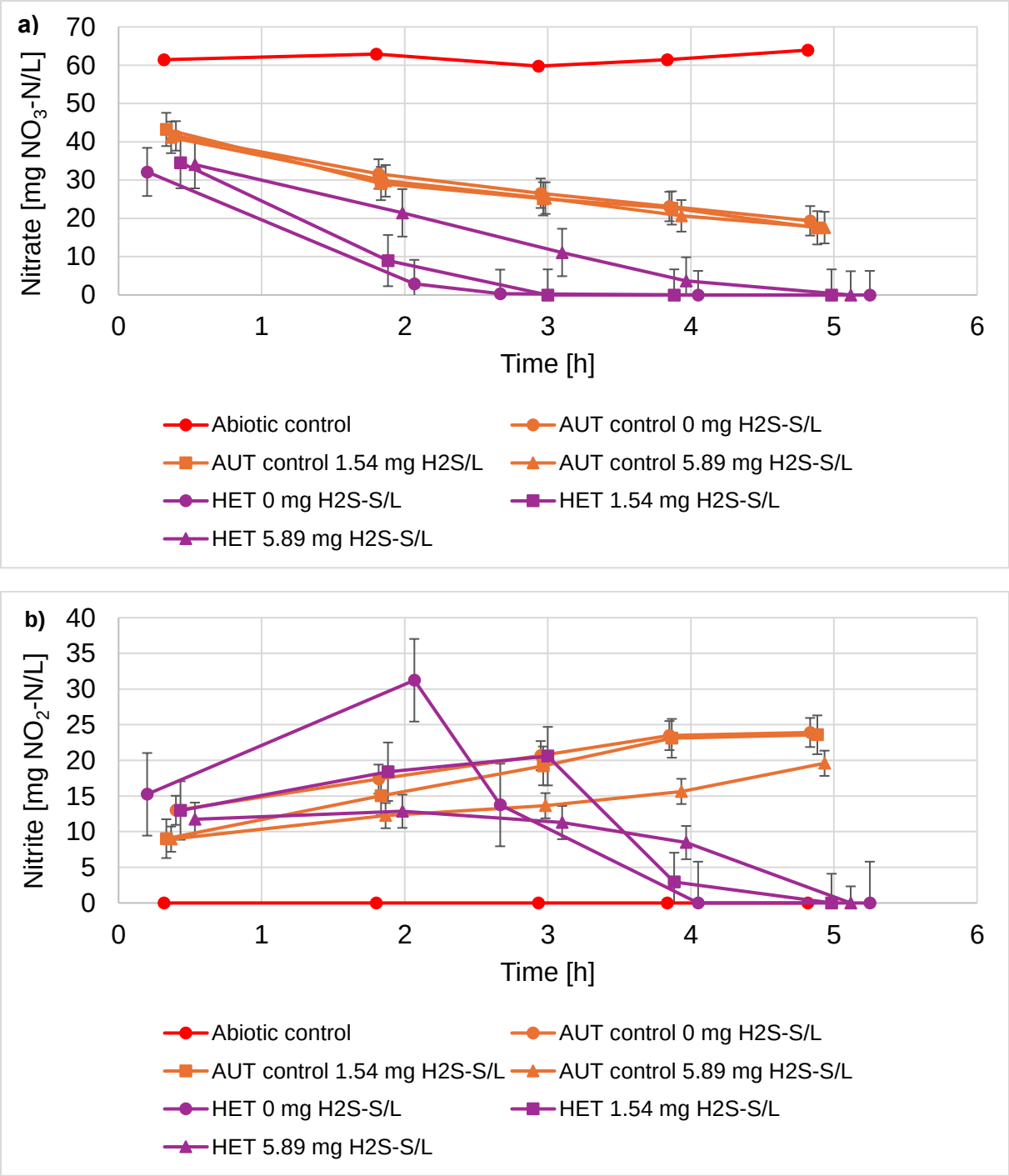


*Figure 3.14: The average nitrate [mg $NO_3$-N/ L] (a) and nitrite [mg $NO_2$-N/L] (b) concentrations over time for autotrophic (AUT control) and heterotrophic (HET) conditions with three different sulphide concentrations (0, 1.54, and 5.89 mg $H_2S$-S/L). For each condition, the average was taken over the triplicates and vertical error bars are shown. Each abiotic control was performed as a single replicate.*

DIC/DOC measurements (Figure 3.15) confirmed biological activity. Control flasks showed stable DIC DOC profiles, while HET setups displayed a DOC decrease and concurrent DIC increase, consistent with active HD and acetate consumption.

The increase in DIC reflects the $CO_2$ production from the HD. However, at elevated $H_2S$ concentrations, a lower DOC decrease was observed. This, together with the lowered $r_{max}$ confirms the inhibitory effect of $H_2S$ on heterotrophic denitrification.

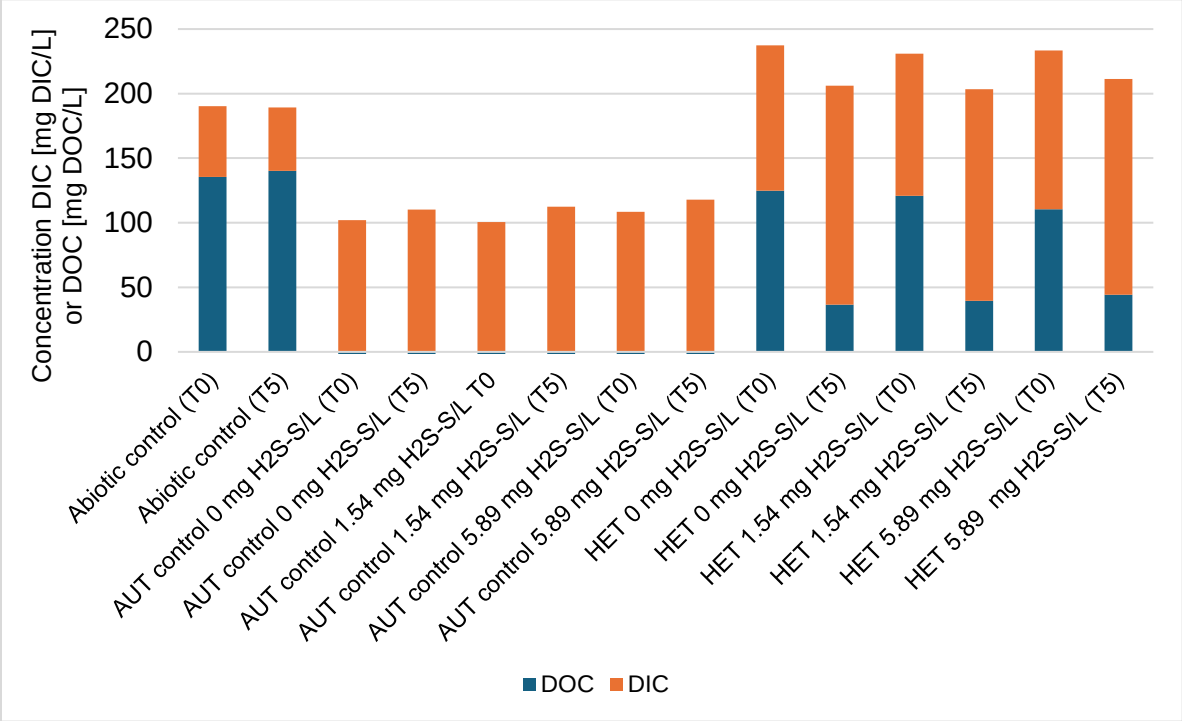


*Figure 3.15: The average DIC and DOC of each condition at the start and end of Test B. The orange bars present the DIC and the blue bars the DOC [mg/L]. The abiotic control was performed as a single replicate.*

### 3.1.4.3 Test B: Indications of autotrophic sulphide-driven denitrification activity

Autotrophic setups in Test B, even the control without $H_2S$, also showed nitrite accumulation, suggesting that SAD was not the sole cause. It could be due to residual COD present in the sludge, inducing slow HD activity. According to J. Oh & Silverstein (1999), nitrite buildup without further reduction occurs when acetate-COD is limiting. However, it cannot be confirmed that HD is the main contributor to these rates, as $r_{max}$'s do not differ significantly. Moreover, no clear DOC was detected at T0 in the DIC/DOC analysis, but cell lysis may have released COD too large to pass through the filter, and thus not measured as DOC. Notably, the autotrophic setup with the highest sulphide dosed showed the lowest nitrite buildup, despite similar nitrate removal rates. This might indicate minor SAD, as autotrophs could use nitrite for sulphur oxidation. However, this contribution is probably very small compared to the heterotrophic contribution in this setup. Table A.9 supports this, showing that only the autotrophic 5.89 mg $H_2S$-S/L setup reached S/N ratios high above stoichiometric thresholds for complete SAD.

This suggest SAD may have occurred, potentially explaining the more rapid TDS drops and reduced inhibition of HD. However, to confirm this, higher nitrate dosages would have been required to extend the test duration, as nitrate became depleted towards the end. Lastly, Autotrophic flasks showed no DOC decrease and minimal DIC change, consistent with limited SAD activity (Figure 3.15).

#### 3.1.4.4 Apparent growth kinetics in heterotrophic- and mixed-favoured conditions

To quantitatively asses inhibition, microbial growth was modelled using Monod kinetics with an added inhibition term. Figure 3.16 illustrates the decline in microbial growth with rising $H_2S$ concentrations for both tests. Model-based μmax values were derived using Ki values obtained from Lineweaver-Burk plots (Figure A.6), yielding $K_{i,H2S-NO3}$ values of 1.43 (Test A) and 7.62 mg $H_2S$-S/L (Test B). Because SAD could not be fully excluded in Test B, a range of $K_i$ values was considered, correcting for possible SAD activity. This resulted in $K_{i,H2S-NO3}$ between 4.26 and 7.62 mg $H_2S$-S/L. Further testing is needed to refine these estimates. The lower limit of the $K_i$ from Test B aligns reasonably with literature values (~3.88 mg $H_2S$-S/L at pH 7.5), while the upper value is nearly twice as high. Also, the lower value from Test A (1.43 mg $H_2S$-S/L) suggests stronger inhibition. This discrepancy may be due to decreasing TDS (and thus $H_2S$) levels over the test (decreased inhibition) or diffusion limitations in more flocculated sludge (Stewart, 2003).

Modelled $\mu_{max}$ values for Test A were 0.01036, 0.00701, and 0.00966 $h^{-1}$ for 0, 0.66, and 4.26 mg $H_2S$-S/L, respectively. In Test B, growth decreased more clearly with rising inhibitor levels: 0.01713, 0.01425, and 0.00966 $h^{-1}$ for 0, 1.54, and 5.89 mg $H_2S$-S/L. This stronger inhibition in Test A was likely due to previously discussed factors. Observed $\mu_{max}$ values confirm these trends. For Test A: 0.01036 ± 0.00015, 0.00589 ± 0.00024, and 0.00253 ± 0.00014 $h^{-1}$ (0–4.26 mg $H_2S$-S/L). For Test B: 0.01713 ± 0.00057, 0.01667 ± 0.00011, and 0.00993 ± 0.00038 $h^{-1}$ (0–5.89 mg $H_2S$-S/L).

While the highest-$H_2S$ setups showed no significant difference ($p > 0.05$), the intermediate concentrations differed significantly ($p < 0.05$).

In Figure A.6, the Lineweaver-Burk plot illustrates the relationship derived from a non-competitive model. Pure heterotrophic activity was assumed. The observed slopes of 67.35 (a) and 7.66 (b) provide the basis for determining the $K_{i,H2S-NO3}$ for HD.

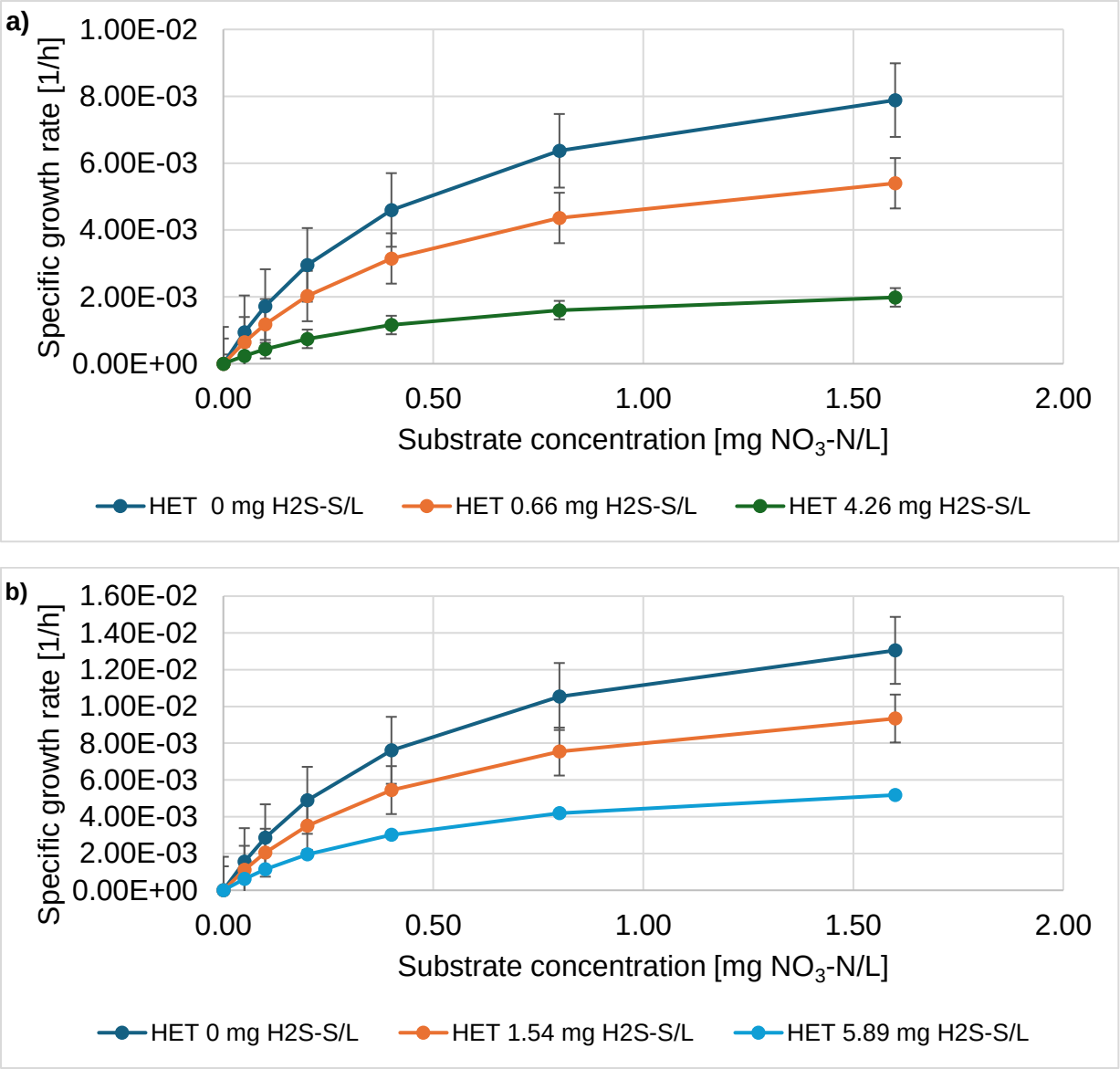


*Figure 3.16: Comparison of the specific growth rates [1/h] for fresh sludge over different substrate concentrations [mg NO3-N/L] in HET conditions under different inhibitor concentrations Test A (a) (0, 0.66 and 4.26 mg $H_2S$-S/L) and Test B (b) (0, 1.54 and 5.89 mg $H_2S$-S/L).*

### 3.1.4.5 Influence of dosing times

When sulphide was dosed at the start of the experiment, a stronger inhibitory effect was observed compared to later dosing moments. This is a notable finding, as it clearly impacts the biological kinetics of the system. It is therefore hypothesized that in sewer systems, the timing of dosing presents a classic "chicken-or-egg" scenario: if nitrified urine is dosed before hydrogen sulphide forms, inhibition is expected to be lower.

Conversely, if sulphide is already present before nitrate addition (anaerobic to anoxic conditions), stronger inhibition may occur. While the latter scenario would reduce the required dose of nitrified urine, it may result in increased odor formation and corrosion.

In addition, no significant nitrite accumulation was observed in Test A under MIXED conditions, whereas Test B showed clear patterns of nitrite accumulation followed by consumption. This suggests that the sequence and timing of nitrate and sulphide availability not only affect inhibition, but also influence the intermediate dynamics of the denitrification pathway in a mixed setup.

### 3.1.5 Mini-batch test 2: TDS losses at varying biomass concentration

To better understand the unexpected decline in TDS during the HET inhibition test, an additional experiment was carried out to explore whether TDS losses are proportional to the amount of active sludge added. Since no electron donors or acceptors were present during this phase (except for TDS), biological activity could not account for the observed decrease. However, IC results do show the presence of nitrate. This is possibly due to insufficient washing of the sludge. Figure 3.17 reveals a strong linear correlation between biomass concentration and TDS losses between the moment of dosing (T0-1) and the first sampling (T0).

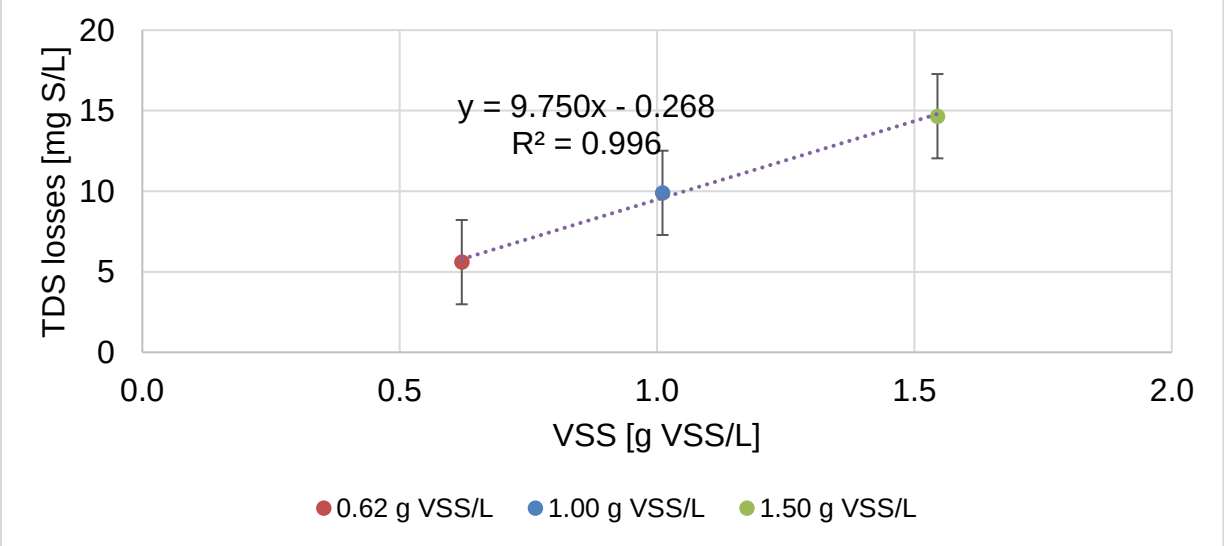


*Figure 3.17: The average TDS concentration [mg S/L] per average of the active biomass concentration [g VSS/L] for three different conditions, each performed in duplicate.*

The observation that higher biomass concentrations resulted in greater early TDS reductions suggests a likely role for adsorption mechanisms, where negatively charged sulphide ions ($HS^-$ and $S^{2-}$) bind to positively charged sites on the sludge, matrix, such as protonated amines or metal ions (*e.g.*, $Fe^{3+}$, $Ca^{2+}$) associated with organic material.

This form of chemisorption is typically stronger and more irreversible than physical adsorption. Bagreev et al. (2001) acknowledges this sulphur adsorption capability of sewage sludge, here the sulphide binds to iron, zinc or calcium's positive charges on the edges of the sludge particles.

Visual observations during the test align with this interpretation. Under sulphide dosing conditions, the sludge acquired a blackish coloration, indicative of iron sulphide (FeS) precipitation (Figure A.3). However, the absence of the greyish-white tint typically associated with calcium sulphide precipitates could suggest either a limited role of calcium or simply that the lighter hue was masked by the dominant FeS blackening. Together, these findings highlight the importance of considering abiotic sulphide removal pathways, notably adsorption and precipitation, when interpreting TDS dynamics in sludge systems exposed to sulphide.

## 3.1.6 General comparison of biomass growth and kinetic modelling

### 3.1.6.1 Biomass growth model for HD versus SAD of fresh sludge

Figure 3.18 presents the specific growth rates derived from the experiments. For SAD, both enriched and fresh sludge were included to reflect real sewer conditions, where microbial communities vary depending on *i.a.* sulphur exposure. Zones with frequent sulphide input tend to host more adapted autotrophic populations, while areas with low sulphur input contain less specialized biofilms.

The highest observed $r_{max}$ for HD (without $H_2S$ inhibition) was 303.3 ± 4.3 mg $NO_3$-N/ (g VSS d). This is considerably higher than the maximal SAD rate in fresh sludge (48.28 ± 18.52 mg $NO_3$-N/ (g VSS d)). Similarly, the HD's $\mu_{max}$ (0.01036 ± 0.0041 $h^{-1}$) exceeded that of $HS^-$-enriched autotrophs (0.00638 ± 0.0049 $h^{-1}$). These findings suggest more nitrate dosing is required in heterotrophic dominated zones, unless sulphur is present in significant amounts. Rising $H_2S$ concentrations progressively inhibit HD activity, favouring SAD. At very low nitrate levels, HD can still dominate even under high $H_2S$ (*e.g.*, 16.7 mg $H_2S$-S/L) (Figure 3.18). As nitrate starts to increase, autotrophs gradually outcompete them despite their lower nitrate affinity.

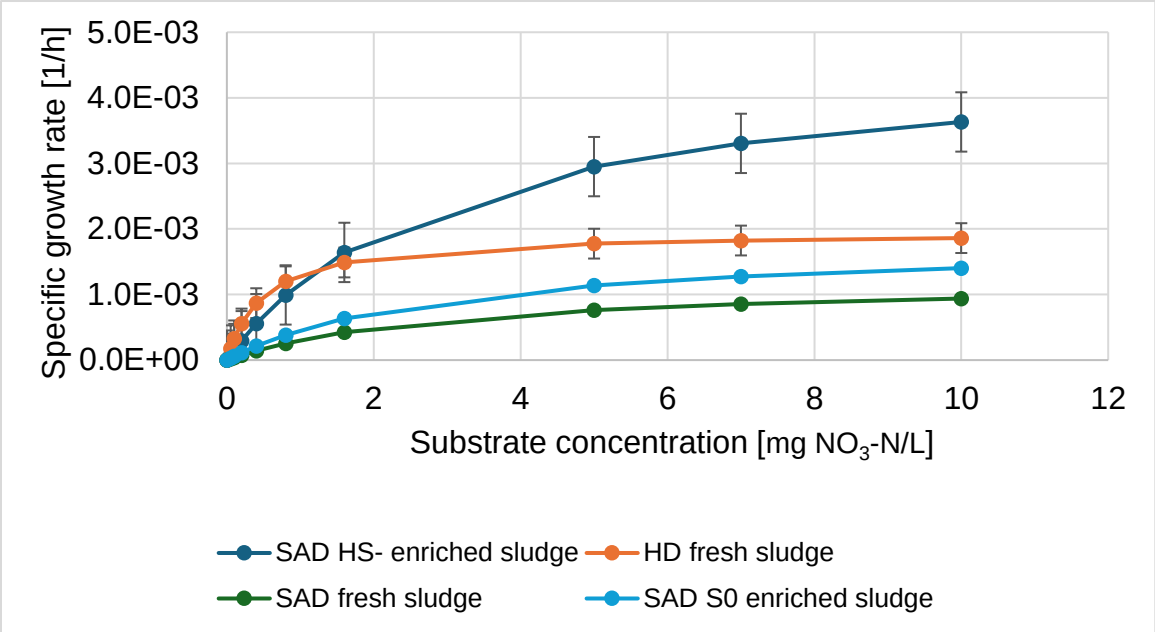


*Figure 3.18: A comparison of the average specific growth rate [1/h] per substrate concentration [g $NO_3$-N/L], for the maximal observed heterotrophic activity, and autotrophic activity of fresh, $S^0$ enriched and $HS^-$ enriched sludge. Every test was performed in triplicate.*

Figure 3.19 compares biomass growth kinetics of fresh sludge, $HS^-$-enriched sludge, and $S^0$-enriched sludge at 30 mg $NO_3$-N/L. These results provide insight into microbial dynamics across varying sulphur conditions. In $H_2S$ hotspots, SAD become dominant due to their adaptation to elevated sulphur, while in low-sulphur areas, HD prevail and autotrophic activity is minimal. A microbial adaptation phase is expected when sludge from low-sulphur zones is suddenly exposed to high $H_2S$ concentrations. A typical range for $H_2S$ in the sewer is difficult to give, as it depends on various factors. Typical $H_2S$ concentrations in sewers vary widely but can reach up to 16 mg $H_2S$-S/L, depending on conditions (Sutherland-Stacey, n.d.).

The observed $r_{max}$ in these experiments for $S^0$ and fresh sludge are 72.16 ± 14.05 mg $NO_3$-N/ (g VSS d) and 48.29 ± 18.53 mg $NO_3$-N/ (g VSS d), which are lower compared to the $r_{max}$ of the $HS^-$ enrichment ($r_{max}$ equals 186.78 ± 14.45 mg $NO_3$-N/ (g VSS d)), possibly due to adaptation needs, and since $S^0$ is a very stable compound which is slower oxidized compared to $HS^-$. At low inhibitor concentrations the heterotrophic growth rate starts to decrease significantly, highlighting their sensitivity. From a concentration of 10 mg $H_2S$-S/L (41.67 mg S/L, pH 7.5) the $HS^-$ enriched autotrophic growth starts to dominate.

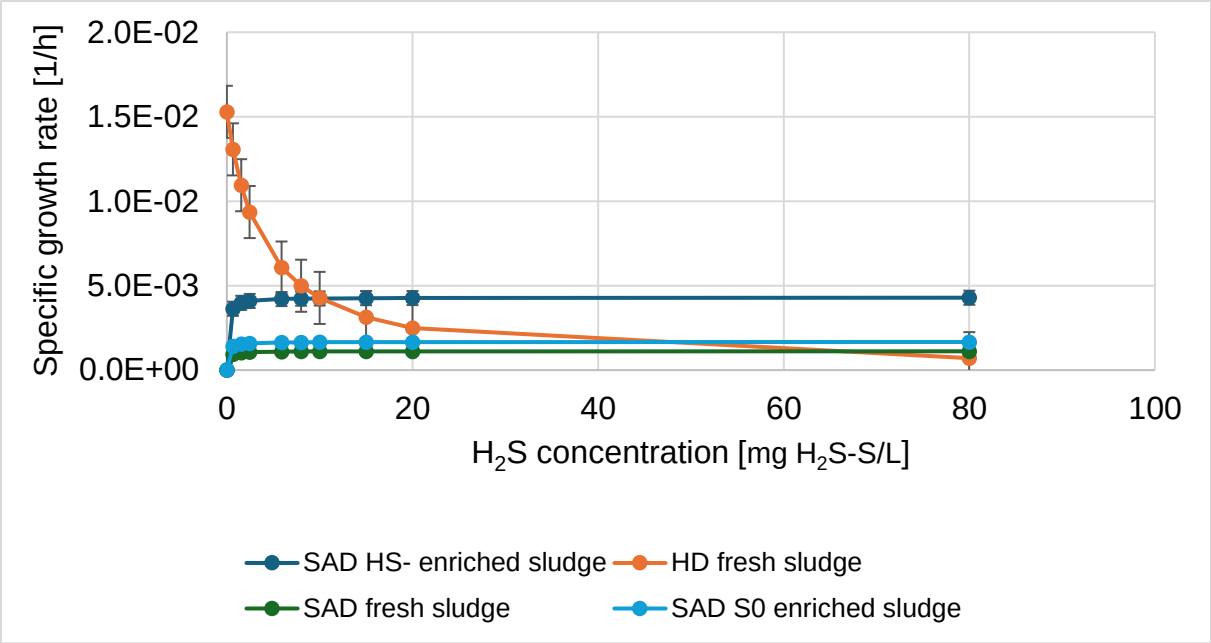


*Figure 3.19: Comparison of the average specific growth rate [1/h] for a fixed substrate concentration (30 mg $NO_3$-N/L) versus the $H_2S$ concentration [mg $H_2S$-S/L], for the maximal observed heterotrophic activity, and autotrophic activity of fresh, $S^0$ enriched and $HS^-$ enriched sludge. Every test was performed in triplicate.*

## 3.2 Nitrified urine dosing

### 3.2.1 Nitrified urine dosing demand

To estimate the required nitrate dosing to maintain anoxic conditions, a simplification of reality is made as temperature (21°C) and pH (7.5) are kept constant. Table 3.4 summarizes the key parameters used to estimate the nitrate dosing required to maintain a target concentration of 30 mg $NO_3$-N/L in the sewer. These include realistic domestic wastewater values for COD and $H_2S$, inhibition constants determined in this thesis, literature-based microbial yields, and realistic HRTs for gravity sewers. The inhibition constant used for this calculation was based on the worst case scenario for N-dosing. Meaning, a higher $K_i$ causes the lowest inhibitory effects, thus more dosing requirements.

Biological nitrate demand ($C_{NO3,demand}$) was estimated under various HRTs and microbial conditions: pure heterotrophic, pure autotrophic, and two MIXED scenarios (MIXED 1 and MIXED 2). In general, MIXED conditions are conditions in which both suphide and COD are present as electron acceptor. In these conditions, both HD and SAD activity are expected.

MIXED 1 reflects sludge with minimal sulphide adaptation (95% HD, 5% SAD), while MIXED 2 represents partially sulphide-adapted sludge (52% HD and 42% SAD), based on batch test results. A simplified Monod-based expression incorporating inhibition, to reflect real-world dynamics, was used:

$$r = r_{max} \cdot \frac{1}{1+K_I} \text{ and } C_{NO3,demand} = r.X.HRT$$

With:

$C_{NO3,demand}$: Nitrate demand of the denitrifiers [mg $NO_3$-N/L].

r: The nitrate removal rate accounting for inhibition [mg $NO_3$-N/ (g VSS h)].

X: The biomass concentration [g VSS/L].

HRT: Hydraulic retention time [h].

*Table 3.4: Overview of parameters used to calculate the nitrate demand for in-sewer dosing in a gravity sewer.*

| **Parameter** | **Value** | **Source** |
|---|---|---|
| **COD [mg $O_2$/L]** | 233.60-294.10 | (VMM, n.d.) |
| **$H_2S$ [mg $H_2S$-S/L]** | 5.25-7.00 | (Salehi & Chaiprapat, 2022) |
| **Urine [mg TN/L nitrified]*** | | (Larsen et al., 2021) |
| **$\rho_{urine}$ [g/mL]** | 1.03 | (Malik, n.d.) |
| **$K_{i,H2S-NO3}$ [mg $H_2S$-S/L]** | 7.62 | Results thesis |
| **$Y_{HET/NO3}$ [g VSS/ g $NO_3$-N]** | 0.82 | (Di Capua et al., 2019)(Di Capua et al., 2019) |
| **$Y_{AUT/NO3}$ [g VSS/ g $NO_3$-N]** | 0.74 ($S^0$ oxidation)<br>0.61 (sulphide oxidation) | |
| **$K_{NO3, HET}$ [mg $NO_3$-N/L]** | 0.50 | (Calise et al., 2020) |
| **$K_{NO3,AUT}$ [mg $NO_3$-N/L]** | 3.00 | (S.-E. Oh et al., 2000) |
| **X [g VSS/L]** | 0.40 | (Sharma et al., 2023) |
| **$r_{max,HET}$ [mg $NO_3$-N/ (g VSS h)]** | 12.63 | Results thesis |
| **$r_{max, AUT}$ [mg $NO_3$-N/ (g VSS h)]** | 7.78 | Results thesis |
| **$r_{max,MIXED}$ [mg $NO_3$-N/ (g VSS h)]** | 4.13 | Results thesis |
| **HRT [h]** | 0.50-9.00 | - |

*Calculated based on Larsen et al. (2021).

Nitrified urine dosing requirements increased significantly with longer HRT (Table A.2). For example, under pure autotrophic conditions (High Sulphide), the required dosing rose by approximately 82%, from 31.53 mg $NO_3$-N/L at HRT 0.5 h to 57.52 mg $NO_3$-N/L at HRT 9 h. A similar trend was observed for the pure heterotrophic community (Low Sulphide), where the dosing requirement increased by around 81%, from 31.49 to 56.86 mg $NO_3$-N/L. MIXED 1 (High COD, Low Sulphide; 95% HD, 5% SAD) showed an increase of ~81%, from 31.49 to 56.89 mg $NO_3^-$-N/L, while MIXED 2 (High COD, Low Sulphide; 52% HD, 48% SAD) exhibited a similar rise of ~82%, from 31.52 to 57.43 mg $NO_3$-N/L. In contrast, variations in COD and sulphide concentrations had only a minor effect on dosing needs compared to the influence of HRT. These findings highlight that both HRT and microbial community composition are key determinants in optimizing nitrified urine dosing for in-sewer denitrification.

### 3.2.2 Application potential

To illustrate the application potential of the proposed in-sewer pretreatment strategy, a scenario was simulated for a gravity sewer system serving an apartment complex of 100 residents. The wastewater produced per person was assumed to be 110 L/pp/d. Also, a urine separation efficiency of 80% and nitrification efficiency of 90% were assumed. For this application, the values obtained from 3.2.1 were used.

Figure 3.20 shows the percentage of the residents from the building that need to source separate in order to obtain a stable value of 30 mg $NO_3$-N/L in the sewer system at four different retention times. These conditions were simulated for pure heterotrophic, pure autotrophic and MIXED conditions. The red line indicates the maximum possible dosing contributors in the 100 resident building. All values above this line show there is an external (chemical) nitrate dosing need, probably coming from a non-renewable source. Depending on the HRT, COD and sulphide concentrations, and microbial community, 47–86% of urine needs to be source separated to meet denitrification demand.

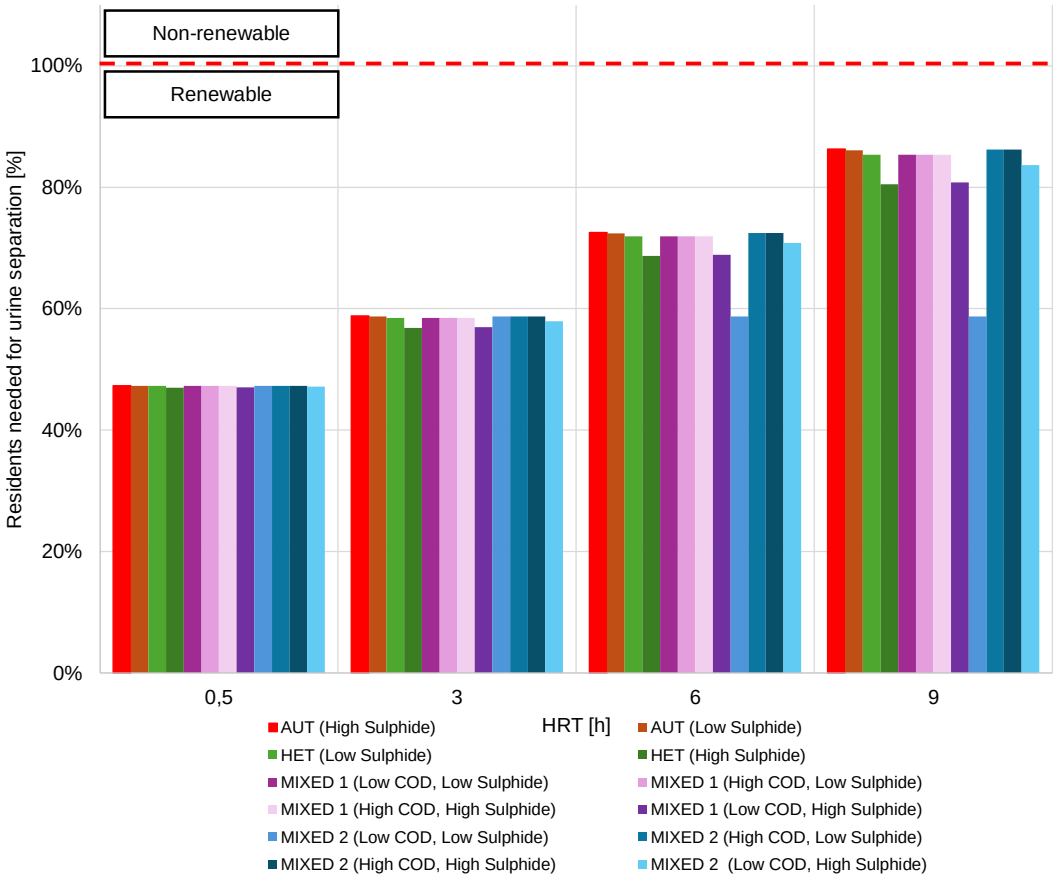


*Figure 3.20: Percentage of residents required to participate in urine source separation under varying HRTs (0.5, 3, 6, and 9). Shown for pure autotrophic, pure heterotrophic, and MIXED conditions. MIXED 1 consists of 95% HD and 5% SAD; MIXED 2 consists of 52% HD and 48% SAD. $H_2S$ acts as inhibitor for HD. Conditions include Low COD (233.60 mg $O_2$/L) and High COD (294.10 mg $O_2$/L), but also Low Sulphide (5.25 mg $H_2S$-S/L), and High Sulphide (7.00 mg $H_2S$-S/L).*

Overall, the results show that nitrate demand generally increases with longer HRTs, particularly under heterotrophic and mixed conditions, due to prolonged microbial interaction with the nitrate present in the waste water. Additionally, higher inhibitor concentrations such as COD and $H_2S$ reduce nitrate consumption, as microbial denitrification is suppressed. If the calculated urine separation efficiencies would exceed 100%, the required nitrate cannot be practically supplied by the residents' urine alone. This scenario demonstrates the application potential of using nitrified urine as an alternative nitrate source to the sewer system to mitigate odors, lower sewer corrosion, and methane emissions, by maintaining anoxic conditions.

# 4. Conclusion and future outlook

This study explored the maximum nitrate removal potential of SAD and acetate-based HD under nitrate-limiting conditions. Using batch experiments and kinetic modelling, the following conclusions were drawn in response to the research questions:

**What are the maximum achievable $r_{max}$ [mg $NO_3$-N/(g VSS d)] of heterotrophic and autotrophic sulphide-driven denitrification?**

Denitrification rates are influenced by various factors, including temperature, pH, substrate availability, inhibitor concentrations, and the degree of microbial enrichment. In this study, all rates were conducted under controlled conditions (T = 21°C, pH = 7.5) allowing for consistent comparison across tests. The maximum $r_{max}$ for HD using fresh sludge was found to be **303.3 ± 4.3** mg $NO_3$-N/ (g VSS d). In contrast, SAD using fresh sludge initially resulted in much lower rates, with only **48.29 ± 18.53** mg $NO_3$-N/ (g VSS d) removed. However, enrichment with sulphur substrates clearly increased the autotrophic activity. $S^0$ enrichment increased the rate to **72.16 ± 14.05** mg $NO_3$-N/ (g VSS d), while $HS^-$ enrichment yielded the highest autotrophic rate of **186.78 ± 14.45** mg $NO_3$-N/ (g VSS d). These $r_{max}$ values are consistent with those reported in literature: 11-740.48 mg $NO_3$-N/ (g VSS d) (HD), 35.37-168.56 mg $NO_3$-N/ (g VSS d) (SAD, $HS^-$), and 38.88-534 mg $NO_3$-N/ (g VSS d) (MIXED).

The results confirm the initial hypothesis: HD shows higher $r_{max}$ values than SAD under similar conditions, due to slower autotrophic kinetics. Nevertheless, at elevated $H_2S$ levels, known to inhibit HD, enriched autotrophic cultures achieved competitive growth rates (Figure 3.19). These $r_{max}$ values are not only relevant for modelling, but also critical to estimate the nitrate dose required to maintain anoxic sewer conditions.

**How do HD and SAD interact in a MIXED setup?**

MIXED conditions were expected to promote synergistic nitrate removal via complementary substrate use and $H_2S$ mitigation. Yet, experiments showed a substrate-driven shift in dominance: high acetate-COD levels favoured HD, potentially even in the enriched sludge. Furthermore, HD and SAD did show some signs of possible co-operation, as no nitrite accumulation was observed under these MIXED conditions, while sulphate oxidation was mostly observed towards the end. On top of this, DIC DOC data showed a decrease in both DIC and DOC, pointing out the activity

of both groups. The reduced $r_{max}$ observed under high COD conditions in the SAD-enriched sludge might also indicate a possible inhibitory effect of acetate. Further testing is required to verify this hypothesis and elucidate the underlying mechanisms. Understanding this dynamic is crucial, as it may influence microbial behaviour in the sewer and, consequently, impact nitrate dosing for effective $H_2S$ control.

Interestingly, no significant difference in overall nitrate removal was observed between fresh sludge (predominantly HD) and sulphide-enriched sludge (with increased SAD activity). Maximum nitrate removal rates were 119.07 ± 13.71 and 108.55 ± 20.55 mg $NO_3$-N/(g VSS d) for fresh and enriched sludge, respectively. Nonetheless, the $r_{max}$ of pure HD and SAD indicated a change in microbial community composition. Moreover, the enriched sludge showed a clear lag phase, likely indicating minimal initial HD activity and a delayed onset of HD dominance under inhibitory conditions. In COD-rich tests, $S^0$ was the main product, with later conversion to sulphate. Under these conditions, removal rates were lower than in HD-dominant systems, but notably higher than in fresh autotrophic sludge.

Overall, these findings point to substrate ($NO_3$)-driven competition rather than cooperation, although indirect benefits, such as sulphide removal by SAD mitigating $H_2S$ inhibition of HD, may still play a role.

**What is the $K_{i,H2S-NO3}$ of fresh sewage sludge from Aquafin Aartselaar?**

Sulphide dosing has a clear inhibitory effect on HD activity, with the extent of inhibition strongly influenced by the timing of sulphide dosing. When sulphide was added at the start of the test (Test A), inhibition was more severe, resulting in a $K_{i,H2S-NO3}$ of 1.43 mg $H_2S$-S/L. But, dosing sulphide during denitrification (Test B) seemed to lower the sensitivity. The was possibly due to either the delayed inhibitor exposure or the more enriched and pre-activated sludge used in this test. In Test B, activity reductions of 4.86 ± 1.0% and 56.47 ± 1.0% were observed at 1.54 and 5.89 mg $H_2S$-S/L, respectively. As SAD could not be entirely excluded, the $K_{i,H2S-NO3}$ yielded was 4.26-7.62 mg $H_2S$-S/L. Strong sulphide losses at the start of the experiments were likely due to abiotic adsorption, as removal scaled with sludge concentration. These findings are crucial for understanding microbial dynamics in sewer biofilms and should be integrated into nitrate dosing strategies, as sulphide inhibition can significantly impact in-sewer denitrification performance and odour control efficiency.

**How much nitrified urine [mg $NO_3$-N/L] must be dosed to the sewer (reactor) to maintain anoxic conditions?**

Nitrified urine dosing needs increased with HRT across all tested conditions. Under purely autotrophic conditions, the requirements ranged from 31.53 to 57.52 mg $NO_3$-N/$L_{sewage}$. Purely heterotrophic communities exhibited higher demands, ranging from 31.50 to 57.37 mg $NO_3$-N/L. MIXED 1 (95% heterotrophic, 5% autotrophic) showed a slightly lower requirement (31.49–56.89 mg $NO_3$-N/L), while MIXED 2 (52% heterotrophic, 48% autotrophic) demonstrated a more moderate range of 31.52 to 57.43 mg $NO_3$-N/L. Variations in COD and sulphide levels had only minor effects compared to the influence of HRT. These findings highlight the significant impact of microbial community composition on nitrified urine dosing strategies.

The **simulation** made showed the influence of HRT, microbial composition and inhibitor ($H_2S$) presence on the dosing requirements and if urine separation alone is feasible enough to maintain these anoxic conditions. Longer HRTs, especially under heterotrophic and mixed conditions with high heterotrophic abundancy, resulted in higher nitrate demand due to the higher substrate affinity and faster growth of the heterotrophic organisms. Furthermore, higher concentrations of inhibitor reduce nitrate needs by suppressing microbial activity. The simulation showed that nitrified urine dosing as standalone technique is enough to maintain anoxic conditions in the sewer, thus external dosing of the unsustainable chemical nitrate becomes unnecessary.

**Future Outlook**

Lastly, to further unravel the complex interactions between heterotrophic and autotrophic denitrifiers, future experiments could investigate the impact of mixing different ratios of enriched and fresh sludge. This would help simulate the spatial heterogeneity found in real sewer biofilms, where certain zones experience persistent $H_2S$ exposure while others do not. Long-term studies would also be valuable to observe how microbial communities stabilize over time and to assess how sustained acetate-COD availability influences SAD activity and potential microbial coexistence. Ultimately, integrating these microbial dynamics into full-scale models could enhance the reuse of nitrate from urine and pave the way for more sustainable, resource-efficient strategies for odour and corrosion control in sewers.

# 5.Appendix

*Table A.1: Overview of techniques closely related to the thesis, showing the scale of the experiment and compounds dosed and measured. The crosses indicate in which study a batch test was performed.*

| Topic | Compound Dosed | Batch Test | Compound Measured | Source |
|---|---|---|---|---|
| Nitrified urine impact | Nitrified urine, sewage, $Ca(NO_3)_2$ | OUR batch | COD, TKN, $NH_4^+$ (EFF) | (F. Jiang et al., 2011, p. 20) |
| Mixotrophic interactions with nitrified urine dosage | $Ca(NO_3)_2$, $CH_3COONa$, $S^{2-}$ | x | $NO_3^-$, $NO_2^-$, $S^{2-}$, $SO_4^{2-}$, VFA, COD | (F. Jiang et al., 2013b) |
| Nitrified urine impact in sewers | Nitrified urine, $NO_3^-$ | | $NO_3^-$, $NO_2^-$, $NH_4^+$, $H_2S$ | (Oosterhuis & Van Loosdrecht, 2009) |
| $NO_3^-$ dose optimalisation | $S^{2-}$, $SO_4^{2-}$, $HS^-$, thiosulfate, $NO_3^-$, VFA | x | $H_2S$, $S^{2-}$, $NO_3^-$ | (Gutierrez et al., 2008) |
| S/N ratio on SAD | $Na_2S.0.5H_2O$, $NO_3^-$ | x | $S^{2-}$, $SO_4^{2-}$, $NO_3^-$, $NO_2^-$, TAN | (Dolejs et al., 2015) |
| Investigation of the HAD process | Synthetic wastewater, $Na_2S.9H_2O$, $NaAc.3H_2O$, $NO_3^-$ | | $NO_3^-$, acetate, $S^{2-}$, $NO_2^-$, $SO_4^{2-}$, $S^0$ | (G. Xu et al., 2015) |
| $S^{2-}$ on mixotrophic denitrification dominated by *Thauera* | $CH_3COONa$, $NO_3^-$, $S^{2-}$ | x | $NO_3^-$, $S^{2-}$, $NO_2^-$, total organic carbon (TOC), $SO_4^{2-}$, thiosulfate | (Liang et al., 2020b) |
| $S^{2-}$ oxidation AD | Thiosulfate, $KNO_3$, $S^0$, $Na_2S.7H_2O$ | x | $NO_3^-$, $NO_2^-$, thiosulfate | (Cardoso et al., 2006) |
| Simultaneous HD-SAD for N, S and C removal | $NaNO_3$, $Na_2S_2O_3.5H_2O$, $CH_3COOK$ | x | $NO_3^-$, $NO_2^-$, thiosulfate acetate, $SO_4^{2-}$ | (Peirano et al., 2020) |
| Cross effect T, pH and FA on AD | $NaNO_3$, $S^{2-}$ | x | $S^{2-}$, $NO_3^-$, FA | (Fajardo et al., 2014) |
| $N_2O$ under nitrifying and denitrifying conditions | $NaNO_3$, $CH_3COONa$ | x | $NO_2^-$, $NH_4^+$, $N_2O$ | (Wunderlin et al., 2012) |
| S-driven $N_2O$ emissions in mixotrophs | Synthetic wastewater, $Na_2S$, $NaNO_3$, glucose | x | $N_2O$, $NO_2^-$, $NO_3^-$, $SO_4^{2-}$, TDS | (Yu et al., 2023) |
| Different C-sources for denitrification | $CH_3COONa$, (m)ethanol, glucose | x | Denitrification rates | (Cherchi et al., 2009b) |

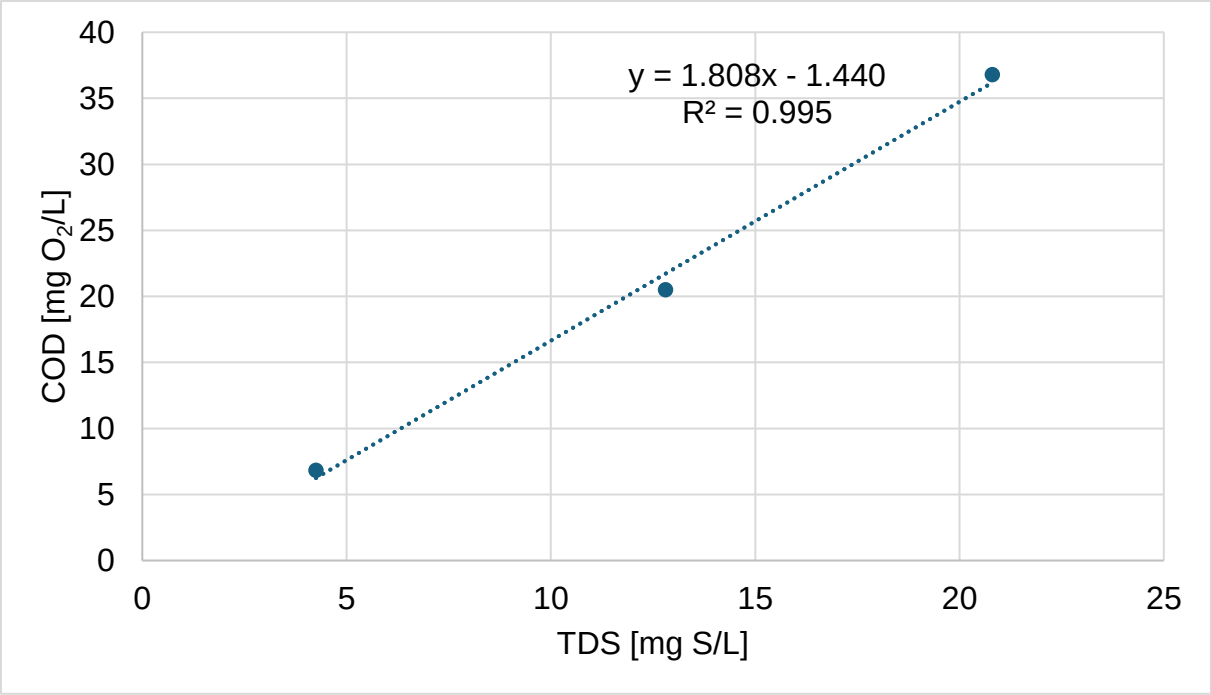


*Figure A.1: The measured COD concentrations [mg $O_2$/L] over the measured TDS concentrations [mg S/L] for three different TDS concentrations.*

*Table A.2 Part 1: Parameters, setup and philosophy of the test to determine the maximal denitrification performance for HD, SAD and MIXED.*

| **Parameter + concentration** | **Abiotic control** | **Heterotrophs** | **Autotrophs** | **MIXED** | **Philosophy** |
|---|---|---|---|---|---|
| **$Ca(NO_3)_2.4H_2O$**<br>**[mg $NO_3$-N/L]** | 30 | 30 | 30 | 30 | Nitrate dosage is based on Table 1.2. This value was multiplied by biomass concentration, based on the duration. Here, nitrate is the limiting substrate. |
| **$Na_2S.xH_2O$**<br>**[mg S/L]** | 47.07 | x | 47.07 | 26.00 | **SAD**: **S/N of 1.569** was chosen (slightly above stoichiometric ratio of 1.43 g S/ g $NO_3$-N) to be not S limiting and obtain max denitrification. Dolejs et al. (2015) reported that an S/N ratio > 6.41 g S/ g $NO_3$-N inhibited denitrification.<br><br>**MIXED**: Opted for a lower S/N since low sulphur concentrations would inhibit HD, therefore a lower concentration was chosen. On top of this the MIXED conditions were performed in fed-batch to ensure less inhibition of the HD. |
| **$CH_3COONa$ [mg $O_2$/L]** | 210 | 210 | x | 210 | A **COD/N of 7** was chosen since COD/N < 5.3 g $O_2$/g $NO_3$-N would be insufficient according to (Dolejs et al., 2015). There should be enough electron donor present to avoid limitations.<br><br>However, COD may not be too high in MIXED conditions, otherwise SAD inhibition (Table 1.3b). |

*Table A.2 Part 2: Parameters, setup and philosophy of the test to determine the maximal denitrification performance for HD, SAD and MIXED.*

| **Parameter + concentration** | **Abiotic control** | **Heterotrophs** | **Autotrophs** | **MIXED** | **Philosophy** |
|---|---|---|---|---|---|
| **$NaHCO_3$ [mg/L]** | 30 | 30 | 30 | 30 | To make sure autotrophs and MIXED did not enter **inorganic carbon limitations** (the inorganic carbon could be removed due to sparging) |
| **Synthetic medium [mL]** | 207 | 226 | 209 | 245 | Medium was added to ensue reproducibility across tests, and to eliminate potential limitations in trace elements. The total amount of parameters is around 300 mL at the beginning of the test to take 50 mL for DIC DOC and TSS VSS measurements. |
| **Nitrified urine [mg $NO_3$-N/L]** | 30 | 30 | 30 | 30 | To have a source of nitrified urine. This will also be present in the sewer reactor, therefore dosing it makes the test more representative. |
| **Sludge [ g VSS/L]** | x | 0.5 | 0.5 | 0.5 | To ensure enough time for sampling a low VSS concentration was chosen<br>The fresh sludge was activated by aeration. |

*Table A.3: Parameters, setup and philosophy of the test to determine the maximal denitrification performance SAD using $S^0$ enriched sludge.*

| **Parameter + concentration** | **Abiotic control*** | **Autotrophs S/N 0.75** | **Autotrophs S/N 1** | **Autotrophs S/N 1.5** | **Philosophy*** |
|---|---|---|---|---|---|
| **$Ca(NO_3)_2.4H_2O$ [mg $NO_3$-N/L]** | 60 | 60 | 60 | 60 | The amount of N dosed is chosen based on maximal SAD rates obtained in 'Denitrification performance-Fresh sludge (Aquafin Zuid)' |
| **$Na_2S.xH_2O$ [mg TDS-S/L]**** | 90 | 45 | 60 | 90 | Dosing was performed in fed-batch formation. The total concentration wanted to be dosed was distributed equally over each timeframe. Three different S/N ratios were chosen to see their effect on SAD. The lower ratio is a bit more realistic to sewer conditions since we expect excess nitrate. |
| **$NaHCO_3$ [mg/L]** | 30 | 30 | 30 | 30 | x |
| **Synthetic medium [mL]** | 274 | 205 | 205 | 205 | x |
| **Nitrified urine [mg $NO_3$-N/L]** | 60 | 60 | 60 | 60 | x |
| **Sludge [g VSS/L]** | x | 0.5 | 0.5 | 0.5 | x |

*the empty cells follow the same philosophy as Table A.2. ** shows the total concentration dosed at the end of the test.

*Table A.4: Parameters, setup and philosophy of the test to determine the maximal denitrification performance of SAD using $HS^-$ enriched sludge.*

| **Parameter + concentration** | **Abiotic control*** | **Mixed control S/N 1.5** | **Autotrophs S/N 1.5** | **Philosophy*** |
|---|---|---|---|---|
| **$Ca(NO_3)_2.4H_2O$ [mg $NO_3$-N/L]** | 60 | 60 | 60 | x |
| **$Na_2S.xH_2O$ [mg TDS-S/L]** | 90 | 90 | 90 | The choice of the highest S/N was based on results of 'SAD performance-$S^0$ enriched sludge' showing the highest SAD |
| **$NaHCO_3$ [mg/L]** | 7.50 | 6.63 | 6.63 | x |
| **Synthetic medium [mL]** | 244 | 211 | 216 | x |
| **Nitrified urine [mg $NO_3$-N/L]** | 60 | 60 | 60 | x |
| **Sludge [g VSS/L]** | x | 1.0 | 1.0 | To enhance microbial activity and accelerate observable responses, a higher substrate concentrations was applied. This approach allows for shorter test duration while enabling clearer detection of SAD. |

*the empty cells follow the same philosophy as Table A.2.

*Table A.5 Part 1: Parameters, setup and philosophy of the test to determine the inhibition concentration for HD performance.*

| **Parameter + concentration** | **Abiotic control** | **Autotrophic control (1) S/N 0** | **Autotrophic control (2) S/N 0.08** | **Authotrophic control (3) S/N 0.283** | **HD inhibition S/N 0** | **HD inhibition S/N 0.167** | **HD inhibition S/N 0.567** | **Philosophy*** |
|---|---|---|---|---|---|---|---|---|
| $Ca(NO_3)_2.4H_2O$ [mg $NO_3$-N/L] | 60 | 60 | 60 | 60 | 60 | 60 | 60 | Based on previous tests: ~180 mg $NO_3$-N/ g VSS/d is the maximal obtained HD rate (S/N 0). Work with 1 g VSS/L and duration of max 8h. |
| $CH_3COONa$ [mg $O_2$/L] | 420 | x | x | x | 420 | 420 | 420 | x |
| $Na_2S.xH_2O$ [mg $H_2S$-S/L]<br><br>Test A<br>Test B | 4.29<br>5.89 | x | 0.66<br>1.54 | 4.29<br>5.86 | x | 0.66<br>1.54 | 4.29<br>5.86 | concentrations are based on literature: Liang et al. (2020) observed 50% inhibition at ~3.88 mg $H_2S$-S/L and 71% inhibition at ~17.43 mg $H_2S$-S/L (pH 7.5). |

*Table A.5 Part 2: Parameters, setup and philosophy of the test to determine the inhibition concentration for HD performance.*

| **Parameter + concentration** | **Abiotic control** | **Autotrophic control (1) S/N 0** | **Autotrophic control (2) S/N 0.08** | **Autotrophic control (3) S/N 0.283** | **HD inhibition S/N 0** | **HD inhibition S/N 0.167** | **HD inhibition S/N 0.567** | **Philosophy*** |
|---|---|---|---|---|---|---|---|---|
| $NaHCO_3$ [mg/L] | 30 | 30 | 30 | 30 | 30 | 30 | 30 | x |
| Synthetic medium [mL] | 253 | 252.6 | 250.1 | 244.1 | 247.1 | 244.6 | 238.6 | x |
| Nitrified urine [mg $NO_3$-N/L] | 60 | 60 | 60 | 60 | 60 | 60 | 60 | x |
| Sludge [g VSS/L] | x | 1.0 | 1.0 | 1.0 | 1.0 | 1.0 | 1.0 | x |
| HCl (1 M) [mL] | 0.667 | x | 0.196 | 0.667 | x | 0.196 | 0.667 | To correct the pH to the desired range when sulphur is added. |

*the empty cells follow the same philosophy as Table A.4.

*Table A.6: Proposed setup of minibatch test 1, alongside the parameters dosed, their concentrations and philosophy of choice.*

| Parameter + concentration | Flask A | Flask B | Philosophy* |
|---|---|---|---|
| m($K_2HPO_4$) [g] | 0.35 | 0.35 | Phosphate buffer added to keep the pH neutral. |
| m($KH_2PO_4$) [g] | 0.24 | 0.24 | |
| $Na_2S.xH_2O$ [mg $H_2S$-S/L] | 15 | 45 | Two different sulphur concentrations were chosen to see if the trend remains constant. |
| Volume (tap water added) [mL] | 246.25 | 238.75 | Trace elements. |
| DO [mg $O_2$/L] | ≤ 0.50 | ≤ 0.50 | X |

*the empty cells follow the same philosophy as Table A.1.

*Table A.7: Proposed setup of mini batch test 2, alongside the parameters dosed, their concentrations and philosophy of choice.*

| Parameter + concentration | Abiotic control | Low VSS | Medium VSS | High VSS | Philosophy* |
|---|---|---|---|---|---|
| $Na_2S.xH_2O$ [mg $H_2S$-S/L] | 17 | 17 | 17 | 17 | These concentrations were based on the ones used for the heterotrophic inhibition test. |
| $NaHCO_3$ [mg/L] | 30 | 30 | 30 | 30 | X |
| Synthetic medium [mL] | | | | | X |
| DO [mg $O_2$/L] | ≤ 0.5 | ≤ 0.5 | ≤ 0.5 | ≤ 0.5 | X |
| Ph | 7.5-8.0 | 7.5-8.0 | 7.5-8.0 | 7.5-8.0 | X |
| Sludge [g VSS/L] | x | 0.62 | 1.00 | 1.50 | A higher VSS concentration is hypothesized to show more adsorption. |
| HCl (1 M) [mL] | 0.67 | x | 0.67 | 0.67 | To correct the pH to the desired range when sulphur is added. |

*the empty cells follow the same philosophy as Table A.2.

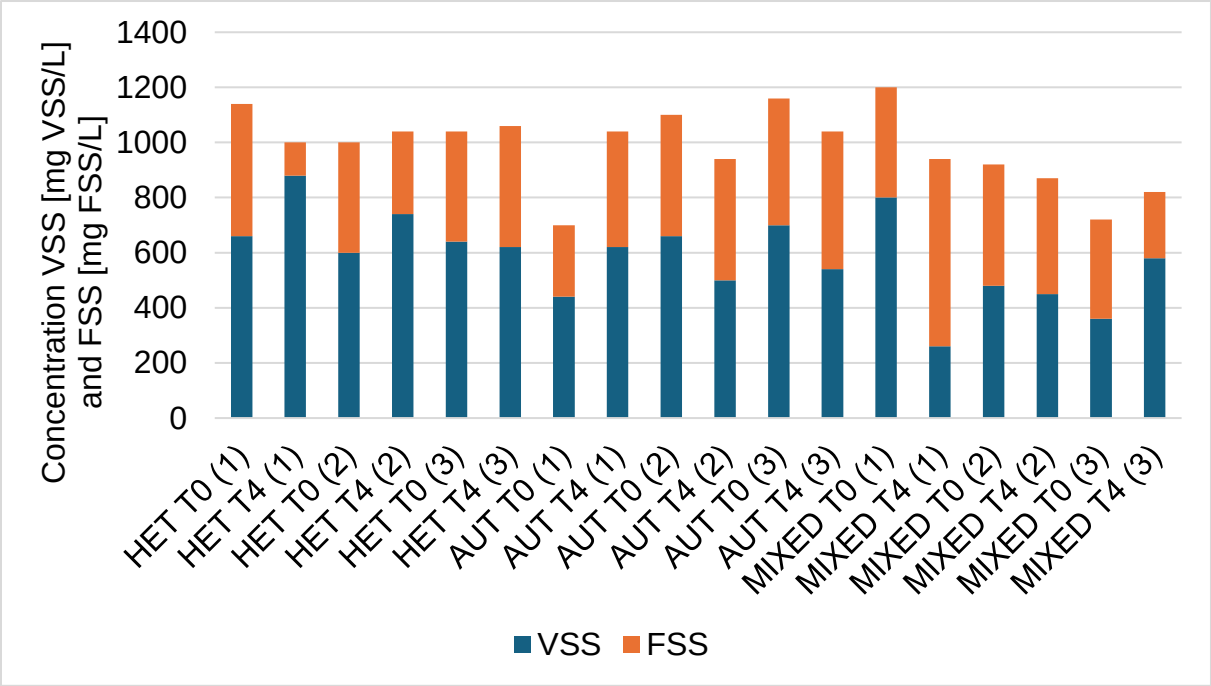


*Figure A.2: Volatile suspended solids (VSS) and Fixed suspended solids (FSS) concentrations for each flask at the start (T0) and end (T4) of the experiment.*


*Figure A.3: FeS precipitation in sludge causing the blackish color (left) compared with the same sludge without sulphur dosing (right).*

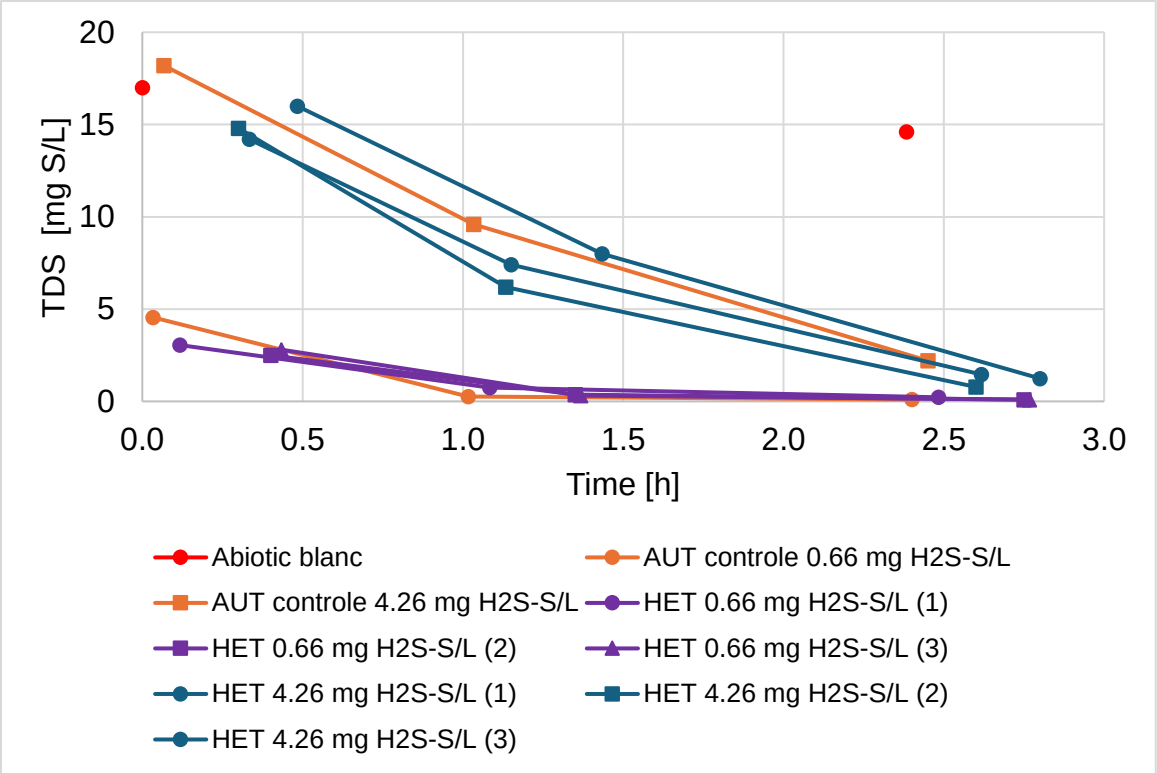


*Figure A.3: TDS concentration [mg S/L] per time [h] for Test A.*

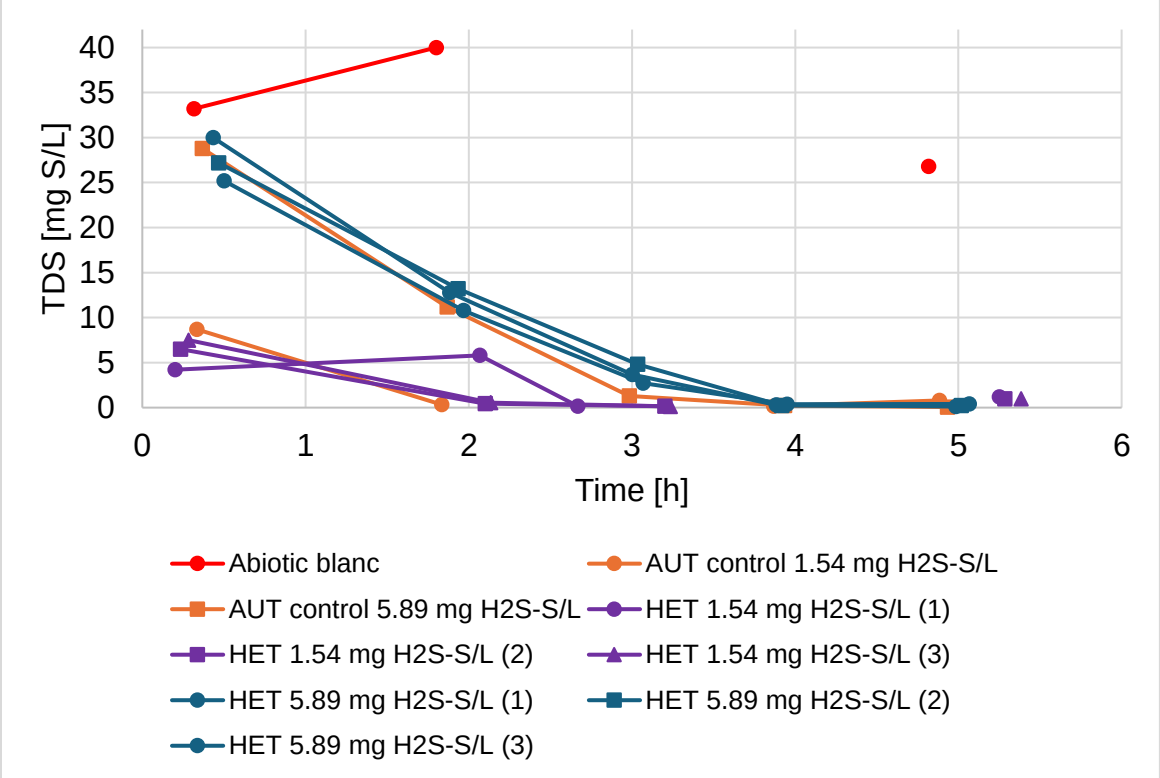


*Figure A.5: TDS concentration [mg S/L] per time [h] for Test B.*

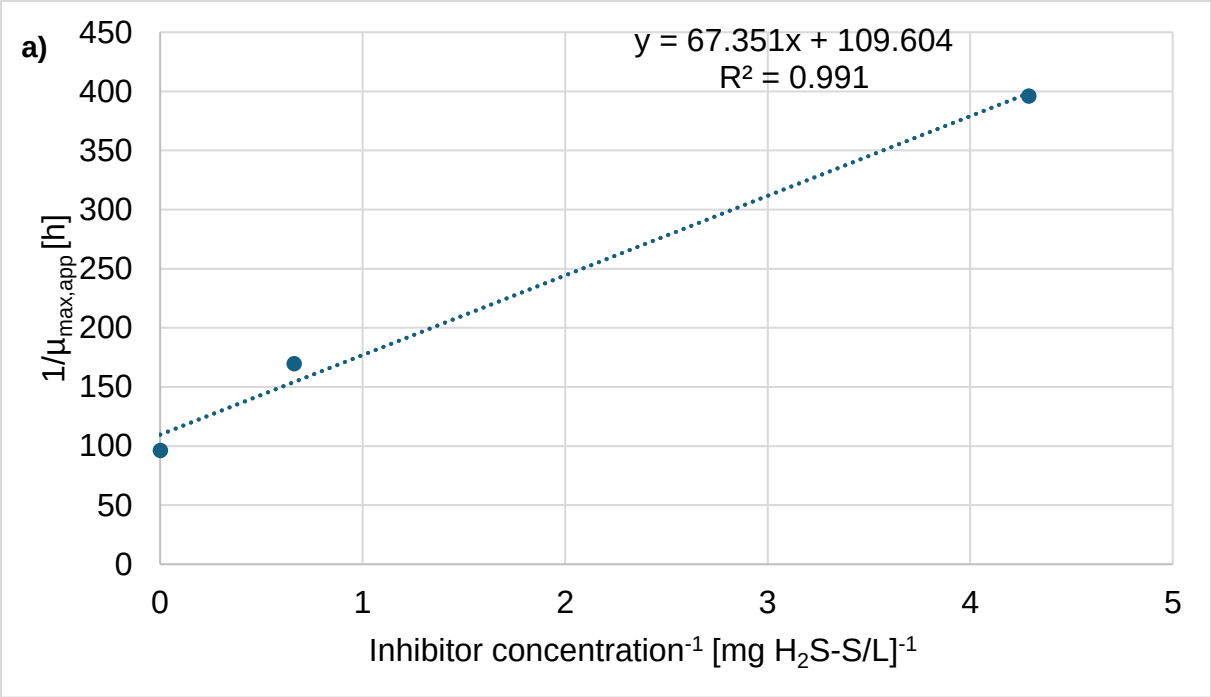


*Figure A.6: Display of a non-competitive Lineweaver-Burk inhibition plot of the inverse maximal observed growth rate [h] over the inverse of the inhibitor [mg $H_2S$-S/L]-1 for Test A (a) and Test B (b). The slope of the plot equals $1/\mu_{max}.K_{i,H2S-NO3}$.*

*Table A.8: Overview of the observed acetate-COD/N and S/N [g/g] across the autotrophic (AUT control) and heterotrophic (HET) conditions with different $H_2S$ concentrations (0, 0.66, 4.26 mg $H_2S$-S/L).*

| **Sample With inhibitor concentrations [mg $H_2S$-S/]** | **Acetate-COD/N removed over test (g $O_2$/g $NO_3$-N)** | **S/N removed over test (g S/g $NO_3$-N)** |
|---|---|---|
| AUT control 0 | - | - |
| AUT control 0.66 | - | 0.59 |
| AUT control 4.26 | - | 3.08 |
| HET 0 (1) | 3.46 | - |
| HET 0 (2) | 3.06 | - |
| HET 0 (3) | 6.51 | - |
| HET 0.66 (1) | -2.44 | 0.16 |
| HET 0.66 (2) | 0.32 | 0.15 |
| HET 0.66 (3) | 1.38 | 0.19 |
| HET 4.26 (1) | -14.82 | 2.11 |
| HET4.26 (2) | -1.45 | 2.60 |
| HET 4.26 (3) | -4.88 | 1.64 |

*Table A.9: Overview of the observed acetate-COD/N and S/N removal [g/g] across the autotrophic (AUT control) and heterotrophic (HET) conditions with different $H_2S$ concentrations (0, 1.54, 5.89 mg H2S-S/L).*

| **Sample With inhibitor concentrations [mg $H_2S$-S/]** | **Acetate-COD/N removed over test (g $O_2$/g $NO_3$-N)** | **S/N removed over test (g S/g $NO_3$-N)*** |
|---|---|---|
| **AUT CONTROL 0** | - | - |
| **AUT CONTROL 1.54** | - | 0.38 |
| **AUT CONTROL 5.89** | | 1.40 |
| **HET 0 (1)** | 3.21 | - |
| **HET 0 (2)** | 6.00 | - |
| **HET 0 (3)** | 4.96 | - |
| **HET 1.54 (1)** | 3.77 | 0.17 |
| **HET 1.54 (2)** | 8.44 | 0.29 |
| **HET 1.54 (3)** | 6.07 | - |
| **HET 5.89 (1)** | 4.82 | 15.26 |
| **HET 5.89 (2)** | 5.90 | - |
| **HET 5.89 (3)** | 6.77 | - |

**The S/N removed values for the HET flasks are corrected for the nitrate removed through HD assuming nitrate removal is solely true heterotrophic or autotrophic-sulphur driven denitrification.*

*Table A.10 Part 1: Concentration nitrified-urine needed under varying HRTs (0.5, 3, 6, and 9). Shown for pure autotrophic, pure heterotrophic, and MIXED conditions. MIXED 1 consists of 95% HD and 5% SAD; MIXED 2 consists of 52% HD and 48% SAD. $H_2S$ acts as an inhibitor for HD. Conditions include Low COD (233.60 mg $O_2$/L) and High COD (294.10 mg $O_2$/L), but also Low Sulphide (5.25 mg $H_2S$-S/L), and High Sulphide (7.00 mg $H_2S$-S/L).*

| **Condition + inhibitor concentration** | **HRT** | **Nitrified urine dosing need [mg $NO_3$-N/L]** |
|---|---|---|
| AUT (High COD) | 0.5 | 31.53 |
| AUT (High COD) | 3.0 | 39.17 |
| AUT (High COD) | 6.0 | 48.35 |
| AUT (High COD) | 9.0 | 57.52 |
| AUT (Low COD) | 0.5 | 31.52 |
| AUT (Low COD) | 3.0 | 39.12 |
| AUT (Low COD) | 6.0 | 48.25 |
| AUT (Low COD) | 9.0 | 57.37 |
| HET (Low Sulphide) | 0.5 | 31.49 |
| HET (Low Sulphide) | 3.0 | 38.95 |
| HET (Low Sulphide) | 6.0 | 47.91 |
| HET (Low Sulphide) | 9.0 | 56.86 |
| HET (High Sulphide) | 0.5 | 31.49 |

*Table A.10 Part 2: Concentration nitrified-urine needed under varying HRTs (0.5, 3, 6, and 9). Shown for pure autotrophic, pure heterotrophic, and MIXED conditions. MIXED 1 consists of 95% HD and 5% SAD; MIXED 2 consists of 52% HD and 48% SAD. $H_2S$ acts as an inhibitor for HD. Conditions include Low COD (233.60 mg $O_2$/L) and High COD (294.10 mg $O_2$/L), but also Low Sulphide (5.25 mg $H_2S$-S/L), and High Sulphide (7.00 mg $H_2S$-S/L).*

| **Condition + inhibitor concentration** | **HRT** | **Nitrified urine dosing need [mg $NO_3$-N/L]** |
|---|---|---|
| HET (High Sulphide) | 3.0 | 38.95 |
| HET (High Sulphide) | 6.0 | 47.91 |
| HET (High Sulphide) | 9.0 | 56.86 |
| MIXED 1 (Low COD, Low Sulphide) | 0.5 | 31.49 |
| MIXED 1 (Low COD, Low Sulphide) | 3.0 | 38.96 |
| MIXED 1 (Low COD, Low Sulphide) | 6.0 | 47.92 |
| MIXED 1 (Low COD, Low Sulphide) | 9.0 | 56.88 |
| MIXED 1 (High COD, Low Sulphide) | 0.5 | 31.49 |
| MIXED 1 (High COD, Low Sulphide) | 3.0 | 38.96 |
| MIXED 1 (High COD, Low Sulphide) | 6.0 | 47.93 |
| MIXED 1 (High COD, Low Sulphide) | 9.0 | 56.89 |
| MIXED 1 (High COD, High Sulphide) | 0.5 | 31.49 |
| MIXED 1 (High COD, High Sulphide) | 3.0 | 38.96 |
| MIXED 1 (High COD, High Sulphide) | 6.0 | 47.93 |
| MIXED 1 (High COD, High Sulphide) | 9.0 | 56.89 |
| MIXED 1 (Low COD, High Sulphide) | 0.5 | 31.32 |
| MIXED 1 (Low COD, High Sulphide) | 3.0 | 37.94 |
| MIXED 1 (Low COD, High Sulphide) | 6.0 | 45.89 |
| MIXED 1 (Low COD, High Sulphide) | 9.0 | 53.83 |
| MIXED 2 (Low COD, Low Sulphide) | 0.5 | 31.52 |
| MIXED 2 (Low COD, Low Sulphide) | 3.0 | 39.14 |
| MIXED 2 (Low COD, Low Sulphide) | 6.0 | 48.29 |
| MIXED 2 (Low COD, Low Sulphide) | 9.0 | 57.43 |
| MIXED 2 (High COD, Low Sulphide) | 0.5 | 31.52 |
| MIXED 2 (High COD, Low Sulphide) | 3.0 | 39.14 |
| MIXED 2 (High COD, Low Sulphide) | 6.0 | 48.29 |
| MIXED 2 (High COD, Low Sulphide) | 9.0 | 57.43 |
| MIXED 2 (High COD, High Sulphide) | 0.5 | 31.52 |

*Table A.10 Part 3: Concentration nitrified-urine needed under varying HRTs (0.5, 3, 6, and 9). Shown for pure autotrophic, pure heterotrophic, and MIXED conditions. MIXED 1 consists of 95% HD and 5% SAD; MIXED 2 consists of 52% HD and 48% SAD. $H_2S$ acts as an inhibitor for HD. Conditions include Low COD (233.60 mg $O_2$/L) and High COD (294.10 mg $O_2$/L), but also Low Sulphide (5.25 mg $H_2S$-S/L), and High Sulphide (7.00 mg $H_2S$-S/L).*

| **Condition + inhibitor concentration** | **HRT** | **Nitrified urine dosing need [mg $NO_3$-N/L]** |
|---|---|---|
| MIXED 2 (High COD, High Sulphide) | 3.0 | 39.14 |
| MIXED 2 (High COD, High Sulphide) | 6.0 | 48.29 |
| MIXED 2 (High COD, High Sulphide) | 9.0 | 57.43 |
| MIXED 2 (Low COD, High Sulphide) | 0.5 | 31.43 |
| MIXED 2 (Low COD, High Sulphide) | 3.0 | 38.58 |
| MIXED 2 (Low COD, High Sulphide) | 6.0 | 47.17 |
| MIXED 2 (Low COD, High Sulphide) | 9.0 | 55.75 |

# 6. Use of Generative Artificial Intelligence (GenAI)

## Gebruik van Generatieve Artificiële Intelligentie (GenAI) - In te vullen formulier

**Naam student**: Amber Brouns
**Studentennummer**: r0836399

**Geef met "X" aan of het gaat om een cursusopdracht, een BIG-project of een masterproef:**

⊗ Dit formulier heeft betrekking op mijn masterproef.
Titel masterproef: “Golden opportunities in urban sewers: Nitrified urine for heterotrophic and autotorphic in-sewer denitrification, odor and corrosion control”
Promotor: Benjamin Horemans en Siegfried Vlaeminck

O Dit formulier heeft betrekking op een BIG-project.
Titel BIG-project: ...
Promotor: ...

O Dit formulier heeft betrekking op een cursusopdracht.
Cursusnaam: ...
Cursusnummer: ...

**Geef met "X" aan:**

o Ik heb geen GenAI tool gebruikt.
⊗ Ik heb wel een Gen AI tool gebruikt. Geef in dat geval aan welke (bv. ChatGPT/GPT-4/...): ChatGPT

**Geef met "X" aan (mogelijk meerdere keren) op welke manier je de Gen AI tool hebt gebruikt:**

- ⊗ **Als taalassistent voor het herwerken of verbeteren van zelf geschreven teksten zonder nieuwe inhoud toe te voegen.** (Dit gebruik is gelijk aan spelling- en grammaticacheckers en hoef je niet expliciet te vermelden.)
- ○ **Als zoekmachine om eerste informatie te krijgen over een onderwerp of voor een eerste aanzet om op zoek te gaan naar literatuur.** (Deze toepassing is gelijkaardig aan het gebruik van een gewone zoekmachine bij de uitwerking van een persoonlijk werkstuk. Als student ben je verantwoordelijk voor het controleren en verifiëren van de afwezigheid of correctheid van referenties. Ga dus vervolgens zelf op zoek naar wetenschappelijke referenties en voer zelf een analyse van de brondocumenten. Interpreteer, analyseer en verwerk de verkregen informatie; kopieer ze niet zomaar. Indien je vervolgens eigenhandig een tekst opstelt, hoef je het gebruik niet te vermelden.)
- ○ **Om tekstblokken te genereren.** (Wanneer je tekstblokken van GenAI output letterlijk overneemt, dan vermeld je de GenAI bronnen en citeer je, m.a.w. je meldt duidelijk dat het item via GenAI is aangemaakt d.m.v. citatie/referentie.)
- ○ **Om grafieken of figuren te genereren.** (Wanneer je grafieken/figuren van GenAI output letterlijk overneemt, dan vermeld je de GenAI bronnen en citeer je, m.a.w. je meldt duidelijk dat het item via GenAI is aangemaakt d.m.v. citatie/referentie.)
- ○ **Om code te laten genereren als deelaspect binnen een grotere opdracht.** (Let op, dit mag enkel als de docent hier EXPLICIET toestemming voor heeft gegeven.)

- **Anders** (Neem contact op met de docent van de cursus of de promotor van de thesis of het BIG-project. Leg uit hoe je voldoet aan artikel 84 van het examenreglement. Leg uit wat het nut of de toegevoegde waarde van het gebruik van GenAI.)

## Bijkomende richtlijnen en opmerkingen

De faculteit volgt het beleid van KU Leuven om GenAI verantwoord in te zetten. Daarbij is transparantie over het gebruik van GenAI door de student essentieel, waarvoor dit formulier hulp biedt. Onverantwoord en niet-transparant gebruik van GenAI kan beschouwd worden als een onregelmatigheid en gesanctioneerd worden. Studenten die overwegen om GenAI te gebruiken, moeten zich verder informeren via de universitaire website met bijkomende richtlijnen (Hoe GenAI correct te citeren en naar te refereren? Wat is (niet) toegelaten? Tips en aandachtspunten voor een verantwoord gebruik):

https://www.kuleuven.be/onderwijs/student/onderwijstools/artificiele-intelligentie

# 7.Sources


Abdul-Talib, S., Hvitved-Jacobsen, T., Vollertsen, J., & Ujang, Z. (2002). Half saturation constants for nitrate and nitrite by in-sewer anoxic transformations of wastewater organic matter. *Water Science and Technology*, *46*(9), 185–192. https://doi.org/10.2166/wst.2002.0236

An, S., Tang, K., & Nemati, M. (2010). Simultaneous biodesulphurization and denitrification using an oil reservoir microbial culture: Effects of sulphide loading rate and sulphide to nitrate loading ratio. *Water Research*, *44*(5), 1531–1541. https://doi.org/10.1016/j.watres.2009.10.037

Auguet, O., Pijuan, M., Guasch-Balcells, H., Borrego, C. M., & Gutierrez, O. (2015). Implications of Downstream Nitrate Dosage in anaerobic sewers to control sulfide and methane emissions. *Water Research*, *68*, 522–532. https://doi.org/10.1016/j.watres.2014.09.034

Augustyniak, A., Sikora, P., Grygorcewicz, B., Despot, D., Braun, B., Rakoczy, R., Szewzyk, U., Barjenbruch, M., & Stephan, D. (2021). Biofilms in the gravity sewer interfaces: Making a friend from a foe. *Reviews in Environmental Science and Bio/Technology*, *20*(3), 795–813. https://doi.org/10.1007/s11157-021-09582-0

Bagreev, A., Bashkova, S., Locke, D. C., & Bandosz, T. J. (2001). Sewage Sludge-Derived Materials as Efficient Adsorbents for Removal of Hydrogen Sulfide. *Environmental Science & Technology*, *35*(7), 1537–1543. https://doi.org/10.1021/es001678h

Barker, P. S., & Dold, P. L. (1997). General model for biological nutrient removal activated-sludge systems: Model presentation. *Water Environment Research*, *69*(5), 969–984. https://doi.org/10.2175/106143097X125669

Bernal, D., Restrepo, I., & Grueso-Casquete, S. (2021). Key criteria for considering decentralization in municipal wastewater management. *Heliyon*, *7*(3), e06375. https://doi.org/10.1016/j.heliyon.2021.e06375

Biradar, P. M., Roy, S. B., D'Souza, S. F., & Pandit, A. B. (2010). Excess cell mass as an internal carbon source for biological denitrification. *Bioresource Technology*, *101*(6), 1787–1791. https://doi.org/10.1016/j.biortech.2009.10.049

Calise, F., Eicker, U., Schumacher, J., & Vicidomini, M. (2020). Wastewater Treatment Plant: Modelling and Validation of an Activated Sludge Process. *Energies*, *13*(15), 3925. https://doi.org/10.3390/en13153925

Campos, J. L., Carvalho, S., Portela, R., Mosquera-Corral, A., & Méndez, R. (2008). Kinetics of denitrification using sulphur compounds: Effects of S/N ratio, endogenous and exogenous compounds. *Bioresource Technology*, *99*(5), 1293–1299. https://doi.org/10.1016/j.biortech.2007.02.007

Cardoso, R. B., Sierra-Alvarez, R., Rowlette, P., Flores, E. R., Gómez, J., & Field, J. A. (2006). Sulfide oxidation under chemolithoautotrophic denitrifying conditions. *Biotechnology and Bioengineering*, *95*(6), 1148–1157. https://doi.org/10.1002/bit.21084

Cherchi, C., Onnis-Hayden, A., El-Shawabkeh, I., & Gu, A. Z. (2009a). Implication of Using Different Carbon Sources for Denitrification in Wastewater Treatments. *Water Environment Research*, *81*(8), 788–799. https://doi.org/10.2175/106143009X12465435982610

Cherchi, C., Onnis-Hayden, A., El-Shawabkeh, I., & Gu, A. Z. (2009b). Implication of Using Different Carbon Sources for Denitrification in Wastewater Treatments. *Water Environment Research*, *81*(8), 788–799. https://doi.org/10.2175/106143009X12465435982610

Chua, S. L., Liu, Y., Yam, J. K. H., Chen, Y., Vejborg, R. M., Tan, B. G. C., Kjelleberg, S., Tolker-Nielsen, T., Givskov, M., & Yang, L. (2014). Dispersed cells represent a distinct stage in the transition from bacterial biofilm to planktonic lifestyles. *Nature Communications*, *5*(1), 4462. https://doi.org/10.1038/ncomms5462

Coördinatiecomissie Intergraal Waterbeleid. (2014). *Code van goede praktijk voor het ontwerp, de aanleg en het onderhoud van rioleringsystemen: Deel 4: DWA-systemen* (p. 34). Vlaamse

Milieumaatschappij. https://www.integraalwaterbeleid.be/nl/publicaties/code-goede-praktijk-rioleringssystemen/Deel4_DWAsystemen_07_2014.pdf

D'Aquino, A., Kalinainen, N., Auvinen, H., Andreottola, G., Puhakka, J. A., & Palmroth, M. R. T. (2023). Effects of inorganic ions on autotrophic denitrification by Thiobacillus denitrificans and on heterotrophic denitrification by an enrichment culture. *Science of The Total Environment*, *901*, 165940. https://doi.org/10.1016/j.scitotenv.2023.165940

Despot, D., Reinhold, L., & Barjenbruch, M. (2022). Assessment of limited downstream nitrate dosing for sulphide control in pressure sewers: Case study in Germany. *Water Practice and Technology*, *17*(10), 2031–2047. https://doi.org/10.2166/wpt.2022.106

DHI. (2023). *SUMO Database* [Dataset]. DHI. https://www.dhigroup.com

Di Capua, F., Pirozzi, F., Lens, P. N. L., & Esposito, G. (2019). Electron donors for autotrophic denitrification. *Chemical Engineering Journal*, *362*, 922–937. https://doi.org/10.1016/j.cej.2019.01.069

Dolejs, P., Paclík, L., Maca, J., Pokorna, D., Zabranska, J., & Bartacek, J. (2015). Effect of S/N ratio on sulfide removal by autotrophic denitrification. *Applied Microbiology and Biotechnology*, *99*(5), 2383–2392. https://doi.org/10.1007/s00253-014-6140-6

Duque, N., Bach, P. M., Scholten, L., Fappiano, F., & Maurer, M. (2022). A Simplified Sanitary Sewer System Generator for Exploratory Modelling at City-Scale. *Water Research*, *209*, 117903. https://doi.org/10.1016/j.watres.2021.117903

Elefsiniotis, P., & Wareham, D. G. (2007). Utilization patterns of volatile fatty acids in the denitrification reaction. *Enzyme and Microbial Technology*, *41*(1–2), 92–97. https://doi.org/10.1016/j.enzmictec.2006.12.006

European Environment Agency. (2019). *Urban waste water treatment for 21st century challenges*. Environmental Infromation Systems. https://www.eea.europa.eu/publications/urban-waste-water-treatment-for/urban-waste-water-treatment

European Parliament. (2023). *Urban wastewater treatment Updating EU rules*. https://www.europarl.europa.eu/RegData/etudes/BRIE/2023/739370/EPRS_BRI%282023%29739370_EN.pdf

Fajardo, C., Mora, M., Fernández, I., Mosquera-Corral, A., Campos, J. L., & Méndez, R. (2014). Cross effect of temperature, pH and free ammonia on autotrophic denitrification process with sulphide as electron donor. *Chemosphere*, *97*, 10–15. https://doi.org/10.1016/j.chemosphere.2013.10.028

Fajardo, C., Mosquera-Corral, A., Campos, J. L., & Méndez, R. (2012). Autotrophic denitrification with sulphide in a sequencing batch reactor. *Journal of Environmental Management*, *113*, 552–556. https://doi.org/10.1016/j.jenvman.2012.03.018

Fanning, J. (2000). The chemical reduction of nitrate in aqueous solution. *Coordination Chemistry Reviews*, *199*(1), 159–179. https://doi.org/10.1016/S0010-8545(99)00143-5

Faust, V., Markus, P., Schielke-Jenni, S., Timmer, M. J., De Paepe, J., Ganigué, R., Vlaeminck, S. E., & Udert, K. M. (2024). Conditions for successful nitrogen removal from source-separated urine by partial nitritation/anammox. *PLOS Water*, *3*(5), e0000235. https://doi.org/10.1371/journal.pwat.0000235

Fittschen, I., & Hahn, H. H. (1998). Characterization of the municipal wastewaterpart human urine and a preliminary comparison with liquid cattle excretion. *Water Science and Technology*, *38*(6), 9–16. https://doi.org/10.2166/wst.1998.0231

Fu, X., Hou, R., Yang, P., Qian, S., Feng, Z., Chen, Z., Wang, F., Yuan, R., Chen, H., & Zhou, B. (2022). Application of external carbon source in heterotrophic denitrification of domestic sewage: A review. *Science of The Total Environment*, *817*, 153061. https://doi.org/10.1016/j.scitotenv.2022.153061

Gadekar, S., Nemati, M., & Hill, G. A. (2006). Batch and continuous biooxidation of sulphide by Thiomicrospira sp. CVO: Reaction kinetics and stoichiometry. *Water Research*, *40*(12), 2436–2446. https://doi.org/10.1016/j.watres.2006.04.007

Gao, R., Zhang, Z., Zhang, T., Liu, J., & Lu, J. (2020). Upstream Natural Pulsed Ventilation: A simple measure to control the sulfide and methane production in gravity sewer. *Science of The Total Environment*, *742*, 140579. https://doi.org/10.1016/j.scitotenv.2020.140579

Gao, Z., Zhang, Z., Li, Q., Wu, H., Wang, M., Tian, X., Wang, A., & Li, J. (2024). Improving contaminant removal and inhibiting CH4 and H2S emissions from septic tanks: Nitrified human urine as a source of electron acceptor. *Science of The Total Environment*, *951*, 175410. https://doi.org/10.1016/j.scitotenv.2024.175410

Gill, L. W., O'Luanaigh, N., Johnston, P. M., Misstear, B. D. R., & O'Suilleabhain, C. (2009). Nutrient loading on subsoils from on-site wastewater effluent, comparing septic tank and secondary treatment systems. *Water Research*, *43*(10), 2739–2749. https://doi.org/10.1016/j.watres.2009.03.024

Guerriero, G., Mattei, M. R., Papirio, S., Esposito, G., & Frunzo, L. (2022). Modelling the effect of SMP production and external carbon addition on S-driven autotrophic denitrification. *Scientific Reports*, *12*(1), 7008. https://doi.org/10.1038/s41598-022-10944-z

Guisasola, A., De Haas, D., Keller, J., & Yuan, Z. (2008). Methane formation in sewer systems. *Water Research*, *42*(6–7), 1421–1430. https://doi.org/10.1016/j.watres.2007.10.014

Gundlach, J., Bryla, M., Larsen, T. A., Kristoferitsch, L., Gründl, H., & Holzner, M. (2021). Novel NoMix toilet concept for efficient separation of urine and feces and its design optimization using computational fluid mechanics. *Journal of Building Engineering*, *33*, 101500. https://doi.org/10.1016/j.jobe.2020.101500

Gutierrez, O., Mohanakrishnan, J., Sharma, K. R., Meyer, R. L., Keller, J., & Yuan, Z. (2008). Evaluation of oxygen injection as a means of controlling sulfide production in a sewer system. *Water Research*, *42*(17), 4549–4561. https://doi.org/10.1016/j.watres.2008.07.042

Haaningnielsen, A., Lens, P., Vollertsen, J., & Hvitvedjacobsen, T. (2005). Sulfide–iron interactions in domestic wastewater from a gravity sewer. *Water Research*, *39*(12), 2747–2755. https://doi.org/10.1016/j.watres.2005.04.048

Horemans, B. (2023, 2024). *Microbial Processes for Biobased Circular Economy: Chapter 7 Sulphur Management & Recovery*.

Huang, C., Liu, Q., Li, Z.-L., Ma, X., Hou, Y.-N., Ren, N.-Q., & Wang, A.-J. (2021). Relationship between functional bacteria in a denitrification desulfurization system under autotrophic, heterotrophic, and mixotrophic conditions. *Water Research*, *188*, 116526. https://doi.org/10.1016/j.watres.2020.116526

Huang, S., Yu, D., Chen, G., Wang, Y., Tang, P., Liu, C., Tian, Y., & Zhang, M. (2021). Realization of nitrite accumulation in a sulfide-driven autotrophic denitrification process: Simultaneous nitrate and sulfur removal. *Chemosphere*, *278*, 130413. https://doi.org/10.1016/j.chemosphere.2021.130413

Hvitved-Jacobsen, T., Vollertsen, J., & Nielsen, A. H. (2013). Chapter 3: Microbiology in Sewer Networks. In *Sewer Processes: Microbial and Chemical Process Engineering of Sewer Networks, Second Edition* (0 ed., pp. 75–105). CRC Press. https://doi.org/10.1201/b14666

Jahn, A., & Nielsen, P. H. (1998). Cell biomass and exopolymer composition in sewer biofilms. *Water Science and Technology*, *37*(1). https://doi.org/10.1016/S0273-1223(97)00751-8

Jiang, F., Chen, Y., Mackey, H. R., Chen, G. H., & Van Loosdrecht, M. C. M. (2011). Urine nitrification and sewer discharge to realize in-sewer denitrification to simplify sewage treatment in Hong Kong. *Water Science and Technology*, *64*(3), 618–626. https://doi.org/10.2166/wst.2011.491

Jiang, F., Liang, Z.-S., Peng, G.-L., Qian, J., & Chen, G.-H. (2013a). Nitrogen removal capacity of simultaneously autotrophic and heterotrophic denitrification in a sewer receiving nitrified source-separated urine. *Water Practice and Technology*, *8*(1), 33–40. https://doi.org/10.2166/wpt.2013.005

Jiang, F., Liang, Z.-S., Peng, G.-L., Qian, J., & Chen, G.-H. (2013b). Nitrogen removal capacity of simultaneously autotrophic and heterotrophic denitrification in a sewer receiving nitrified source-separated urine. *Water Practice and Technology*, *8*(1), 33–40. https://doi.org/10.2166/wpt.2013.005

Jiang, G., Gutierrez, O., Sharma, K. R., & Yuan, Z. (2010). Effects of nitrite concentration and exposure time on sulfide and methane production in sewer systems. *Water Research*, *44*(14), 4241–4251. https://doi.org/10.1016/j.watres.2010.05.030

Jiang, G., Sun, J., Sharma, K. R., & Yuan, Z. (2015). Corrosion and odor management in sewer systems. *Current Opinion in Biotechnology*, *33*, 192–197. https://doi.org/10.1016/j.copbio.2015.03.007

Jimenez, J., Bott, C., Love, N., & Bratby, J. (2015). Source Separation of Urine as an Alternative Solution to Nutrient Management in Biological Nutrient Removal Treatment Plants. *Water Environment Research*, *87*(12), 2120–2129. https://doi.org/10.2175/106143015X14212658613884

Jin, P., Shi, X., Sun, G., Yang, L., Cai, Y., & Wang, X. C. (2018). Co-Variation between Distribution of Microbial Communities and Biological Metabolization of Organics in Urban Sewer Systems. *Environmental Science & Technology*, *52*(3), 1270–1279. https://doi.org/10.1021/acs.est.7b05121

Kalogo, Y., & Verstraete, W. (1999). Development of anaerobic sludge bed (ASB) reactor technologies for domestic wastewater treatment: Motives and perspectives. *World Journal of Microbiology and Biotechnology*, *15*(5), 523–534. https://doi.org/10.1023/A:1008950121308

Kang, J.-H., Namgung, H.-G., Cho, J.-I., Yoo, S. S., Lee, B.-J., & Ji, H. W. (2020). Removal of Hydrogen Sulfide in Septic Tanks for Treating Black Water via an Immobilized Media of Sulfur-Oxidizing Bacteria. *International Journal of Environmental Research and Public Health*, *17*(3), 684. https://doi.org/10.3390/ijerph17030684

Kleerebezem, R., & Mendezà, R. (2002). Autotrophic denitrification for combined hydrogen sulfide removal from biogas and post-denitrification. *Water Science and Technology*, *45*(10), 349–356. https://doi.org/10.2166/wst.2002.0368

Knowles, R. (1982). Denitrification. *Microbiological Reviews*, *46*(1), 43–70. https://doi.org/10.1128/mr.46.1.43-70.1982

Koenig, A., & Liu, L. (2004). Autotrophic Denitrification of High–Salinity Wastewater Using Elemental Sulfur: Batch Tests. *Water Environment Research*, *76*(1), 37–46. https://doi.org/10.2175/106143004X141564

Kou, Z., Huo, P., Qi, X., Gu, Y., Huang, X., & Liang, P. (2024). Effect of dissolved oxygen on sulfur autotrophic denitrification and how to address it: An experimental and modelling work. *Water Research*, *267*, 122415. https://doi.org/10.1016/j.watres.2024.122415

Lan, L., Zhao, J., Wang, S., Li, X., Qiu, L., Liu, S., & Bin Nasry, A. A. N. (2019). NO and N2O accumulation during nitrite-based sulfide-oxidizing autotrophic denitrification. *Bioresource Technology Reports*, *7*, 100190. https://doi.org/10.1016/j.biteb.2019.100190

Larsen, T. A., Riechmann, M. E., & Udert, K. M. (2021). State of the art of urine treatment technologies: A critical review. *Water Research X*, *13*, 100114. https://doi.org/10.1016/j.wroa.2021.100114

Li, W., Zheng, T., Ma, Y., & Liu, J. (2019). Current status and future prospects of sewer biofilms: Their structure, influencing factors, and substance transformations. *Science of The Total Environment*, *695*, 133815. https://doi.org/10.1016/j.scitotenv.2019.133815

Li, Y., Liu, L., & Wang, H. (2022). Mixotrophic denitrification for enhancing nitrogen removal of municipal tailwater: Contribution of heterotrophic/sulfur autotrophic denitrification and bacterial community. *Science of The Total Environment*, *814*, 151940. https://doi.org/10.1016/j.scitotenv.2021.151940

Liang, Z., Sun, J., Zhan, C., Wu, S., Zhang, L., & Jiang, F. (2020a). Effects of sulfide on mixotrophic denitrification by *Thauera* -dominated denitrifying sludge. *Environmental Science: Water Research & Technology*, *6*(4), 1186–1195. https://doi.org/10.1039/C9EW01014A

Liang, Z., Sun, J., Zhan, C., Wu, S., Zhang, L., & Jiang, F. (2020b). Effects of sulfide on mixotrophic denitrification by *Thauera* -dominated denitrifying sludge. *Environmental Science: Water Research & Technology*, *6*(4), 1186–1195. https://doi.org/10.1039/C9EW01014A

Libralato, G., Volpi Ghirardini, A., & Avezzù, F. (2012). To centralise or to decentralise: An overview of the most recent trends in wastewater treatment management. *Journal of Environmental Management*, *94*(1), 61–68. https://doi.org/10.1016/j.jenvman.2011.07.010

Lin, H.-W., Rabaey, K., Keller, J., Yuan, Z., & Pikaar, I. (2015). Scaling-Free Electrochemical Production of Caustic and Oxygen for Sulfide Control in Sewers. *Environmental Science & Technology*, *49*(19), 11395–11402. https://doi.org/10.1021/acs.est.5b02188

Lu, H., Chandran, K., & Stensel, D. (2014). Microbial ecology of denitrification in biological wastewater treatment. *Water Research*, *64*, 237–254. https://doi.org/10.1016/j.watres.2014.06.042

Lu, H., Huang, H., Yang, W., Mackey, H. R., Khanal, S. K., Wu, D., & Chen, G.-H. (2018a). Elucidating the stimulatory and inhibitory effects of dissolved sulfide on sulfur-oxidizing bacteria (SOB) driven autotrophic denitrification. *Water Research*, *133*, 165–172. https://doi.org/10.1016/j.watres.2018.01.022

Lu, H., Huang, H., Yang, W., Mackey, H. R., Khanal, S. K., Wu, D., & Chen, G.-H. (2018b). Elucidating the stimulatory and inhibitory effects of dissolved sulfide on sulfur-oxidizing bacteria (SOB) driven autotrophic denitrification. *Water Research*, *133*, 165–172. https://doi.org/10.1016/j.watres.2018.01.022

Malik, M. A. (n.d.). *1.7: Density and Specific Gravity Measurements*. Chemistry LibreTexts. 1.7: Density and specific gravity measurements - Chemistry LibreTexts

Manconi, I., Carucci, A., & Lens, P. (2007). Combined removal of sulfur compounds and nitrate by autotrophic denitrification in bioaugmented activated sludge system. *Biotechnology and Bioengineering*, *98*(3), 551–560. https://doi.org/10.1002/bit.21383

Maurer, M., Rothenberger, D., & Larsen, T. A. (2005). Decentralised wastewater treatment technologies from a national perspective: At what cost are they competitive? *Water Supply*, *5*(6), 145–154. https://doi.org/10.2166/ws.2005.0059

Metcalf, & Eddy. (2014). Chapter 7: Fundamentals of Biological Treatment. In G. Tchobanoglous, D. H. Stensel, R. Tsuchihashi, F. Burton, M. Abu-Orf, G. Bowden, W. Pfrang, Metcalf & Eddy, Inc, &

Albert Einstein College of Medicine (Eds.), *Wastewater engineering: Treatment and resource recovery* (Fifth Edition). McGraw-Hill Education.

Mohanakrishnan, J., Gutierrez, O., Sharma, K. R., Guisasola, A., Werner, U., Meyer, R. L., Keller, J., & Yuan, Z. (2009). Impact of nitrate addition on biofilm properties and activities in rising main sewers. *Water Research*, *43*(17), 4225–4237. https://doi.org/10.1016/j.watres.2009.06.021

Möhle, R. B., Langemann, T., Haesner, M., Augustin, W., Scholl, S., Neu, T. R., Hempel, D. C., & Horn, H. (2007). Structure and shear strength of microbial biofilms as determined with confocal laser scanning microscopy and fluid dynamic gauging using a novel rotating disc biofilm reactor. *Biotechnology and Bioengineering*, *98*(4), 747–755. https://doi.org/10.1002/bit.21448

Muller, Inc. (2024). *Gravity Sewer Mains & How They Work*. Muller.

Oh, J., & Silverstein, J. (1999). Acetate Limitation and Nitrite Accumulation during Denitrification. *Journal of Environmental Engineering*, *125*(3), 234–242. https://doi.org/10.1061/(ASCE)0733-9372(1999)125:3(234)

Oh, S.-E., Kim, K.-S., Choi, H.-C., Cho, J., & Kim, I. S. (2000). Kinetics and physiological characteristics of autotrophic dentrification by denitrifying sulfur bacteria. *Water Science and Technology*, *42*(3–4), 59–68. https://doi.org/10.2166/wst.2000.0359

Oosterhuis, M., & Van Loosdrecht, M. C. M. (2009). Nitrification of urine for H2S control in pressure sewers. *Water Practice and Technology*, *4*(3), wpt2009059. https://doi.org/10.2166/wpt.2009.059

Otterpohl, R., Braun, U., & Oldenburg, M. (2004). Innovative technologies for decentralised water-, wastewater and biowaste management in urban and peri-urban areas. *Water Science and Technology*, *48*(11–12), 23–32. https://doi.org/10.2166/wst.2004.0795

Paing, J., Picot, B., Sambuco, J. P., & Rambaud, A. (2000). Sludge accumulation and methanogenic activity in an anaerobic lagoon. *Water Science and Technology*, *42*(10–11), 247–255. https://doi.org/10.2166/wst.2000.0654

Pan, Y., Ye, L., & Yuan, Z. (2013). Effect of H2S on N2O Reduction and Accumulation during Denitrification by Methanol Utilizing Denitrifiers. *Environmental Science & Technology*, *47*(15), 8408–8415. https://doi.org/10.1021/es401632r

Pang, Y., Hu, L., & Wang, J. (2022). Mixotrophic denitrification using pyrite and biodegradable polymer composite as electron donors. *Bioresource Technology*, *351*, 127011. https://doi.org/10.1016/j.biortech.2022.127011

Park, K., Lee, H., Phelan, S., Liyanaarachchi, S., Marleni, N., Navaratna, D., Jegatheesan, V., & Shu, L. (2014). Mitigation strategies of hydrogen sulphide emission in sewer networks – A review. *International Biodeterioration & Biodegradation*, *95*, 251–261. https://doi.org/10.1016/j.ibiod.2014.02.013

Peirano, C., Guerrero, L., Barahona, A., Montalvo, S., Huiliñir, C., Da Silva, C., & Borja, R. (2020). Assessment of simultaneous autotrophic–heterotrophic denitrification with high removal of nitrogen, sulfur and carbon: Optimization through response surface methodology. *Journal of Chemical Technology & Biotechnology*, *95*(3), 631–638. https://doi.org/10.1002/jctb.6244

Phscale Core Team. (2024, June 4). *The Importance of pH in Sewage Water Treatment*. The Importance of pH in Sewage Water Treatment. https://phscale.org/water-ph/ph-of-sewage-water/

Pikaar, I., Flugen, M., Lin, H.-W., Salehin, S., Li, J., Donose, B. C., Dennis, P. G., Bethke, L., Johnson, I., Rabaey, K., & Yuan, Z. (2019). Full-scale investigation of in-situ iron and alkalinity generation for efficient sulfide control. *Water Research*, *167*, 115032. https://doi.org/10.1016/j.watres.2019.115032

Pikaar, I., Li, E., Rozendal, R. A., Yuan, Z., Keller, J., & Rabaey, K. (2012). Long-term field test of an electrochemical method for sulfide removal from sewage. *Water Research*, *46*(9), 3085–3093. https://doi.org/10.1016/j.watres.2012.03.013

Randall, D. G., & Naidoo, V. (2018). Urine: The liquid gold of wastewater. *Journal of Environmental Chemical Engineering*, *6*(2), 2627–2635. https://doi.org/10.1016/j.jece.2018.04.012

Ren, D., Zuo, Z., Xing, Y., Ji, P., Yu, T., Zhu, D., Liu, Y., & Huang, X. (2022). Simultaneous control of sulfide and methane in sewers achieved by a physical approach targeting dominant active zone in sediments. *Water Research*, *211*, 118010. https://doi.org/10.1016/j.watres.2021.118010

Reyes-Avila, J., Razo-Flores, E., & Gomez, J. (2004). Simultaneous biological removal of nitrogen, carbon and sulfur by denitrification. *Water Research*, *38*(14–15), 3313–3321. https://doi.org/10.1016/j.watres.2004.04.035

Rocher, V., Laverman, A. M., Gasperi, J., Azimi, S., Guérin, S., Mottelet, S., Villières, T., & Pauss, A. (2015). Nitrite accumulation during denitrification depends on the carbon quality and quantity in wastewater treatment with biofilters. *Environmental Science and Pollution Research*, *22*(13), 10179–10188. https://doi.org/10.1007/s11356-015-4196-1

Roothans, N., Van Loosdrecht, M. C. M., & Laureni, M. (2025). Metabolic labour division trade-offs in denitrifying microbiomes. *The ISME Journal*, *19*(1), wraf020. https://doi.org/10.1093/ismejo/wraf020

Salehi, R., & Chaiprapat, S. (2022). Predicting H2S emission from gravity sewer using an adaptive neuro-fuzzy inference system. *Water Quality Research Journal*, *57*(1), 20–39. https://doi.org/10.2166/wqrj.2021.018

Sharma, E., Sivakumar, M., Kelso, C., Zhang, S., Shi, J., Gao, J., Gao, S., Zhou, X., & Jiang, G. (2023). Effects of sewer biofilms on the degradability of carbapenems in wastewater using laboratory scale bioreactors. *Water Research*, *233*, 119796. https://doi.org/10.1016/j.watres.2023.119796

Shen, Q., Fangying, J., Jiazhi, W., Dexin, F., Qian, Z., Lei, J., Anrong, C., & Li, K. (2020). *The influence mechanism of temperature on solid phase denitrification based on denitrification performance, carbon balance, and microbial analysis*.

Smets, I. (2024, 2025). *Wastewater Treatment Technology Biodegradation: Carbon and nutrient removal*.

Soliman, M., & Eldyasti, A. (2018). Ammonia-Oxidizing Bacteria (AOB): Opportunities and applications—a review. *Reviews in Environmental Science and Bio/Technology*, *17*(2), 285–321. https://doi.org/10.1007/s11157-018-9463-4

Stewart, P. S. (2003). Diffusion in Biofilms. *Journal of Bacteriology*, *185*(5), 1485–1491. https://doi.org/10.1128/JB.185.5.1485-1491.2003

Sun, J., Hu, S., Sharma, K. R., Ni, B.-J., & Yuan, Z. (2014). Stratified Microbial Structure and Activity in Sulfide- and Methane-Producing Anaerobic Sewer Biofilms. *Applied and Environmental Microbiology*, *80*(22), 7042–7052. https://doi.org/10.1128/AEM.02146-14

Sun, J., Hu, S., Sharma, K. R., Ni, B.-J., & Yuan, Z. (2015). Degradation of methanethiol in anaerobic sewers and its correlation with methanogenic activities. *Water Research*, *69*, 80–89. https://doi.org/10.1016/j.watres.2014.11.004

Sun, Q., Fang, Y.-K., Liu, W.-Z., Xie, N., Dong, H., Guadie, A., Liu, Y., Cheng, H.-Y., & Wang, A.-J. (2023). Synergistic between autotrophic and heterotrophic microorganisms for denitrification using bio-S as electron donor. *Environmental Research*, *231*, 116047. https://doi.org/10.1016/j.envres.2023.116047

Sun, Y., & Nemati, M. (2012). Evaluation of sulfur-based autotrophic denitrification and denitritation for biological removal of nitrate and nitrite from contaminated waters. *Bioresource Technology*, *114*, 207–216. https://doi.org/10.1016/j.biortech.2012.03.061

Sutherland-Stacey, L. (n.d.). *Research Employee DCM Process Control Ltd. PO Box 113233 Newmarket Auckland 1149, New Zealand phone: + 64 9 520 3774 fax: + 64 9 520 3779 email: Nzoffice@ dcmprocesscontrol.com www.dcmprocesscontrol.com*.

Talaiekhozani, A., Bagheri, M., Goli, A., & Talaei Khoozani, M. R. (2016). An overview of principles of odor production, emission, and control methods in wastewater collection and treatment systems. *Journal of Environmental Management*, *170*, 186–206. https://doi.org/10.1016/j.jenvman.2016.01.021

Team Economie en Nematoden, Biological Recovery & Re-use Technology, WIMEK, Vijn, M., & Weijma, J. (2020). *Menselijke urine als meststof voor eetbare planten: Inzameling, medicijnresten, wet- en regelgeving en maatschappelijke acceptatie*. Wageningen University & Research, Wetenschapswinkel. https://doi.org/10.18174/516515

Terpstra, P. M. J. (1999). Sustainable water usage systems: Models for the sustainable utilization of domestic water in urban areas. *Water Science and Technology*, *39*(5), Fit. https://doi.org/10.1016/S0273-1223(99)00088-8

Udert, K., & Jenni, S. (2013). Chapter 20: Biological nitrogen conversion processes. In J. Lienert (Ed.), *Source Separation and Decentralization for Wastewater Management* (pp. 291–302). IWA Publishing.

Udert, K., & Lienert, J. (Eds.). (2013). Chapter 17: Wastewater composition. In E. Friedler, D. Buttler, & Y. Alfiya, *Source Separation and Decentralization for Wastewater Management* (pp. 241–254). IWA Publishing.

Verma, S., Kuila, A., & Jacob, S. (2023). Role of Biofilms in Waste Water Treatment. *Applied Biochemistry and Biotechnology*, *195*(9), 5618–5642. https://doi.org/10.1007/s12010-022-04163-5

VMM. (n.d.). *Indicator influent- en effluentvrachten van RWZI's Toestan, grafieken en evolutie doorheen de jaren*. Vlaamse Milieumaatschappij (VMM). https://vmm.vlaanderen.be/feiten-cijfers/water/riolering-en-waterzuivering/indicator-influent-en-effluentvrachten-van-rwzis?

VMM. (2024). *Watergebruik door huishoudens*. https://www.vmm.be/publicaties/watergebruik-door-huishoudens

Wang, D., Xu, S., Jiang, C., Wang, X., Yang, D., Kuai, B., & Zhuang, X. (2023). The effects, mechanisms, and applications of sulfide as both an inhibitor and electron donor in novel biological nitrogen removal process. *Science of The Total Environment*, *894*, 164784. https://doi.org/10.1016/j.scitotenv.2023.164784

Wang, H., Chen, N., Feng, C., & Deng, Y. (2021). Insights into heterotrophic denitrification diversity in wastewater treatment systems: Progress and future prospects based on different carbon sources. *Science of The Total Environment*, *780*, 146521. https://doi.org/10.1016/j.scitotenv.2021.146521

Wang, S., Zhu, H., Zheng, G., Dong, F., & Liu, C. (2022). Dynamic Changes in Biofilm Structures under Dynamic Flow Conditions. *Applied and Environmental Microbiology*, *88*(22), e01072-22. https://doi.org/10.1128/aem.01072-22

Wang, T., Guo, Z., Shen, Y., Cui, Z., & Goodwin, A. (2020). Accumulation mechanism of biofilm under different water shear forces along the networked pipelines in a drip irrigation system. *Scientific Reports*, *10*(1), 6960. https://doi.org/10.1038/s41598-020-63898-5

Wang, X., Wang, W., Zhang, Y., Zhang, J., Li, J., Wang, S., & Chen, G. (2019). Isolation and characterization of Acinetobacter sp. JQ1004 and evaluation of its inhibitory kinetics by free ammonia. *Desalination and Water Treatment*, *147*, 316–325. https://doi.org/10.5004/dwt.2019.23757

Weissenberger, J. (2002). *Betonkorrosion ein Forschungprojekt aus Norwegen. Schwefelwasserstroff in Abwassersystemen*. https://link.springer.com/content/pdf/10.1007/s00506-012-0380-4.pdf?pdf=inline%20link

Withers, P. J., Jordan, P., May, L., Jarvie, H. P., & Deal, N. E. (2014). Do septic tank systems pose a hidden threat to water quality? *Frontiers in Ecology and the Environment*, *12*(2), 123–130. https://doi.org/10.1890/130131

World Health Organisation. (2024). *Guidelines for safe recreational water environments: Volume 1. Coastal and fresh waters* (No. WHO/HEP/ECH/WASH/2024.3). World Health Organization. https://iris.who.int/bitstream/handle/10665/376869/9789240094703-eng.pdf?sequence=1

Wunderlin, P., Mohn, J., Joss, A., Emmenegger, L., & Siegrist, H. (2012). Mechanisms of N2O production in biological wastewater treatment under nitrifying and denitrifying conditions. *Water Research*, *46*(4), 1027–1037. https://doi.org/10.1016/j.watres.2011.11.080

Xu, G., Feng, C., Fang, F., Chen, S., Xu, Y., & Wang, X. (2015). *The heterotrophic-combined-with-autotrophic denitrification process: Performance and interaction mechanisms*. https://doi.org/doi.org/10.2166/wst.2015.097

Xu, G., Peng, J., Feng, C., Fang, F., Chen, S., Xu, Y., & Wang, X. (2015). Evaluation of simultaneous autotrophic and heterotrophic denitrification processes and bacterial community structure analysis. *Applied Microbiology and Biotechnology*, *99*(15), 6527–6536. https://doi.org/10.1007/s00253-015-6532-2

Xu, J., Yang, L., & Zhou, X. (2023). A systematical review of blackwater treatment and resource recovery: Advance in technologies and applications. *Resources, Conservation and Recycling*, *197*, 107066. https://doi.org/10.1016/j.resconrec.2023.107066

Xu, Z., Chen, X., Li, H., Wan, D., & Wan, J. (2020). Combined heterotrophic and autotrophic system for advanced denitrification of municipal secondary effluent in full-scale plant and bacterial community analysis. *Science of The Total Environment*, *717*, 136981. https://doi.org/10.1016/j.scitotenv.2020.136981

Yang, G., Xu, Q., Wang, D., Tang, L., Xia, J., Wang, Q., Zeng, G., Yang, Q., & Li, X. (2018). Free ammonia-based sludge treatment reduces sludge production in the wastewater treatment process. *Chemosphere*, *205*, 484–492. https://doi.org/10.1016/j.chemosphere.2018.04.140

Yu, C., Qiao, S., & Zhou, J. (2023). Sulfide-driven nitrous oxide recovery during the mixotrophic denitrification process. *Journal of Environmental Sciences*, *125*, 443–452. https://doi.org/10.1016/j.jes.2021.12.003

Yuan, Y., Bian, A., Chen, F., Xu, X., Huang, C., Chen, C., Liu, W., Cheng, H., Chen, T., Ding, C., Li, Z., & Wang, A. (2019). Continuous sulfur biotransformation in an anaerobic-anoxic sequential batch reactor involving sulfate reduction and denitrifying sulfide oxidization. *Chemosphere*, *234*, 568–578. https://doi.org/10.1016/j.chemosphere.2019.06.109

Zhan, M., Zeng, W., Wu, C., Chen, G., Meng, Q., Hao, X., & Peng, Y. (2024). Impact of organic carbon on sulfide-driven autotrophic denitrification: Insights from isotope fractionation and

functional genes. *Water Research*, *255*, 121507. https://doi.org/10.1016/j.watres.2024.121507

Zhang, L., De Schryver, P., De Gusseme, B., De Muynck, W., Boon, N., & Verstraete, W. (2008). Chemical and biological technologies for hydrogen sulfide emission control in sewer systems: A review. *Water Research*, *42*(1–2), 1–12. https://doi.org/10.1016/j.watres.2007.07.013

Zhang, L., Keller, J., & Yuan, Z. (2009). Inhibition of sulfate-reducing and methanogenic activities of anaerobic sewer biofilms by ferric iron dosing. *Water Research*, *43*(17), 4123–4132. https://doi.org/10.1016/j.watres.2009.06.013

Zhang, Z., Zhang, C., Yang, Y., Zhang, Z., Tang, Y., Su, P., & Lin, Z. (2022). A review of sulfate-reducing bacteria: Metabolism, influencing factors and application in wastewater treatment. *Journal of Cleaner Production*, *376*, 134109. https://doi.org/10.1016/j.jclepro.2022.134109

Zhou, Y., Pijuan, M., & Yuan, Z. (2007). Free nitrous acid inhibition on anoxic phosphorus uptake and denitrification by poly-phosphate accumulating organisms. *Biotechnology and Bioengineering*, *98*(4), 903–912. https://doi.org/10.1002/bit.21458

Zumft, W. G. (1997). Cell biology and molecular basis of denitrification. *Microbiology and Molecular Biology Reviews*, *61*(4), 533–616. https://doi.org/10.1128/mmbr.61.4.533-616.1997